Piers, jetties and related structures exposed to waves:

Guidelines for hydraulic loadings

Kirsty McConnell
William Allsop
Ian Cruickshank

HR Wallingford

dti
Department of Trade and Industry

ThomasTelford

Preface

Trade with coastal nations requires jetties against which vessels may berth to discharge/accept cargo. For small vessels, these facilities can often be constructed in sheltered locations where hydraulic and other loadings are relatively small. However, the demand in recent years has been for much larger vessels, which require longer jetties in significantly deeper water. In these locations the construction of protective breakwaters can be prohibitively expensive and therefore increasingly jetties or their approach trestles are being constructed without breakwaters in exposed locations.

There is a significant need for clear guidance on prediction methods, formulae and coefficients to determine those hydraulic loads needed in the design of such jetties exposed to extreme conditions.

These guidelines aim to bring together existing guidance for the hydraulic design of jetties into a single document. They also introduce new methodologies for the prediction of wave loads on jetties derived from extensive laboratory testing undertaken specifically for the production of these guidelines.

The project to develop these guidelines was undertaken by HR Wallingford and was part-funded by the Department of Trade and Industry Construction Programme Partners in Innovation Scheme. The contract was CI 39/5/125 (cc 1821). A number of Project Partners formed a Steering Committee for the project that directed the technical content of the project and also provided matching funds. These organisations were:

- BP Amoco
- CJ Associates
- Costain
- Halcrow
- HR Wallingford
- Kier
- Jacobs
- Peter Fraenkel Maritime
- Posford Haskoning
- Mott MacDonald
- Mouchel Parkman
- Seacore
- Shell Global Solutions
- University of Liverpool

Contributions from the Steering Committee in the form of case study information, photographs and sections of text are gratefully acknowledged. These are acknowledged in the document where appropriate.

Valuable contributions were obtained from colleagues at HR Wallingford, in particular: Richard Whitehouse who provided assistance and review on the discussion of scour issues; Mike Pomfret and Amjad Mohamed-Saleem who carried out a literature review and collated information on case studies; Matteo Tirindelli and Giovanni Cuomo who carried out the

Contents

1. Introduction

1.1. BACKGROUND – WHY ARE 'EXPOSED JETTIES' CONSTRUCTED?

Traditionally marine terminals have been constructed in naturally sheltered locations or protected by breakwaters so hydraulic and other marine loadings on structures are relatively small. However, there are occasions when jetties have to be constructed in 'exposed' locations and hence may be subject to large and complex direct and indirect hydraulic loadings. A typical exposed jetty under construction is shown in Figure 1.1.

In recent years there has been an increased demand for the development of large single use industrial terminals (especially those for Liquid Natural Gas (LNG), and Liquid Petroleum Gas (LPG)) which require deep water and sheltered berths, but little shelter to the approach trestles carrying the delivery lines. These terminals are often required in remote locations where there is no shelter, no existing infrastructure and the construction of new protective breakwaters for the whole facility is not cost effective. Therefore, in many instances the jetties and/or their approach trestles are being constructed in exposed locations without breakwater protection. This has resulted in the design and construction of facilities with a degree of exposure beyond the bounds of most general experience.

Other examples of exposed jetties include small jetties on open coasts in tropical regions serving small fishing communities, ferry services and emergency access to remote locations. For most of the design life, the environmental conditions may be benign but occasionally cyclone and hurricane conditions hit, putting the exposed jetty under significant hydraulic loading.

It is estimated that in the past 15 years the market value of 'exposed' jetties designed by UK consultants is in the order of £5 billion. It is likely that this market will continue to grow, but that growth up to now has been inhibited as the confidence in design methods was not sufficiently robust.

Figure 1.1.   *Typical exposed jetty under construction (courtesy Besix–Kier)*

1.2.   TYPICAL DESIGN ISSUES AND THE NEED FOR FURTHER GUIDANCE

Since the early 1980s, there have been repeated and persistent requests from designers and contractors for better guidance and information for the design of exposed jetties, as existing British and European Standards do not adequately address the design issues.

A significant need is for clear guidance on prediction methods, formulae and coefficients to determine wave slam forces down onto and underneath decks, and against vertical elements. Data on uncertainties are needed for probabilistic simulations, and validated methods are needed to combine wave slam and pile loadings (particularly short-duration slam forces) on long jetties.

Information and guidance presently used in assessing hydraulic loads and related responses for exposed jetties has been of limited reliability, and has been difficult to source. In particular, there has been no knowledge on wave slam loads down onto decks from above, very little knowledge on wave slam forces on projecting elements, and even less on slam underneath decks. New guidance on these aspects is given in Chapter 5 of this document, based on an extensive series of physical model tests undertaken to support the preparation of this guidance.

Design guidance is well developed in the two environments of 'coastal', where structures withstand shallow sea conditions, and 'offshore', where oil and gas exploration has led to the development of sophisticated deepwater designs for these large and often unique projects. However, exposed jetties are in an environment which spans the gap between coastal and offshore. Consequently, the design requirements are neither completely aligned to one nor the other environment and the guidance on how to apply theories and practice has not historically been clear.

1.3. OBJECTIVES OF THESE GUIDELINES

These guidelines address many of the problems described above and in doing so provide the following benefits.

- Reduce design uncertainties and hence improve safety
- Where appropriate, reduce design and construction costs
- Support the development of more appropriate designs
- Reduce environmental risks from failure of jetty pipelines
- Improve safety for construction and operational staff
- Demonstrate improved design techniques in case study examples.

This new guidance will assist designers to ensure that exposed jetties are adequately designed for the environment to which they are exposed and remain serviceable throughout their planned life.

1.4. USE OF THESE GUIDELINES

The design methods derived in these guidelines represent state-of-the-art knowledge and are based on a comprehensive set of physical model tests. However, the designer must take full recognition of the various limits of applicability and uncertainties in the design process. The designer should confirm and check the design for the particular location and conditions envisaged, which may necessitate specific model testing to be undertaken.

1.5. STRUCTURE OF THE GUIDELINES

These guidelines are structured in five parts:

- Chapter 1 has summarised the need for the guidelines and their objectives
- Chapter 2 provides a definition of exposed jetties
- Chapter 3 provides details of design methodologies and design criteria
- Chapters 4, 5, 6 and 7 describe the design methods available to assess hydraulic loading and scour effects
- Chapters 8 briefly highlights construction and maintenance issues to be considered in the hydraulic design process
- Chapter 9 contains the references used in this work.

2. Definitions of exposed jetties, typical locations and exposures

2.1. DEFINITION OF AN EXPOSED JETTY

The British Standard for Maritime Structures, BS 6349 Pt 2 (1998) defines a jetty as:

'a structure providing a berth or berths at some distance from the shore'

BS 6349 sub-divides (quay and) jetty structures into the following categories:

- Sheet walls
- Sheet piled walls
- Timber
- Concrete
- Steel
- In-situ concrete piled walls
- Diaphragm walls
- Soldier piles and sheeting
- Gravity walls
- Concrete
- Masonry
- Precast reinforced concrete

- Concrete caissons
- Cellular sheet piled walls
- Double-wall sheet piled structures
- In-situ mass concrete walls
- In-situ reinforced concrete walls
- Diaphragm walls
- Monoliths
- Suspended deck/open piled structures
- All vertical piles
- All vertical piles plus horizontal tie backs
- Vertical and raking piles
- All raking piles.

Within these guidelines an 'exposed jetty' is defined as:

'A solid vertical or open piled structure, possibly with cross-bracing, providing a berth or berths constructed in a location where wave forces have a significant influence on the design'

'These structures can be remote from the land in deep water (where the influence of shallow water is small) or in exposed locations such as marginal quays (where the influence of shallow water impacts are more significant)'

When considering hydraulic design parameters, four main categories of structures exist:

- simple solid quays/jetties
- open piled jetties
- marginal jetties/quays
- rubble mound causeway.

These are described in the following sections.

The majority of exposed jetties in deep water locations are open piled structures. As part of the process of developing these guidelines, new laboratory studies were undertaken that primarily focused on these types of structures. Some reference is made to other structure types where appropriate.

2.1.1. Simple solid quays
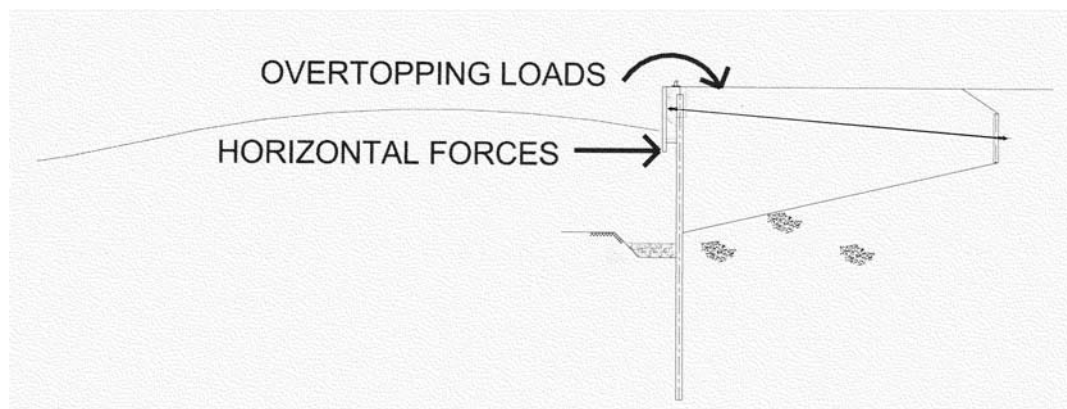
Figure 2.1.   Typical vertical-faced solid quay

These structures (Figure 2.1) are essentially vertically sided, formed by stone blockwork, concrete blocks, or in situ (shuttered) concrete, with or without sheet pile containment. The jetty deck/crest is probably at a uniform (horizontal) level. This structure type offers complete blockage to longshore currents and, under wave attack, may be treated as a vertical wall or breakwater. These jetties are generally quite short in length, and may be designed with little if any analysis of their hydraulic effects, or of wave or current loadings. Solid jetty heads may also be constructed at the end of a piled approach jetty (Figure 2.2). Design methods for these structures are discussed in Section 4.3.
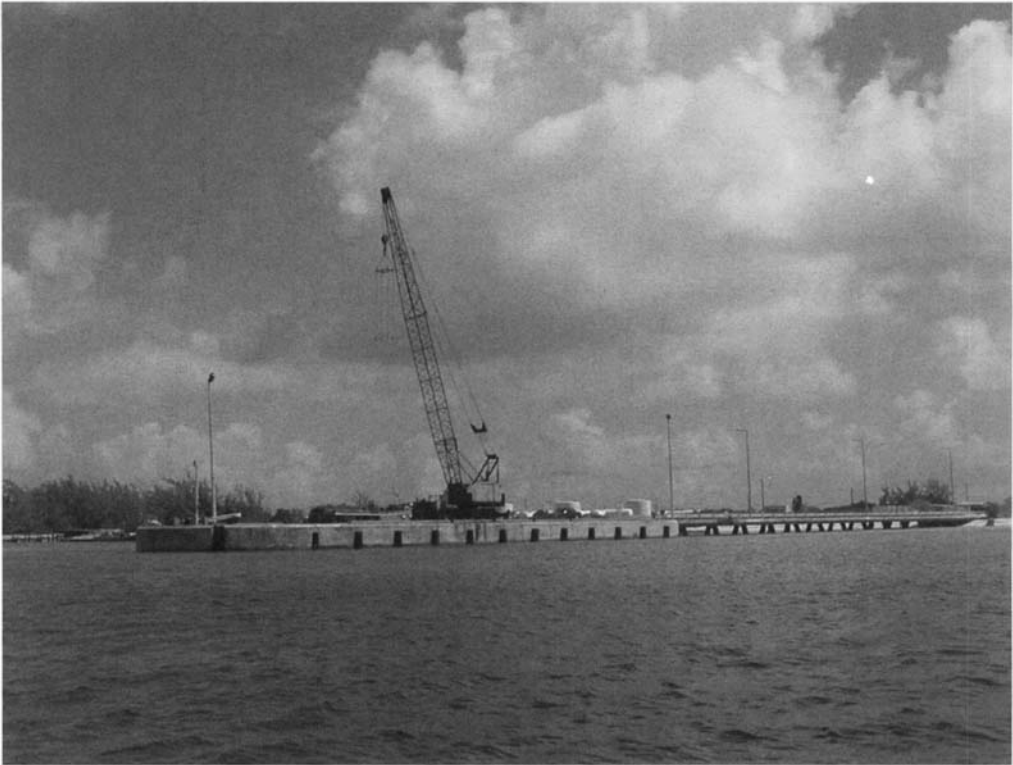
Figure 2.2.   Open piled jetty with solid quay at jetty head (courtesy Mott MacDonald)

2.1.2. Open piled jetties

These structures may be very long in the direction of wave travel (Figure 2.3), 2–4 km have been known, with longer ones currently being planned. They are often configured approximately normal to the shoreline. A typical plan layout is shown in Figure 2.4 and a cross-section in Figure 2.5. Vessel mooring forces are often absorbed by free-standing mooring and fender dolphins, rather than by the jetty head, and any head structure is usually relatively small in plan area. These types of jetties are common at LNG/LPG import and export terminals.
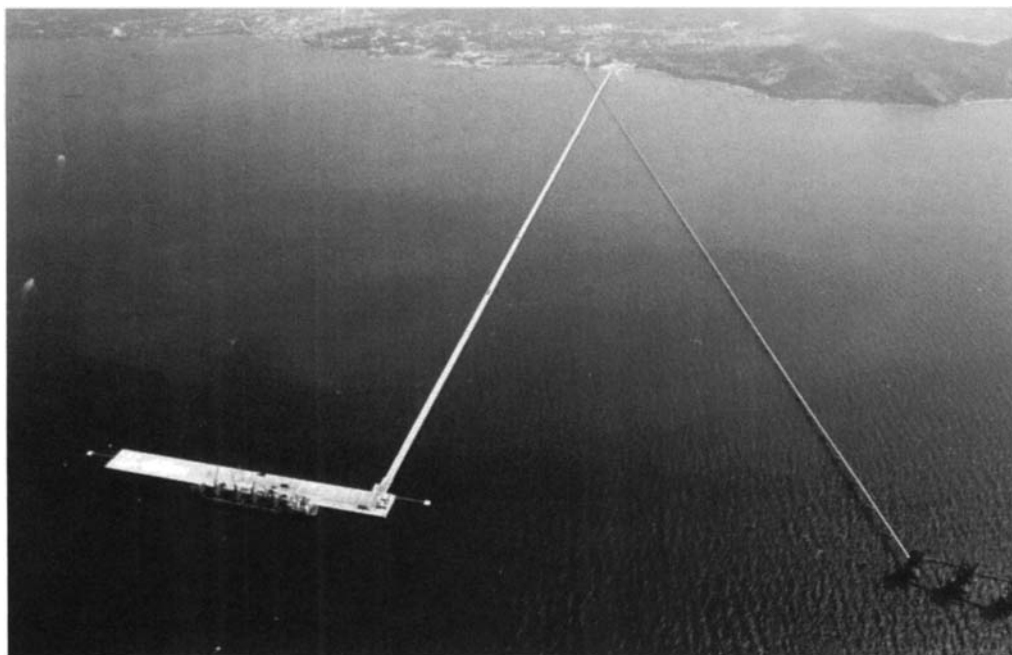
Figure 2.3.   Sri Racha Jetty, Thailand (courtesy Kier)
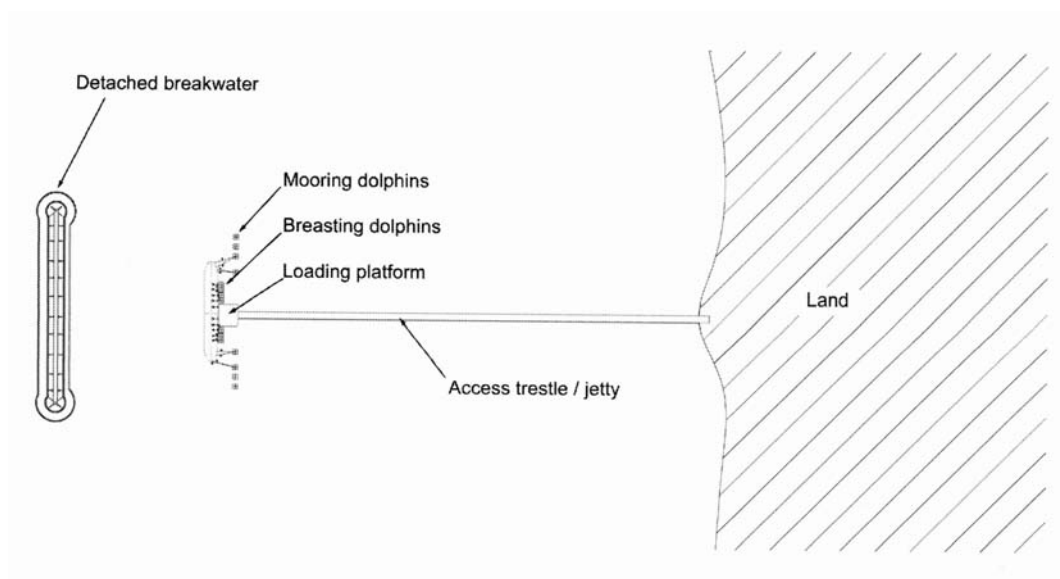
Figure 2.4.   Typical plan of open piled jetty
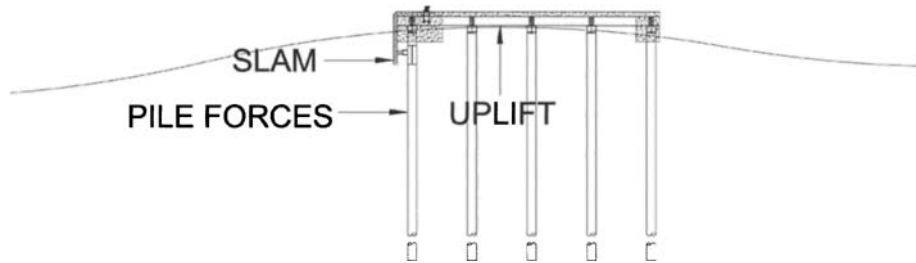
Figure 2.5. *Typical section of open piled jetty*

Figure 2.6. *Small coastal jetty (courtesy Mott MacDonald)*

These jetties are constructed with open piles to minimise interruption of waves, currents and sediment movement along the coastline, and to minimise wave forces onto the structure. A typical jetty is shown in Figure 2.6. For oil or gas cargoes where cargo transfer is by flexible hoses or marine loading arms with swivel joints, these types of jetties are typically designed to be so high that there is always an 'air gap' between the crest of the extreme design wave and the underside of the jetty deck. The air gap is provided to eliminate the occurrence of wave loads on the jetty deck and protect topside equipment. The jetty deck elevation may, however, be dictated by berth operations and vessel draught and freeboard, to ensure efficient design and operation of loading arms. Where the air gap is not sufficient and loading occurs on

the underside of the jetty deck, deck elements may be damaged or removed by the force of wave action. An example of a small coastal jetty is shown in Figure 2.7.
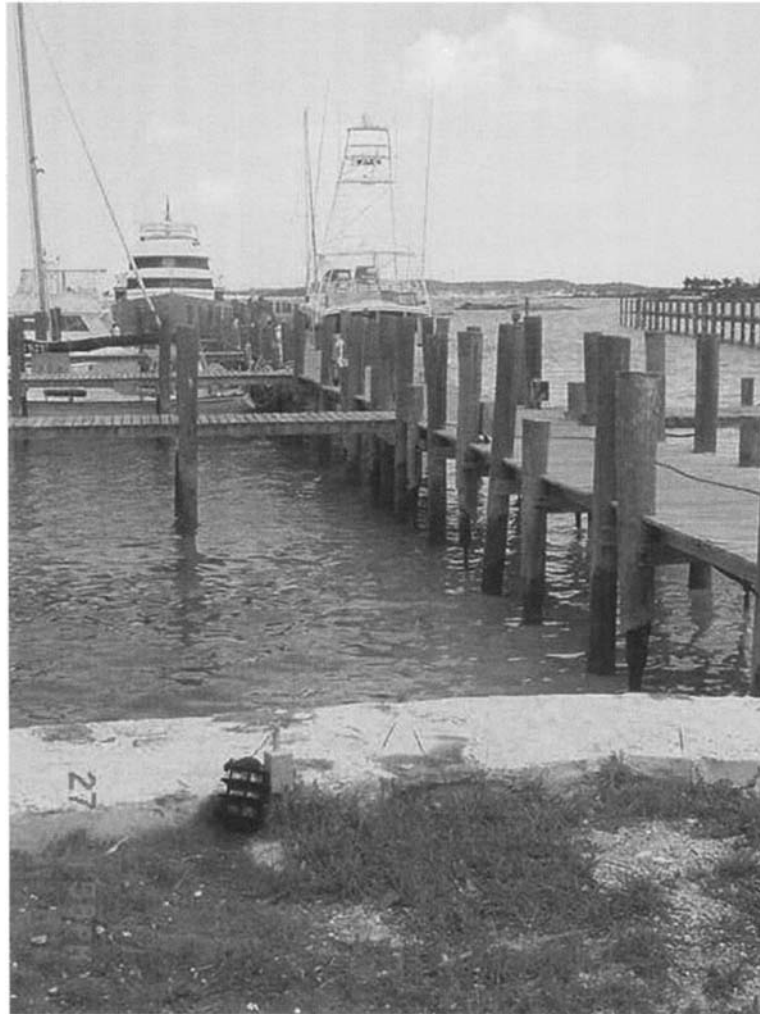
Figure 2.7.   Small timber jetty (courtesy Doug Ramsay)

2.1.3. Rubble mound causeway

Many jetties use this form of construction (see Figure 2.8) along much of their nearshore (shallow water) length, where placement of rock is an economic solution and wave conditions are limited due to shallower water and wave breaking effects. These structures will have an impact on littoral drift, by interrupting sediment transport along the coast. This may lead to erosion downdrift of the structure in regions where sediment transport is high.

OVERTOPPING LOADS

WAVE FORCES→
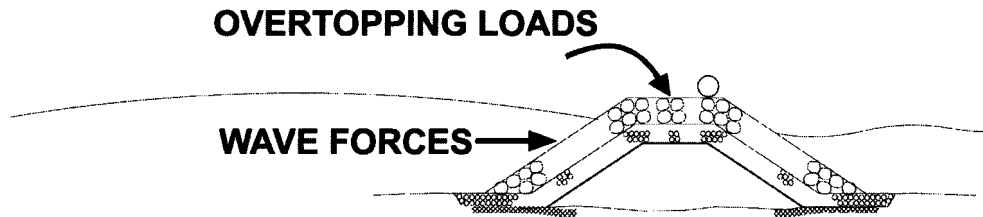
Figure 2.8.   Typical rubble mound causeway section

Design rules for these sections may be derived from design methods for rubble mound breakwaters/seawalls, see for example the *Rock Manual*, CIRIA/CUR (1991) or design guidance for rubble mounds by Burcharth (1994). No special consideration is given in this document to this jetty type.

2.1.4. Marginal jetties/quays

These structures share features of the other three structure types. Generally a piled deck used for cargo handling is constructed over a marginal slope, which is armoured, usually by rock (Figure 2.9). The vertical face is required for berthing against while the rock armour slope assists in dissipation of wave energy. The quay structure may also accommodate vessel mooring loads through fenders. The deck level for these quays is generally set much lower than for open-piled structures, often driven by the levels of surrounding paved areas and access roadways. As a result, extreme storm conditions can generate wave slam forces on structural elements, and can cause overtopping impacts onto the upper deck. Wave shoaling and run-up on the armoured slope may also generate significant uplift forces on the deck, which can cause damage of the deck, as illustrated in Figure 2.10. The detail at the top of the armoured slope is also particularly vulnerable, as wave energy can be concentrated in this location, causing armour damage.
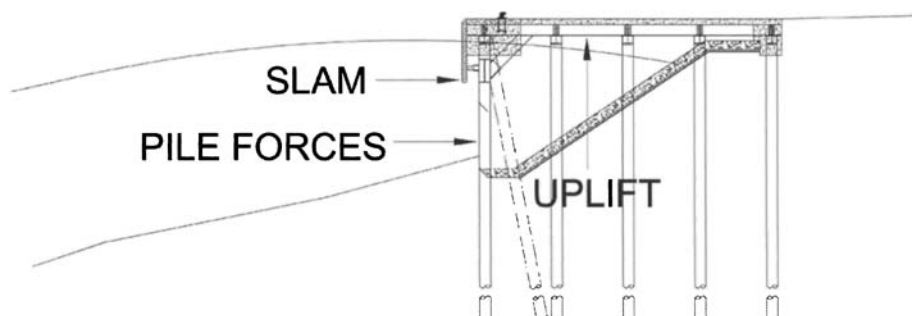
Figure 2.9.   *Typical marginal quay*

Figure 2.10.   *Failure of an exposed jetty deck caused by wave uplift forces (courtesy Han–Padron Associates)*

2.2.   TYPICAL LOCATIONS

Exposed jetties are constructed worldwide. Some structures (at their most exposed outer ends) can be remote from the land in deep water, where shallow water effects are small. Some sites or structures may still be exposed to large waves, such as marginal quays in regions subject to cyclones or hurricanes. At these sites, shallower water may allow breaking wave effects to become more significant.

Whilst exposed jetties are constructed worldwide, they tend to provide a more economical solution where dominant wave conditions are relatively calm and more severe wave conditions and storms are relatively rare and/or limited to a short period of the year (as for locations subject to monsoon conditions).

2.3. TYPICAL EXPOSURES AND THRESHOLDS

Typical operational thresholds and structure design thresholds are given in Tables 2.1 and 2.2, based on historical experience.

Table 2.1. Summary of typical operating thresholds based on historical experience*

Description	Operating condition	Typical limiting wave height, H_s (m)	Typical limiting wind speed, V (30 second) (m/s)	Loads
Good weather	Berthing and mooring and cargo operations can be carried out	Small ships 0.5 m Larger ships 1.0 m	12 m/s	Berthing loads on fenders, Line pull on hooks, alongside forces on fenders, Loading operational forces (e.g. loading arms extended)
Bad weather	Berthing not possible, if ship already moored can stay alongside – some cargo operations may be acceptable	Small ships 0.75 m Larger ships 1.5 m	15 m/s	Line pull on hooks, Alongside forces on fenders, Loading operational forces (e.g. loading arms extended)
Very bad weather	If already moored, ship can stay alongside, but cargo operations unsafe	Small ships 1.0 m Larger ships 2.0 m	20 m/s	Alongside forces on fenders, Non-loading operational forces (e.g. loading arms stowed)
Storm	Ship will have to leave berth	Design storm, e.g. 1 in 100 year or more extreme	Design storm, e.g. 1 in 100 year or more extreme	Non-loading operational forces (e.g. loading arms stowed)

* This does not necessarily infer good practice as every design should consider the appropriate operating threshold for its use and location (see also Section 3.2.2)

Table 2.2. Summary of structure design thresholds

Description	Inundation criteria	Damage criteria	Typical limiting wave return period, H_s (m)*
No inundation	Possible inundation of jetty superstructure support members but no slam under decks, no inundation of topside equipment or access areas	No damage to topsides, no damage to structure	1 in 10 years
Inundation of deck ('white-water condition')	Minimal slam under decks, limited inundation of access areas and topside equipment	Limited damage to topsides – will not significantly disrupt future operations	1 in 100 years
Survivability ('green-water condition')	Slam under decks, widespread inundation of access areas and topside equipment	Loss of topsides – only exceptionally long-lead replacement items intact. Main structure remains intact, gangways etc. lost/damaged	1 in 250 years

* The reader is referred to Section 3.2.2 for a discussion on current guidance for the selection of appropriate design conditions

3. Aspects of design

3.1. INTRODUCTION

This section discusses the key hydraulic design aspects that need to be considered for jetty structures. Hydraulic design issues are identified in Table 3.1 and summarised in Figure 3.1, with cross-references to relevant sections of the document.

Table 3.1. Location of technical guidance

Design aspect	Hydraulic design issues	Document section
Select structure design life	Encounter probability of design event	3.3
Vertical walls:	Calculate wave forces	4.3
Piled jetties:		
Deck superstructure	Is deck to be above maximum wave crest?	5.2
	Is deck in zone of wave action?	5.3
	If yes, calculate wave forces on superstructure:	
	– horizontal forces on beams and decks	5.5.3
	– vertical forces on beams and decks	5.5.2
	– impacts on beams and decks	5.5.4
Pile diameter, spacing, depth	Forces on piles:	
	– currents	3.2.5
	– waves	4.2.1
	Scour around piles:	
	– currents	7.2
	– waves	7.3
Berth and fendering design	Berthing loads	6.1
	Mooring and breasting forces	6.2
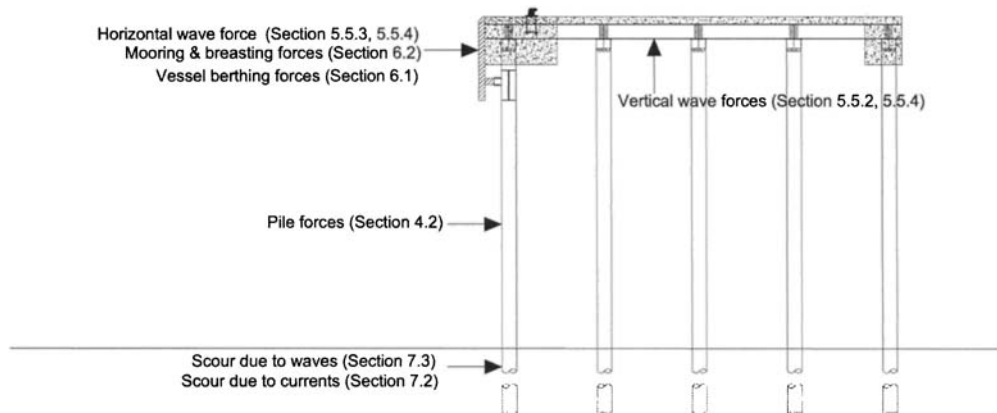
Figure 3.1.   Typical loadings and location of technical guidance

3.2.   HYDRAULIC AND RELATED LOADS

Hydraulic loadings to be considered vary significantly between different structure types. The main hydraulic design issues to be considered are summarised in the following sub-sections. Their relative importance for the various types of structure is summarised in Table 3.2.

3.2.1. Quasi-static wave loads

Quasi-static loads are slowly varying wave-induced forces, where the duration of the loading is typically of the order of 0.25 to 0.5 times the incident wave period. The magnitude of quasi-static forces is generally a function of the incident wave height.

Wave drag and inertia forces on piles

To determine wave forces for piles and related elements, Morison's equations are used with appropriate coefficients. Relatively little information is available for the particular configurations of exposed jetties, but methods to apply Morison's method for a single extreme wave are well established – see for example the *Coastal Engineering Manual*, Section VI, Burcharth and Hughes (2001). Little guidance is available for random waves, nor on phasing of loads along the length of multiple pile structures. The effects of wave obliquity, short-crestedness and reflected waves on wave loads are not well defined and the designer should consider whether detailed physical modelling or other studies are required to fully address these issues.

Table 3.2. Structure types and important design issues

	(a) Solid, vertical wall	(b) Rubble mound	(c) Open piled	(d) Marginal quay
Wave/current drag or inertia wave loads (quasi-static)	Usually design case, resisted by weight	Act on armour units, armour sizing	Frequent but moderate significance	Rare and moderate
Wave overtopping loads	Possibly important but often ignored	Important and usually predicted	Usually ignored but can be very dangerous	Usually ignored but can be very dangerous
Uplift forces	Methods available, but often ignored	Methods available and easily predicted	Seldom predicted, no reliable methods	Seldom predicted, no reliable methods
Wave slam or impact forces	New methods now available	Methods available	Not well predicted	Not well predicted
Vessel mooring loads	Moderate	Not important	Significant	Frequent and significant
Vessel impact loads	Not significant design case for the jetty	Not significant design case for the jetty	May be critical	May be important
Local bed scour	May be severe	Less than for (a), but may be significant	Only local and for limited cases	Can be an issue in estuaries due to high currents
Shoreline morphology changes	Potentially significant	Potentially significant	Usually very small	Seldom significant
Future sea level rise	Important	Important	Important	Important

Note: this list is for general guidance only. The designer should identify the issues of concern for any particular scenario, where the relative importance of various issues may differ from that identified here.

Quasi-static wave (momentum) loads on vertical walls and related elements

For vertical or composite walls, quasi-static wave loads may be estimated using methods based on Goda's equations originally developed for caisson breakwaters (see Goda (1985), CIRIA/CUR (1991), BS 6349 Pt 1). Guidance for evaluating the effects of obliquity and short-crestedness is given by Battjes (1982).

3.2.2. Wave overtopping loads

Wave overtopping induced impact loads acting downwards on decks

The loads induced on a deck by the impact of overtopping water have not been predicted by any established method. Research studies are being undertaken as part of the VOWS ('Violent Overtopping of Waves at Seawalls') project by Edinburgh, Sheffield and Manchester Metropolitan Universities which have identified example loads due to severe overtopping events, but no generic methods are known. Downwards acting inundation loads were measured in the physical model tests and are discussed in Chapter 5.

3.2.3. Wave uplift forces

Quasi-static wave pressures acting upwards on walls or other submerged elements

Quasi-static wave pressures acting upwards on submerged elements may be predicted using simple wave theories, or Goda's method originally developed for caisson breakwaters on rubble foundations (see Goda (1985), CIRIA/CUR (1991), BS 6349 Pt 1 (2000)). Vertical wave forces on the underside of decks are discussed in Chapter 5, based on the results of new model tests.

Impact or slam loads acting upwards on decks or other elements

Impact or slam loads acting upwards on the deck or other elements cannot be predicted by any generic method. Test measurements of wave impacts are reported in Chapter 5.

3.2.4. Wave slam forces

Wave impact/slam forces acting in the direction of wave travel on fenders, beams or other projecting elements

Wave impact/slam forces acting in the direction of wave travel on fenders, beams or other projecting elements can be estimated (with low reliability) using adaptations of methods by Goda (1985), Blackmore and Hewson (1984) or Müller and Walkden (1998), or by calculations using slam coefficients in Morison's equations.

3.2.5. Current forces

Loads imposed on exposed structures by tidal or fluvial currents can be classified as:

(a) drag (or in line) forces parallel to the flow direction
(b) cross flow forces, transverse to the flow direction.

Current drag forces are principally steady and the oscillatory component is only significant when its frequency approaches a natural frequency of the structure. Cross-flow forces are entirely oscillatory for bodies symmetrical to the flow. Further guidance and methods of force calculation are given in BS 6349 Part 1, BSI (2000) and Sumer and Fredsøe (1997).

3.2.6. Vessel induced loads

Vessel berthing loads on jetty

Vessel berthing forces are taken by the jetty and/or independent berthing structures, usually through fenders, as vessels come to come to rest at the berth. Structural design methods are generally based on vessel energies and on the characteristics of the fender systems. Dynamic conditions are usually simplified to static equivalent loads. These forces can be assessed using guidance given in BS 6349 Pt 4 (1994).

Vessel mooring and breasting forces

- Mooring forces are due to wind, wave and current forces pushing the vessel *off* or along berth and the load being transferred to the structure through mooring lines
- Breasting forces are due to wind, wave and current forces pushing the vessel *onto* or along berth and the load being transferred to the structure through fenders.

There are uncertainties in the load transfer from vessel to structure and modelling is often undertaken to assess loads. A series of look-up graphs are given in Chapter 6 for a typical vessel and mooring configuration.

3.2.7. Bed scour or morphological change

Lowering of sea bed at or close to pile or wall

Lowering of the sea bed at or close to piles or walls due to waves and currents can be estimated by methods suggested by Whitehouse (1998). These are described in more detail in Chapter 7. Where underkeel clearances are small, propeller and bow/stern thruster scour may be an issue. For further guidance on propeller scour, see PIANC (1997), EAU (1996) and Römisch and Hering (2002).

Interruption of coastal processes such that morphology of adjoining shoreline is altered

The impact of structures on coastal processes and shoreline morphology can be studied by flow and sediment transport modelling.

3.2.8. Future sea level rise

Consideration should be given to predictions of future changes in sea level over the lifetime of the structure. Increases in sea level will not only increase design water levels, but may result in increased design wave heights, particularly in situations where waves break due to depth-limiting effects. These effects may require jetty deck levels to be raised to provide the required performance at a later stage of the structure design life. The latest work by the Intergovernmental Panel on Climate Change (IPCC, 2001) considers a wide range of scenarios to predict a worldwide rise in mean sea level by 2050 in the range 5–32 cm, and 9–88 cm by 2100. The designer should consider local future sea level change in conjunction with future predicted changes in land elevation.

3.3. ACCEPTABLE RISK ISSUES

3.3.1. Selection of the design life

Most port structures are designed and constructed for a specific design life. The design life of a structure is taken to be its intended useful life and will depend on the purpose for which it is required. The choice of the design life is a matter to be decided in relation to each project since changes in circumstances and operational practices can make the structure redundant or in need of substantial reconstruction before the end of its physical life. The design life will also be selected based on economic factors, such as the cost of replacement, cost of downtime and availability of other berths during the repair.

For example, a wave height with a return period of 50 years has an annual likelihood of occurring or being exceeded of 0.02 or 2%.

For design events, the return period should be significantly longer than the design life. It is important to emphasise here that due to the stochastic nature of wave conditions and water levels there is still a risk that the design event will be exceeded during the design life. This likelihood of exceedance of the design event during the design life of the structure is termed the encounter probability. As the return period of the design event increases, the encounter probability decreases.

3.3.2. Design event return period

Structures are usually designed to withstand a specific hydraulic design event (or a number of extreme events of different severity). Each such event will probably be a combination of a wave condition and water level, and will have an associated return period, T_R, which indicates the annual likelihood of the design event being exceeded.

Guidance is given in BS 6349 Part 1, BSI (2000), on determining the encounter probability of an event of duration T_R. The encounter probability, p, of an event of a return period, T_R, during the design life, N, can be calculated:

$$p = 1-(1-1/T_R)^N \qquad\qquad (3.1)$$

This function is plotted in BS 6349 Part 7, BSI (1991) (see Figure 3.2).

For example, for an oil terminal with a design life of 25 years and a design event with a 1 in 100 year return period, the probability of that event occurring during the life of the structure is just under 25%.
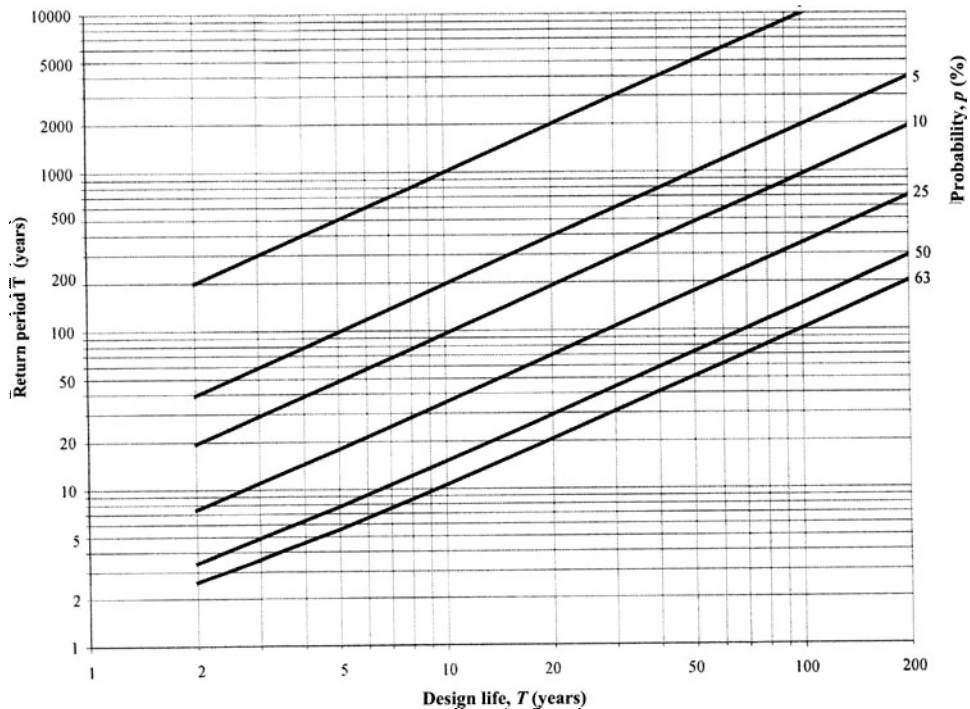
Figure 3.2.   *Encounter probability (after* BS 6349, *Part 7 (1991))*

For structures exposed to loads on a frequent basis, e.g. breakwaters, it is normally not economical or even feasible to design a structure to fully resist such loads with no damage, so the designer should identify a suitable level of risk of exceedance and design the structure for an event with the corresponding return period. For example, for a breakwater with a design life of 50 years, the 1000 year

event has a 5% probability of exceedance. If the structure were to be designed for the return period equal to the design life, then this would have a 63% chance of exceedance. Selection of an appropriate design condition should also be based on an assessment of the consequences of exceedance as this may not always be catastrophic. This forms the basis of risk-based design by evaluating the frequency of occurrence of a certain event against the consequences.

It is the designer's responsibility to define, in discussion with the eventual owner and operator, the acceptable risk for the structure. In general, it can be seen that the return period of the design condition will exceed the given period over which costs are to be optimised.

Structures designed to withstand large events may be more expensive to construct than weaker structures for which the cost of periodical repair has been included. By optimising whole life costs, including downtime, against benefits, it may be possible to establish an acceptable level of risk.

This type of cost optimisation is, however, difficult to achieve in jetty structures, as the degree of damage is difficult to predict, and the consequences of subjecting the jetty deck to unanticipated wave loads may be much more severe than for other classes of structure. In this case, probabilistic simulations may be needed to address the 'air gap' problem (see Section 4.5.2).

Definition of design conditions becomes more complicated when two or more variables (e.g. wave height and water level) need to be considered. In this case, the return period represents the likelihood that both (or all) variables are exceeded at the same time. Some simple guidance on establishing joint probabilities is given in CIRIA (1996). However, specialist studies may be required to establish this joint probability.

3.4. APPROACHES TO DESIGN

3.4.1. Deterministic design

Traditionally, deterministic methods have been adopted for design. An accepted level of loading, termed the Limit State condition, will be determined for the structure. This limit state will correspond to a particular strength of the structure. This may be the Serviceability Limit State (SLS) or the Ultimate Limit State (ULS). Exceedance of the SLS indicates that the structure is not meeting the required performance. Exceedance of the ULS may result in damage to, or failure of, the structure.

It may not be economical to design a structure to resist the most extreme loads. In practice, an acceptable probability of exceedance of the Limit State will be decided upon, by balancing the likelihood of exceedance and consequences of failure. This is the essence of risk-based design. Consequences are usually quantified in monetary terms. However, there are often less tangible consequences that cannot be easily quantified in monetary terms, such as the loss of human life or natural habitats.

An acceptable annual probability of exceedance of the design loading will be determined. The reciprocal of this exceedance probability is the return period, T_R, of

the design event. The design loading for this return period can then be determined from a statistical analysis. Uncertainties in the loading and strength are accounted for by a safety factor, which should always be greater than 1.

The loading is a function of a number of variables. These variables are often stochastic in nature. It is important to note that deterministic methods can be described as being partially probabilistic and risk-based as they are based on design loading at a selected return period, T_R, where the return period is a statistical entity.

A limitation of deterministic methods is that no account is made of loading on the structure other than at a single design level. Other loading cases will have a range of effects on the structure, but will not be identified, nor will their contributions to the overall chance of failure. Events exceeding the design load will obviously affect the structure, but loading below the Limit State can have a cumulative effect on the structure, contributing to structural failure over time.

3.4.2. Probabilistic design

The alternative to the use of simple deterministic methods is to use probabilistic methods. These extend the deterministic approach by using statistical methods to describe the stochastic nature of strength and load instead of applying a safety factor. There are various different types of probabilistic methods each with varying degrees of complexity.

The basic principle of full probabilistic methods is that the distributions of strength and loading are considered instead of single design values, to account for uncertainty and variability in these parameters. This method avoids unnecessary conservatism and can lead to savings in comparison with designs based on deterministic methods.

Generally the methods used in this manual are strongly deterministic, as interactions between elements and failure modes are important but not quantified, and there are very few statistical data available on the uncertainties in loading. Some discussion is given where appropriate on probabilistic methods.

3.4.3. Sensitivity testing

Often uncertainties in the design process can be partially examined using deterministic methods by undertaking sensitivity testing, varying input parameters to assess the impact on response. This might include looking at a range of combinations of wave height and water level with the same joint probability (probability of exceedance of a certain wave height and water level combination).

3.4.4. Input parameters

While deterministic design methods are most common, the input parameters used are often stochastic in nature, with associated probabilities of exceedance, e.g. sea state parameters such as wave height, wave period and water level.

3.5.   DETERMINING DESIGN WAVE CONDITIONS

3.5.1. Prediction of extreme waves

Central to the design process is a need to firstly establish the extreme events for a particular return period and include environmental parameters such as winds, waves, tides and surges, before determining the forces acting on the structure.

Real ocean waves undergo considerable variation as they enter transitional and shallow water. The main processes are:

- wave shoaling
- wave refraction due to the seabed and current
- depth-induced breaking due to bottom friction
- wave reflection, especially where the waves encounter a steep bed slope
- diffraction around structures and shoreline features such as headlands.

Waves approaching a structure such as a long jetty, in transitional water depths (where $1/2 < h/L_p < 1/20$), may be modified by shoaling and refraction processes. Breaking, bottom-friction and reflection are phenomena linked to shallower water.

Figure 3.3.   Wave breaking in calm conditions (checks should be made to assess whether under extreme conditions waves could break onto the deck section)

3.5.2. Wave shoaling and refraction processes

Wave celerity is defined as the speed of propagation of a wave. A variation in celerity implies a consequent variation in wavelength. A wave approaching a sloping sea bed at an angle is characterised by crest velocity variation – the deeper water part of the wave moves faster than the rest. This causes the wave crest to 'bend' towards alignment with the contour. This phenomenon is called refraction and depends on the relationship between wavelength and water depth. This kind of refraction is caused by seabed changes. However, waves may also be refracted by currents, this latter phenomenon being important in the case of tidal entrances or in areas with major ocean currents. All general methods for refraction analysis are based on Snell's law:

$$c_0/c = \sin \alpha_0 / \sin \alpha \tag{3.2}$$

where α and α_0 represent the angle between wave crest and contour line for celerities c and c_0. The subscript zero refers to deep water conditions.

By considering wave energy (for details see Vincent *et al* (2002)), the following relationship can be derived:

$$\frac{H}{H_0} = \sqrt{\frac{1}{2} \cdot \frac{1}{n} \cdot \frac{c_0}{c} \cdot \frac{B_0}{B}} \tag{3.3}$$

where B_0 and B represent the spacing between the orthogonals to the wave fronts, respectively for celerities c_0 and c.

$$n = \left[1 + \frac{\dfrac{4\pi h}{L}}{\sinh \dfrac{4\pi h}{L}} \right] \cdot$$

The above equation can be rewritten as:

$$\frac{H}{H_0} = K_s \cdot K_r \tag{3.4}$$

where

$$K_s = \sqrt{\frac{1}{2} \cdot \frac{1}{n} \cdot \frac{c_0}{c}} \quad \text{(shoaling coefficient)} \tag{3.5}$$

$$K_r = \sqrt{\frac{B_0}{B}} \quad \text{(refraction coefficient)}. \tag{3.6}$$

K_s and K_r are tabulated or may be derived from diagrams given in the *Shore Protection Manual* (CERC, 1984) or the more recent *Coastal Engineering Manual* (USACE, 2002).

A wide range of numerical models are available that take into account the phenomena that influence wave transformation from deep to transitional and shallower water.

3.5.3. Wave theories

Water-wave phenomena are very complex and difficult to describe mathematically because of non-linearities, three-dimensional characteristics and apparent random behaviour. There are several wave theories used to describe surface and water particle motion, and generate theories used in describing wave transformation due to interaction with the bottom and with structures.

For the greater part of last century wave theories have been used to classify finite amplitude waves such as Airy's theory, solitary wave theory, Stokes wave theory and cnoidal wave theory. For shallow water, a cnoidal wave theory often provides an acceptable approximation of simple waves. For very shallow water near the breaker zone, solitary wave theory satisfactorily predicts certain features of the wave behaviour.

Airy (linear) theory is easy to apply, giving a first approximation of a complete theoretical description of wave behaviour, as given in the following equations:

Wavelength:

$$L = cT \tag{3.7}$$

Water surface elevation:

$$\eta(x,t) = \frac{H}{2}\cos(kx - \omega t) \tag{3.8}$$

Horizontal particle velocity:

$$u = \frac{H}{2}\frac{gT}{L}\frac{\cosh[2\pi(z+h)/L]}{\cosh[2\pi h/L]}\cos(kx - \omega t) \tag{3.9}$$

Vertical particle velocity:

$$v = \frac{H}{2}\frac{gT}{L}\frac{\sinh[2\pi(z+h)/L]}{\cosh[2\pi h/L]}\sin(kx - \omega t) \tag{3.10}$$

Horizontal particle acceleration:

$$a_x = \frac{g\pi H}{L}\frac{\cosh[2\pi(z+h)/L]}{\cosh[2\pi h/L]}\sin(kx - \omega t) \tag{3.11}$$

Vertical particle acceleration:

$$a_y = -\frac{g\pi H}{L}\frac{\sinh[2\pi(z+h)/L]}{\cosh[2\pi h/L]}\cos(kx - \omega t) \tag{3.12}$$

Linear wave theory is based on the assumption that waves are small in amplitude. Ocean waves and waves in exposed locations are generally not small in amplitude and engineering design usually requires that the largest, extreme, waves be considered. In order to define these waves more accurately, higher order theories may need to be used. The reader is referred to Demirbilek *et al* (2002) for a comprehensive discussion on wave theories. The ranges of applicability for different wave theories are shown in Figure 3.4. By calculating the parameters h/gT^2 and H/gT^2, Figure 3.4 can be used to identify the most appropriate wave theory for the conditions of interest.
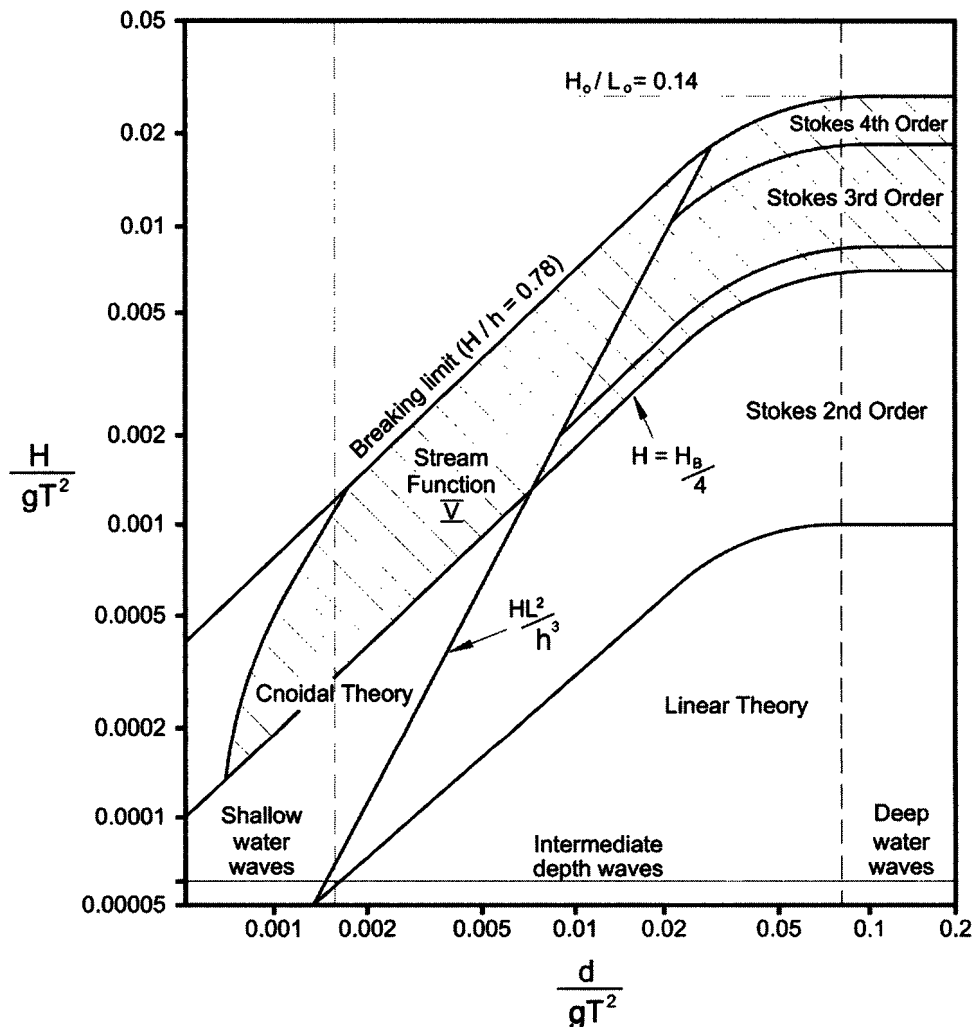
Figure 3.4. *Ranges of applicability of wave theories from Le Mehauté (1976). (As published in USACE (2002))*

30

A number of software packages are available which may be used for such calculations, such as the ACES (Automated Coastal Engineering System) package developed by the Coastal Engineering Research Center (CERC) of the US Army Corps of Engineers (USACE). This package includes linear wave theory, cnoidal wave theory or Fourier series wave theory applications, which may be used to predict water surface elevations.

Detailed studies to derive design wave conditions and to optimise layout may be undertaken using area wave models to represent the wave transformation processes of shoaling, refraction and bed friction. More sophisticated wave models, based on the Boussinesq equations, can also represent wave breaking.

4. Wave forces on vertical elements

4.1. INTRODUCTION

This chapter discusses wave forces on vertical elements of jetty structures. These include piles and vertical faces, such as solid jetty heads or quays. Guidance on these aspects is widely available in literature and design standards. This chapter therefore refers the reader to key sources of existing information.

4.2. WAVE FORCES ON PILES

Piled structures can be classified into two categories:

- small diameter circular structures (diameter/wavelength < 0.2)
- large diameter circular structures (diameter/wavelength > 0.2).

Small diameter piles or cylinders are defined as elements whose presence does not strongly disturb the incident wave field. The usual criterion is that the diameter to wavelength ratio (D/L) should be less than 0.2 otherwise diffraction effects become important.

4.2.1. Small diameter circular structures

For circular or small dimension pile structures (wholly or semi-immersed), design guidelines such as BS 6349 Pt 1 (2000), EAU (1996) and the *Coastal Engineering Manual* (USACE, 2002), refer to Morison's equation for calculations of forces due to non-breaking waves. EAU (1996) suggests a method for wave loads due to breaking waves while the *Coastal Engineering Manual* suggests a method quite similar to the method outlined below but with different values for coefficients. See Burcharth and Hughes (2001).

The method was derived based on the assumption that waves are regular and non-breaking. For a slender, surface-piercing vertical cylinder, subject to a long

crested regular wave, the horizontal force per unit length of the cylinder or pile is given by Morison's equation:

$$F = C_{d}\left(\frac{\rho}{2}\right)Au|u| + C_{m}\rho V\frac{du}{dt} \tag{4.1}$$

where F is the force on pile per metre length in the direction of wave travel at the depth in question, ρ is the density of water, u is the horizontal component of water particle velocity, A is the projected area (m) [for a circular cylinder of diameter D, $A = D$] (m^2/m run of cylinder or pile), V is the displaced volume per unit length. $V = \pi D^2/4$ (m^3/m), C_d is the Morison drag coefficient (proportional to u^2), and C_m is the Morison inertia (mass) coefficient (function of horizontal acceleration, du/dt).

The total force acting on the whole length pile or cylinder should be calculated by integrating the force over the whole of the wetted length.
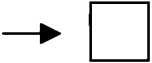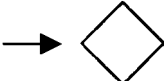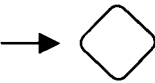
The equation can be more simply described as follows:

F = drag component + inertia component.

The total force is calculated taking account of the phase difference between the drag and inertia components. At the time of occurrence of the maximum drag force (the time of occurrence of the maximum velocity at the wave crest), the inertial term will be zero or near zero (acceleration is zero or near zero at the wave crest). The maximum inertia force occurs at the time of maximum acceleration, when the water surface elevation is at (or close to) the static sea level for the conditions being considered. To identify the maximum combined drag and inertia force the force must be calculated for various time increments during the passage of the wave train.

In order to derive the wave input parameters (velocities and accelerations), it will be necessary to use the appropriate wave theory – see Section 3.4.3. Drag and inertia coefficients C_d and C_m can be derived from graphs given in Burcharth and Hughes (2001) or from BS 6349 Pt 1 (2000). Typical values are summarised in Table 4.1 for various geometries.

Table 4.1.   Drag and inertia coefficients for various pile geometries

Cross-section	Drag coefficient, C_d		Inertia coefficient, C_m
Circular[*]:	Smooth pile	Rough pile	
Det Norske Veritas (1991) for waves	0.7 minimum	1.1 minimum	
American Petroleum Institute (1993) for waves	0.65	1.05	
Nath (1984) for steady flow (high Re)	0.7	1.05	
Offshore test structure data (Sarpkaya and Cakal, 1983) For waves, smooth and rough pile results combined	0.6 to 2.5 median approx. 1.3		2.0[**]
Sarpkaya and Storm (1985) combined waves and current (KC = 60)	0.9	1.5	
Sarpkaya (1986) (KC = 40) review of a wide range of data	0.7	1.2 to 1.4	
Square[**] Direction to flow/waves → □	2.0		2.5
→ ◇	1.6		2.2
Square with rounded corners[**] Direction to flow/waves → ▢	0.6		2.5
→ ◇	0.5		2.5

[*] Information for circular cross-sections extracted from Pos (1991) with relevant updates
[**] Source: BS 6349 Pt 1 (2000)
KC = Keulegan–Carpenter number = UT/D

Figure 4.1.   Fender panel on an exposed jetty – even when the main structural elements are slender and attract relatively little hydraulic load, additional elements such as fender panels can attract more significant load (courtesy Kier)

BS 6349 Part 1 (2000) defines a drag force term (similarly described as above) for uniform prismatic structural members immersed in an uniform current which acts at the centroid of the area normal to the flow and which is given by:

$$F_d = C_d \left(\frac{\rho}{2} \right) A_n u^2 \qquad\qquad (4.2)$$

where F_d is the total drag force acting on pile, u is the incident current velocity, C_d is the dimensionless time-averaged drag force coefficient, and A_n is the area normal to flow in square metres (m^2).

In addition to drag and inertia forces acting on piles, transverse (sometimes called lift) forces may occur. These are caused by vortex or eddy shedding downstream of the pile. Transverse forces act perpendicular to the wave direction and the pile axis. Lift forces depend on the dynamic characteristics of the structure and studies have shown that where dynamic coupling of waves and structure occurs, lift forces can be significantly greater than drag forces. Burcharth and Hughes (2001) quote studies that suggest that for rigid piles the assumption that the transverse force is equal to the drag force will provide a reasonable upper limit.

4.2.2. Large diameter circular structures

Diffraction effects become important when the ratio of the structure diameter to wavelength D/L exceeds 0.2. The theory is based on irrotational flow such that a velocity potential can describe the incident and diffracted wave fields. This is widely applied to concrete or masonry gravity structures and to ship forms or other floating systems with large D/L ratios. BS 6349 Pt 1 (2000) briefly notes the diffraction effects for large circular structures, but suggests referring to other standards for guidance. For fuller discussion on diffraction theory the reader is referred to Tickell (1994) for further references.

4.3. WAVE FORCES ON VERTICAL WALLS

Methods available to describe horizontal non-breaking and breaking wave forces on vertical walls are mainly from the field of breakwater/sea wall engineering.

Solid vertical faced jetties might be constructed from caissons or sheet-piles. Design guidance is given in BS 6349 Pt 7 (1991), EAU (1996) and the USACE (2002) for predicting wave loads on vertical walls. It has been appreciated for many years that similar wave conditions may give rise to dramatically different wave pressures or forces depending on the form of the wave breaking at or close to the wall. Thus the theory used depends on whether the walls are subject to non-breaking (or pulsating), impulsive breaking (impact) or broken wave action.

4.3.1. Non-breaking (pulsating) wave forces

This is the simplest case as the wave motion is relatively smooth. A train of non-breaking waves approaching a vertical wall perpendicularly will be reflected to some degree and form a standing wave pattern.

Methods to calculate wave forces for simple vertical wall structures and pulsating wave conditions are relatively well established. The methods are presented in several standards such as CIRIA/CUR (1991) and BS 6349 Pt 7 (1991) and are not reproduced here.

The main methods used in design manuals to estimate pulsating wave forces on upright walls, breakwaters or sea walls have been derived by numerous authors. These include Hiroi (1919), Ito (1971) and Goda (1974, 1985) for simple vertical walls and composite walls, comprising a vertical face above a rubble toe, and Sainflou (1928) for simple walls in deep water (all the standards refer to this method). Goda's method is the most widely used prediction method for wave forces on vertical walls, although it is used for both non-breaking and breaking waves. The *Shore Protection Manual*, (CERC, 1984) used the Miche–Rundgren formulae to derive the height of the clapotis (a complete standing wave) from which linear hydrostatic pressure can be calculated for shorter non-breaking waves. For waves of low steepness, the *Shore Protection Manual* and the more up to date *Coastal Engineering Manual* (USACE, 2002) recommend Sainflou's method.

4.3.2. Breaking (impact) wave forces

Where waves break at the vertical face of a structure, the resulting impact forces can be substantially more intense than non-breaking wave loads. On most structures, wave impact forces occur infrequently and do not constitute a design condition. For some structures, however, wave impact loads may occur sufficiently frequently and with significant intensity that they need to be considered in the design process. The largest pressures experienced by vertical walls will often result from the direct impact of breaking waves onto the wall. The duration of the impact pressure is very short and its magnitude is highly sensitive to the geometry of the wave front and wall, the deepwater steepness of the incident waves, the beach slope and the degree of air entrainment in the water. For example, the waves may shoal up over a submerged mound or steep approach slope, then form a plunging breaker just seaward of the wall. A major part of the wave momentum is then conveyed to the wall over a very small fraction of the wave period.

Minikin's method (1950, 1963) was developed in the early 1950s to estimate local wave impact pressures caused by a wave breaking directly onto a vertical breakwater or sea wall therefore adequately addressing the problem of impact pressures (see Allsop, 2000). The now superseded *Shore Protection Manual* (CERC, 1984) gave a conservative approach to determining the impact forces using Minikin's method for the estimation of forces and overturning moments arising from an assumed pressure distribution. Minikin's method is not included in the latest edition, (USACE, 2002). There have been other studies carried out like those of Kirkgoz (1982, 1990, 1995) but the general consensus is that conflicts remain in accurately estimating the breaking wave pressure distributions for realistic conditions. The main problems are in identifying the magnitudes and durations (both are needed) of wave impact loads and then applying those loads using dynamic response characteristics of the structure to derive effective loads.

4.3.3. Broken wave forces

For vertical walled structures where waves are depth-limited, wave breaking may significantly reduce waves under largest storms before they reach the structure. These broken waves may reform, but are generally well aerated and much less likely to be transformed into the well-shaped breakers that lead to wave impacts, instead tending to produce a bore of water. Wave forces under broken waves are therefore much lower than impact loads, and may indeed be lower than pulsating loads. Unlike the two previous cases, the same volume of data or theoretical studies for this case is not available.

Guidance given in USACE (2002) suggests a simple procedure, which depends on whether the wall is seaward or shoreward of the water line, but emphasises that it is an approximation since the assumed behaviour is simplified. Guidance in EAU (1996) suggests a method to solve this problem, whilst a method to estimate an average wave pressure from broken wave loads has been developed by Blackmore and Hewson (1984):

$$P_{imax} = \lambda \rho T_p C_b{}^2 \tag{4.3}$$

where λ is an aeration constant, ρ is the water density, T_p is the wave spectral peak period, and C_b is the velocity of the breaker at the wall $= (gd)^{1/2}$.

These methods may be used to make an initial estimate of the horizontal wave force under broken waves, $F_{h,broken}$ to be applied only if $F_{h,broken} < F_{h,Goda}$:

$$F_{h,broken} = h_f P_{imax} \tag{4.4}$$

where h_f is the exposed height of wall over which wave pressures act.

4.3.4. Seaward or negative forces

While most design methods have concentrated on forces that act landward (positive forces), it has been shown that some breakwaters have failed by sliding or rotation seawards, indicating that net seaward or negative forces under a wave trough may indeed be greater than positive wave forces (Allsop, 2000). For the case of jetty or quay structures, consideration will need to be given to the loads acting on the landward side of the structure that may contribute to such a failure mode. Contributing loads may be earth pressures for structures on the coastline or static water level where the structure is surrounded by water.

A review of the literature in McConnell *et al* (1999) identified two prediction methods by Sainflou (1928) and Goda (1985). Both theories are generally based on (relatively) deep-water conditions and non-breaking or pulsating waves. The methods were compared with experimental measurements, which demonstrated that Sainflou's prediction gave relatively good agreement for a certain region of wave height to water depth ratio, H_{si}/d ($0.2 < H_{si}/d < 0.5$) but that it underpredicted in other regions (for $H_{si}/d < 0.2$ and $H_{si}/d > 0.5$). Goda's method generally underpredicted the measurements. Since Sainflou's predictions were closer to the test measurements, this method was modified to improve agreement with the measurements. The modified prediction method calculated $F_{h,min}$ derived from Sainflou's formula, which is then multiplied by a factor which is dependent on whether a probabilistic or deterministic approach is adopted.

Probabilistic approach:

$$F_{h,min} = 1.126 \, F_{Sainflou} \pm 13\% \tag{4.5}$$

Deterministic approach:

$$F_{h,min} = 1.27 \, F_{Sainflou} \tag{4.6}$$

5. Wave forces on horizontal elements

5.1. INTRODUCTION

This chapter concentrates on wave forces on horizontal jetty elements such as decks, beams and the associated superstructure components. Some of the methods discussed here derive from the offshore industry, but most of this chapter describes methods developed within the project to produce these guidelines. As well as bringing together existing information, this chapter provides new guidance on wave forces on deck elements that has been developed from specific physical model studies undertaken as part of the project to develop this guideline document (see Allsop and Cuomo, 2004).

There are two fundamental approaches to designing piled jetty structures in exposed locations with respect to wave forces on the deck:

- Lift the deck structure above the water surface and thereby only design for minimum wave loading imposed on the piles, termed the 'air-gap' approach
- Design the deck to withstand the imposed wave forces. See the example of a jack-up platform with the deck in the zone of wave action (Figure 5.1) and a timber jetty damaged by wave loads in Figure 5.2.

Clearly there is a considerable increase in load arising as a result of the extinction of the air gap between the water surface and the underside of the jetty deck. Hence, when designing a jetty according to the air gap approach, it is important to ensure the presence of an air gap even under extreme conditions, to prevent a sudden increase in loading on the structure, which may result in significant damage and may potentially lead to failure.

Reliable models for determining air gap exceedance and wave forces are therefore required for design. A discussion of the air gap approach is given in Section 5.2 from methods adopted in the offshore industry. A method for estimating the maximum free surface elevation from wave height distributions and hence the probability of extinction of the air gap and occurrence of wave forces on the deck is given in Section 5.3.

Figure 5.1. Wave loads on walking jack-up platform (courtesy Seacore Ltd)

Figure 5.2. Timber jetty damaged due to wave slam underneath deck (courtesy Doug Ramsay)

A review of available design guidance for wave forces on decks is given in Section 5.4. Results of new tests are the presented in Section 5.5, based on studies undertaken to support the development of this document.

In general, existing offshore guidelines/standards indicate that structures cannot survive wave loads that occur when the wave crest is higher than the deck elevation. There have been instances where some offshore platforms have experienced significant loadings on their lower decks during hurricanes and have survived whilst others have failed:

'Experience in the field with platforms subjected to hurricane loading indicates that in some cases, platforms can experience significant (2–3 m) inundation without failures or extensive damage to the supporting structures.' (Bea et al, 1999)

This inconsistency in performance leads to a problem with the amount of importance and detail that is attached to the consideration of these types of loadings in the design of platforms and similar structures such as jetties. This problem is further compounded by case studies, which have shown that the main causes of failure for these types of platform in the past have been wave-in-deck loads and unexpectedly high crest heights. Thus wave loading on decks becomes a significant issue to consider in the design of structures such as jetties and piers. This may include the calculation of local and global loads that are generated by wave impacts on the deck and the verification of the structure's ability to withstand these forces for which it may not originally have been designed.

Consequently, central to the design process is a need to firstly establish the extreme events for a particular return period and to include environmental parameters such as winds, waves, tides and surges, before determining the forces acting on the structure. Following this, there needs to be a rational approach for determining the air gap, and an assessment of wave-in-deck loads if the air gap is exceeded as part of an overall structural assessment for installations.

5.2. 'AIR GAP' APPROACH

5.2.1. Background

As has already been discussed, much previous work on wave forces on decks has been carried out by the offshore industry. Their work has often been more concerned with assessing the relative magnitude of this hazard rather than seeking a full quantification. However, it is recognised that the methods cited here can be expanded to cover the subject area of exposed jetties and piers.

Waves entering the deck of an offshore structure will develop significant loads. It is common practice to attempt to set the deck above reasonably foreseeable wave conditions, although this is not always possible due to operational constraints. Factors to be taken into account when setting the deck level to include an air gap are: the occurrence of more extreme waves than originally estimated for design purposes; estimates of tides and storm surges; estimates of foundation subsidence; and the interaction of large waves with structural components.

The use of a sufficient deck clearance is a tried and tested method within the offshore industry, and is known as the 'air gap' approach. It is an encouraged method used to prevent wave impacts on decks, since wave impacts may effectively determine the reliability of the sub-structure. This has been well demonstrated by case studies of installations in the Gulf of Mexico and the North Sea (Bea *et al*, 1999). If there is insufficient clearance, the incident wave crest elevation exceeds the height location of the platform deck, leading to direct contact between the wave crest and the underside of the deck, termed 'air gap exceedance' or 'air gap extinction'. This will impose loads on the structure not accounted for in the original calculations, as well as impacting on operations and equipment. It is estimated that even a small exceedance of the air gap can generate a significant load, thereby having a major influence on risk and reliability.

Clearly there are differences between the offshore scenario and coastal jetties. While it may be desirable to design the jetty superstructure such that it is sufficiently clear of the maximum extreme wave and water levels, in practice constraints such as vessel dimensions and loading/offloading activities mean that the deck has to be constructed much closer to the water surface. In addition, there will be cost implications to consider. It will be necessary to balance the cost of constructing a higher jetty against the cost of designing elements of the superstructure to resist wave forces, or the cost of maintenance requirements following storm damage. In the case of berthing and mooring dolphins, deck levels are often constrained by vessel dimensions, meaning that these cannot be designed with an air gap. Typical projects where the deck level was set above the maximum wave crest elevation are described in Boxes 5.1 and 5.2.

Figure 5.3.   A small island jetty. Providing sufficient air gap may not be possible when the level of the quay must be low enough to accommodate smaller vessels (courtesy Doug Ramsay)

Box 5.1. Dabhol LNG Facility – Marine Works
(Courtesy Besix–Kier)

Figure 5.4.   Dabhol jetty head (courtesy Besix–Kier)

The marine works at Dabhol (Figure 5.4) were designed to discharge LNG from tankers to the LNG Fuel Jetty Facilities.

The project included a 2300 m long breakwater to provide shelter at the berth, which consisted of:

- Jetty head (with marine unloading arms)
- Four independent berthing dolphins
- Four independent mooring dolphins
- 1.89 km long approachway (1.62 km offshore and 0.270 km onshore) consisting of a 5 m wide pipe track and 5 m wide access road.

The approachway was a composite beam/slab construction with 1.5 m deep prestressed concrete beams and a deck consisting of 130 mm in-situ concrete cast on 180 mm thick precast planks. The jetty head and dolphins were solid reinforced concrete, with the jetty head section being 600 mm thick in-situ concrete cast on 400 mm thick pre-cast planks. All the structures were supported on 762 mm diameter vertical and raking steel piles.

The design is the Contractor's alternative proposal to the conforming design, which included increasing the approachway spans from 20 m to 30 m.

Box continues

Box 5.1. Dabhol LNG Facility – Marine Works (continued)

Deck height

The design condition for the extreme 1:100 year case was H_s = 8 m, T_p = 16 s, T_z = 12 s, water level = +4.1 m CD. The breakwater was designed to reduce the wave height at the jetty head in the operating condition, but as the breakwater would be incomplete during jetty construction the entire jetty was designed for the 100-year storm condition. This resulted in the jetty head and approachway being raised by 4 m to provide 1 m air gap above the crest of the 100-year extreme wave. The berthing and mooring dolphins can become fully submerged during a 100-year storm and were strengthened accordingly.

Box 5.2. Fertiliser jetty, Gulf of Aqaba
(courtesy Mott MacDonald and C J Associates)

The fertiliser jetty at Aqaba (Figure 5.5) is located approx. 20 miles from the Gulf of Aqaba. The jetty was built in 1978–80.
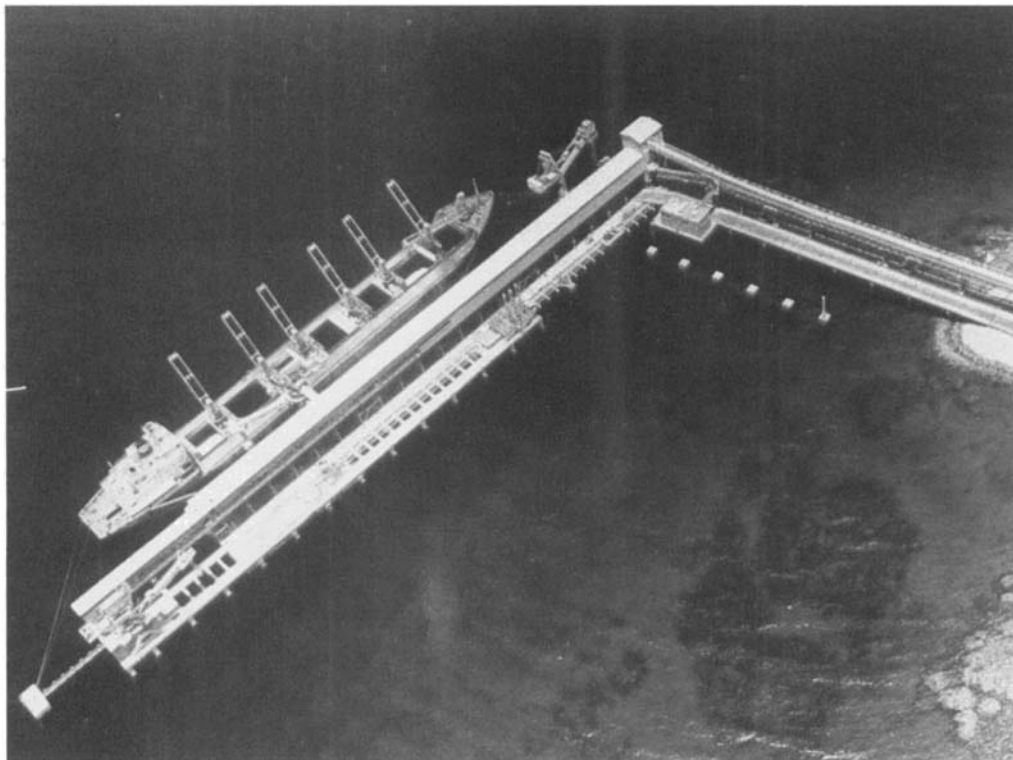

Figure 5.5.   Aqaba jetty – aerial view (courtesy Mott MacDonald and C J Associates)

Box continues

Box 5.2. Fertiliser jetty, Gulf of Aqaba (continued)

Key levels for the jetty are:

MHWS	+1.1 m CD
Seabed at jetty head	-14 m to -18 m CD
Jetty head, deck	+5.6 m CD
Jetty approach road abutment	+5.6 m CD behind jetty head sloping up to +6.55 m CD at

At concept design stage the jetty deck was at +4.75 m CD but during tender design it was raised to +5.6 m CD to allow sufficient clearance between extreme storm wave crests and the underside of the deck slab.

The deck for the Aqaba port expansion (1976–79) had to be kept at a lower level to match the existing berths and to cater for small general cargo vessels.

The structure is constructed on tubular steel piles, 762 mm and 914 mm diameter. Recent inspection has confirmed that the concrete of the fertiliser jetty deck is in good condition.

Figure 5.6. *Aqaba jetty – bulk loading equipment being erected (courtesy Mott MacDonald and C J Associates)*

5.2.2. Selection of air gap

Traditionally designs have been based on API Guidelines (API, 2000), using an historical value of air gap of 1.5 m. However, it is now accepted that this 1.5 m air gap ('safety margin') provides an inconsistent safety margin. This has largely arisen

because the same safety margin has been adapted for different environments despite the varying degree of exposure of the different locations (Smith *et al*, 1999).

In 1996, new regulations (HMSO, 1996) came into force in the UK but did not recommend a particular approach to determining the air gap, nor did they provide extreme environmental parameters for use in the determination of the air gap. Instead it placed the onus on the duty holder to demonstrate that the installation as a whole satisfies the requirement of the regulations. Thus air gap methods were still allowed and preferred for control of the extreme weather hazard. On the other hand, the US/API Recommended Practice retains the historical control that *'the bottom of the lowest deck should be located at an elevation which will clear the calculated crest of the design wave with adequate allowance for safety'*. As the design wave is typically the 1 in 100 year (10^{-2}) wave, the safety level is thus approx. 10^{-2}. In the USA this high failure probability is counteracted with a further risk reduction measure associated with de-manning in the face of storms.

Smith *et al* (1999) examined other approaches in addition to those mentioned above, such as the Norwegian Petroleum Directorate's Offshore Regulations (1994) and the International Organisation for Standardization (ISO) Fixed Steel Structures Standards (draft, 1999). They found that the Norwegian regulations set a more rational requirement regarding the air gap for more uniform platform reliabilities to be achieved. In addition to this, the Norwegian standard was the only one that gave explicit requirements to ensure that the air gap exceedance would not result in major structural damage at a specified high return period (i.e. 10 000 years). Thus the different methods available have led to variations in the air gap exceedance probability, the exact value of which depends on factors such as water depth, fetch, wind and wave climate and tide and surge distributions.

A study was undertaken to estimate the return period associated with the exceedance of an air gap (Smith *et al* 1999). The study used a joint probabilities extreme surface elevation model (developed by Tawn *et al* (1995), see Smith *et al* (1999)) and data for three main UK North Sea locations. The sensitivity of the return period to the location of the installation and the approach taken in estimating the extreme surface elevation were considered.

The study assumed that the air gap for each of the sites had been derived on the basis of the minimum requirements from the pre-1996 UK regulations. Site specific data were used to derive the extreme values. The values of extreme 50-year surface elevation (E_{50}), based on analysis of significant wave height and water level data, were derived using an industry standard approach based on a generalised pareto distribution, a peaks over threshold data reduction technique and a maximum likelihood fitting scheme. Through the use of the joint probabilities model, the true return periods associated with exceedance of the extreme surface elevation (E_{50}) and the air gap (E_{50} + 1.5 m) were estimated. Results are given in Table 5.1.

Table 5.1.   Return periods associated with 50-year surface elevation, E_{50}, and air gap exceedance (after Smith et al, 1999)

Location	E_{50}	E_{50} return period	Air gap return period (E_{50} +1.5 m)
NNS (NORTH)	19.6 m	800 years	3800 years
CNS (CENTRAL)	14.9 m	600 years	>10 000 years
SNS (SOUTH)	8.8 m	850 years	>>10 000 years

There is a regional variation of return periods for this 1.5 m air gap extinction, with shorter return periods being experienced in the northern sector of the North Sea than in the southern sector. The return periods associated with the calculated 50-year extreme surface elevation are in the region of 600 to 850 years. It was thus demonstrated that the pre-1996 methodology (using the prescribed 1.5 m air gap) gave inconsistent safety levels.

For one of the sites, the analysis was extended to consider the effects that different datasets, distributions and analysis techniques have on the resulting air gap exceedance return period. The joint probability model was used as a means of estimating the return period associated with each of the air gap estimates. The results of the study are shown in Table 5.2.

Table 5.2. Airgap estimation for a northern North Sea location (after Smith et al, 1999)

Parameter	Guidance notes	Industry standard generalised distribution			Industry standard generalised pareto distribution			Joint probability model
	E	SE_1	SE_2	SE_3	SE_1	SE_2	SE_3	
50-year extreme surface elevation estimate (m)	17.9	18	19.1	19.4	17.8	19.6	19	16.8
10 000-year extreme surface elevation estimate (m)	24.4	26.6	28.1	28.7	26.3	31.1	27.3	21.8
Deck level[1] (m)	19.4	19.5	20.6	20.9	19.3	21.1	20.5	18.3
Airgap return period	594	681	2 214	2 994	518	3 831	1 931	193
Annual airgap exceedance probability	17×10^{-3}	1.5×10^{-3}	4.5×10^{-4}	3.3×10^{-4}	1.9×10^{-3}	2.6×10^{-4}	5.2×10^{-4}	5.2×10^{-3}

NOTES:
[1]Deck level defined as 50-year surface elevation +1.5 m airgap
All heights relative to Mean Sea Level
SE_1 is derived from the extreme value analysis of surface elevation
SE_2 is derived from the extreme value analysis of H_s and still water level
SE_3 is derived from the extreme value analysis of wave crest elevation and still water level

It can be seen that considerable variation in the estimated air gap extinction return period was found depending on which method of analysis was used. The joint probability based approach of calculating a 50-year extreme water level and adding

the further 1.5 m air gap allowance results in an air gap exceedance return period of 193 years. The longest return period of 3831 years results from the extreme value analysis of significant wave height and still water level.

5.2.3. Determining the probability of air gap exceedance

For the majority of North Sea locations (as those illustrated in Table 5.1), it has been observed that the wave crest height distribution has the greatest influence in determining the probability of exceedance of the air gap. Pre-1996 this was traditionally a value of the extreme 50- or 100-year crest height. Post-1996 this value can be calculated in a number of different ways, with an intermediate step often involving the determination of the most probable maximum individual wave height at the required return period.

One method includes obtaining an estimate of H_s using a measured or hindcast dataset, which is expected to be exceeded on average once in 50 years (H_{s50}), for example. An estimate can then be made of the most probable maximum wave height (H_{50}) which is expected to be exceeded only once in 50 years ($H_{50} = 1.86H_{s50}$). This value can then be used in an appropriate wave theory analysis to determine the most probable maximum wave crest elevation (see Section 5.3) or can be factored to obtain a reasonable estimate of this parameter directly.

The most probable maximum wave height represents the value of the peak in the modified Rayleigh distribution relating to the maximum value of wave height which would be recorded most often in each of a large number of independent 50-year records. It is expected that 63% of the maximum wave heights measured in this 50-year record would be in excess of the most probable maximum value (see Figure 3.2). The annual probability of exceedance of a 50-year wave height is 0.02. This is clearly significant when compared to typical desired annual probabilities of failure of a structure. The studies described above (Table 5.1) showed that, even after tide, surge and air gap allowance are added to the extreme crest elevation, the probability of the installation encountering an individual wave with a crest height which exceeds the air gap is significant.

Thus Smith et al (1999) recommend that an alternative wave height statistic such as the extreme wave height with an annual probability of exceedance of less than 0.0001 (1 in 10 000-year storm) is used. If this probability is used in the method described above, this would imply raising the air gap allowance from 1.5 m to at least 3.5 m.

5.3.   PREDICTION OF EXTREME WAVE CREST ELEVATION, η_{max}

As discussed in Section 5.2, determination of the maximum wave crest elevation is essential for prediction of the occurrence of wave loads on a jetty deck or for determining the air gap allowance if the deck is to be raised clear of the water level.

Any particular wave condition can be described by:

H_s	significant wave height (taken as $H_{1/3}$)
T_m, T_p	mean or peak wave periods
N_z	number of waves during the storm/tide peak
H_{max}	Highest wave (depends on N_z, from laboratory tests was taken as highest of 1000 waves)

Extreme wave heights and elevations vary randomly, so a deterministic prediction of H_{max} is not possible, but a probability density can reasonably be defined for the ratio $H_{max}/H_{1/3}$. Adopting the Rayleigh distribution as a first approximation to the distribution of individual wave heights (valid in deep water, and probably conservative in shallower water) a theoretical relation between H_{max} and $H_{1/3}$ can be derived. The most probable value of H_{max} is given as a modal value of $H_{max}/H_{1/3}$ by Goda (2000) based on Longuet-Higgins (1952), and earlier tests have shown that this value most closely corresponds to wave measurements:

$$(H_{max}/H_{1/3})_{mode} \cong 0.706\sqrt{\ln N_z} \cdot \qquad (5.1)$$

Other wave height distributions can be used on shallow foreshores. A model distribution has been proposed by Battjes and Groenendijk (2000). This model consists of a Rayleigh distribution, or a Weibull distribution with exponent equal to 2, for the lower heights and a Weibull with a higher exponent for the higher wave heights. The parameters of this distribution have been estimated from laboratory data and expressed in terms of local wave energy, depth and bottom slope.

Maximum crest elevations (η_{max}) can be obtained from H_{max} by various non-linear theories. For a range of test conditions used in studies at HR Wallingford, discussed further in Section 5.5 (see Allsop and Cuomo, 2004), it was seen that Stream Function Theory, or Rienecker and Fenton's (1981) Fourier approximation method, can safely be used to derive η_{max} from H_{max}.

Stansberg (1991) gives a rather simpler approximation for crest height in deep water, where the expected maximum crest elevation, η_{max}, for a given wave extreme height, H_{max}, can be obtained by:

$$\eta_{max} = \frac{H_{max}}{2} \cdot \exp\left(\frac{2\pi}{L_m}\frac{H_{max}}{2}\right) \qquad (5.2)$$

where L_m is the wavelength, derived from linear wave theory, using mean wave period (see Section 3.4.3) and H_{max} is the maximum wave height, derived from Equation (5.1).

Stream Function Theory and Fenton's Fourier Theory results were compared with Stansberg and with HR Wallingford's measurements (discussed further in Section 5.5). For the range of conditions tested, there are no evident differences between Stream Function Theory and Fenton's Fourier Theory, while Stansberg's semi-empirical relation gives generally good estimations in deep water considering its simplicity, but higher wave crests tend to be underestimated. It should be noted that Stansberg's approximation is only valid in deeper water. More sophisticated methods discussed above should be used for other conditions.

Software packages are available to undertake higher order wave theory calculations, such as the ACES (Automated Coastal Engineering System) package developed by the Coastal Engineering Research Center (CERC) of the US Army Corps of Engineers (USACE).

Two different case studies for setting the jetty deck level are described in Box 5.3. In case study A the deck level could be located outside the zone of wave activity, so detailed studies were required to ensure that the deck would not experience wave loads for reasonable design conditions. In case study B, operational requirements meant that the zone of wave activity could not be avoided and the design therefore had to allow for inundation of the structure.

Box 5.3. Case studies: Prediction of maximum water surface elevations along a jetty

CASE STUDY A – deck elevation dictated by maximum wave crest elevation (courtesy Mouchel Parkman/KNPC)

Studies were undertaken to derive wave conditions along the line of a new deep water jetty. The jetty will extend into water depths of 18 m. The following stages were undertaken in the study:

- Derivation of offshore wave conditions, including extremes
- Wave transformation to derive wave conditions at the end of the jetty
- Joint probability study of extreme waves and water levels
- Derivation of wave conditions along the line of the jetty and at the shore
- Consideration of jetty elevations.

1. Derivation of offshore wave conditions, including extremes
Offshore deep water extreme wave conditions were derived by hindcasting from wind conditions using the JONSEY computational wave model. This included:

- Review of wind climate data
- Derivation of extreme wind speeds for each directional sector
- Hindcasting of offshore extreme waves from extreme wind speeds using the JONSEY model.

2. Wave transformation to derive wave conditions at the end of the pier
Wave transformation modelling was undertaken using the COWADIS model to transform the design conditions to a location at the end of the jetty. This model includes the effects of wave shoaling, wave refraction due to the seabed and currents, depth-induced breaking, bottom friction and whitecapping, wave growth due to wind, wave blocking. The wave hindcasting and transformation models were calibrated against measured waves from three storms at a location near to the jetty site.

3. Joint probability study of extreme waves and water levels
Extreme water levels and the joint probability of extreme waves and water levels at the end of the jetty were assessed. Several sources of information were used in the assessment of tidal ranges and extreme levels, including field data, numerical model results and inferences from general experience.

Box continues

Box 5.3. Case studies: Prediction of maximum water surface elevations along a jetty (continued)

Expected future sea level rise was assessed based on the latest published data and guidelines.

A simplified method for joint probability extremes prediction was adopted based on an approach described in CIRIA (1996). This assumes that some measure of correlation between extreme waves and water levels is known. It then provides appropriate combinations of large waves and high water levels (each expressed in terms of their marginal, i.e. single variable return periods) with a 100-year joint return period.

4.   Derivation of wave conditions along the line of the jetty and at the shore

Inshore of the jetty head the waves will shoal up and become more asymmetric before being subject to dissipative processes such as seabed friction and wave breaking. The COSMOS model was used to consider wave transformation along the line of the jetty and through the surf zone. This model includes wave refraction, shoaling, seabed friction and breaking. A representative bathymetric profile along the line of the jetty was considered.

The model was used to predict the transformation of the significant waves inshore to give conditions along the line of the jetty. Goda's method (Goda, 1985) was used to derive the ratio of H_{max} to H_s in each depth of water. In order to determine the maximum wave crest elevation, Fourier series wave theory was applied to the maximum wave at a number of points along the jetty to determine the wave asymmetry.

5.   Consideration of jetty elevations

The design ships for the jetty were 20 000 DWT to 360 000 DWT crude and products tankers and loading/unloading operations were to be by loading arms, offering flexibility in setting the deck level. Consequently, in order to eliminate significant vertical wave forces and structure slam it was appropriate to consider a jetty structure that could be generally above the wave crest elevation.

Two criteria were set:

- Main deck soffits to be above the wave crest elevation
- All product pipe racks to be above the wave crest elevation.

This reduced the forces on the major structural elements of the jetty but still allowed some smaller elements such as pipe support steelwork, slops tanks structures and pile bents to be within the wave crest profile.

An example of the variation in wave crest is given in Figure 5.7. Jetty deck level and BOP (Bottom of Pipe) was set at +10.0 m CD.
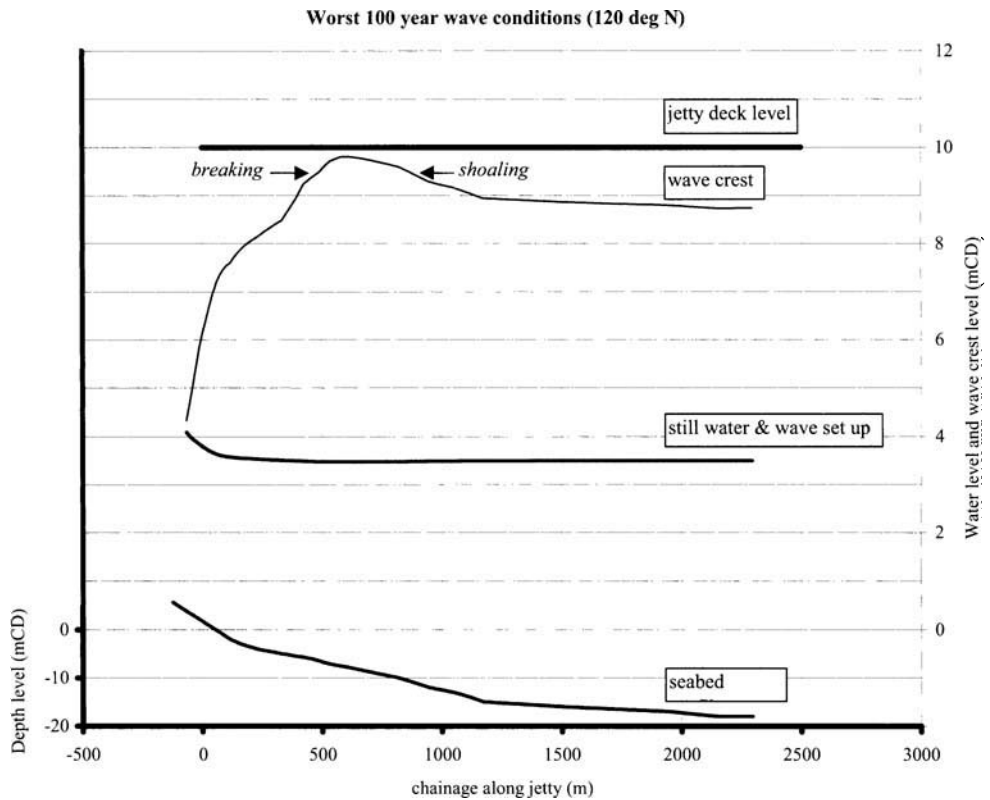
Box continues

Box 5.3. Case studies: Prediction of maximum water surface elevations along a jetty (continued)

Worst 100 year wave conditions (120 deg N)

Figure 5.7. *Profile of wave crest elevation along length of jetty – deck raised above wave zone*

CASE STUDY B – deck elevation dictated by loading/offloading operations (courtesy Mouchel Parkman)

Similar studies were carried out for a multipurpose jetty in Oman. The jetty comprised a heavy load berth, tug and pilot launch berths and a berth for small condensate tankers. In this instance there was little flexibility in setting the deck level as the main deck had to be able to accommodate roll-on roll-off heavy loads transhipped by barges with generally between one and two metres freeboard. Similarly, the condensate tanker, tugs and pilot launches required mooring facilities that were at a low enough level to ensure safe and effective mooring conditions.

It was necessary therefore to set the deck level well within the wave crest elevation, resulting in considerable 'green-water' forces – vertical forces and structure slam.

The jetty structure was designed to withstand these forces, but it was also necessary to consider the impact of damage to the condensate pipelines along the jetty, the condensate loading arm and the likelihood of damage to equipment on the jetty deck in the event of storms. The product pipelines were consequently protected

Box continues

Box 5.3. Case studies: Prediction of maximum water surface elevations along a jetty (continued)

within a concrete trench along the jetty; the loading arm was located on a platform, raising it above the deck level and above the wave crest level. The frequency of 'green water' wave overtopping above deck level was considered in the equipment design on the jetty deck.

An example of the variation in wave crest elevation along the jetty is given in Figure 5.8. Jetty deck level was set at +6.5 m CD and the BOP for the condensate line was set at +6.0 m CD, but with the pipe located within a protective trench.
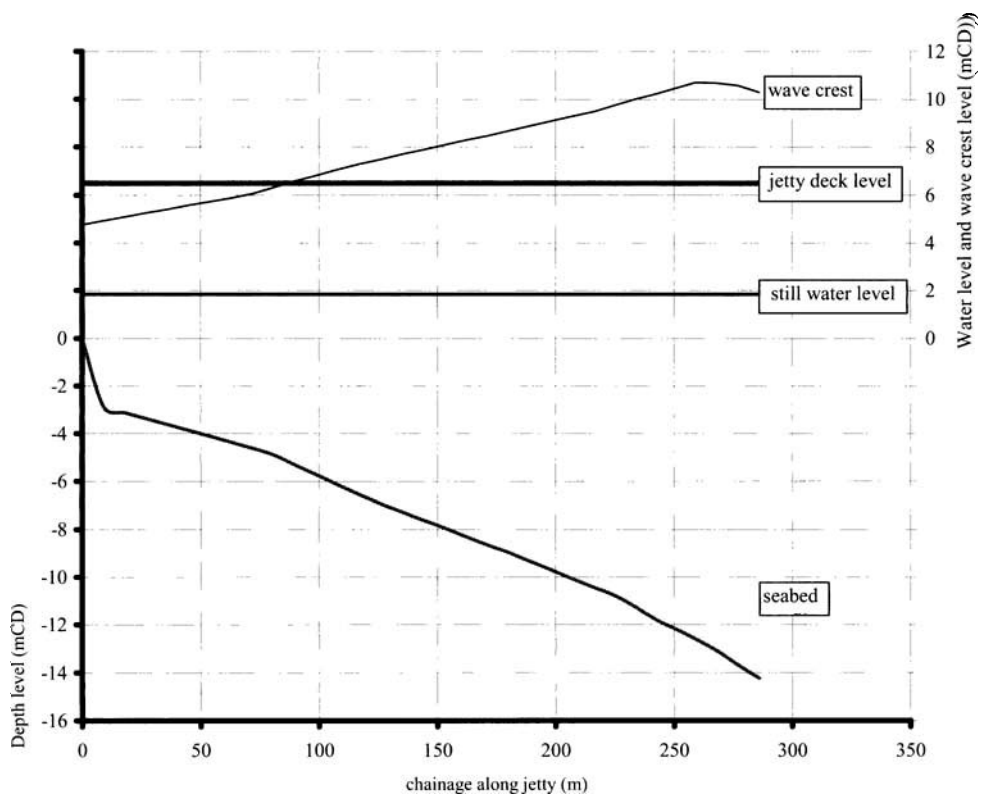
Figure 5.8.   Profile of wave crest elevation along length of jetty – deck in wave zone

5.4. WAVE FORCES ON DECKS

5.4.1. Introduction

This section provides an overview of those wave forces that act on deck elements and discusses guidance available in the literature for evaluating these forces. New design guidance from model tests by HR Wallingford (see Allsop and Cuomo (2004)) is given in Section 5.5.

Much of the existing guidance comes from the offshore industry, where different methods are used to describe wave loading, either globally or using a detailed component approach for the design of structures. Many of these methodologies can be extended to the case of exposed jetties. The global approach is more suited to the overall assessment of issues such as risks from wave-in-deck loading (particularly when sufficient deck information is not available), while the detailed component approach is more suited to the evaluation of individual component damage (or more specific force calculations on structure elements).

Key issues to be considered by the design are slam loads, local structure/wave interaction effects and the dynamic response of the structure to potential short duration loads (impact loading).

Bea *et al* (1999) describe the following theory, based on offshore platforms, that has been developed based on the work of others such as Kaplan (1992) and Isaacson and Prasad (1992).

The total wave force (F_{tw}) 'imposed' on a platform deck can be thought of as a slightly extended modification of Morison's equation, given by the following:

$$F_{tw} = F_b + F_s + F_d + F_l + F_i \tag{5.3}$$

where F_b is the (vertical) buoyancy force (immersed values), F_s is the slamming force, F_d is the drag (velocity dependent) force, F_l is the lift (velocity-dependent, normal to the wave direction), and F_i is the inertia (acceleration-dependent) force.

As the wave crest encounters the platform deck, there is a transfer of momentum from the water to the structure that is reflected as the initial slamming force. As the wave continues to inundate the deck, buoyancy, drag and inertia forces are developed.

The magnitude of the slamming force relative to the peak inundation force will be dependent on the characteristics of the deck. For solid or plated decks there can be a significant downward vertical force developed as the wave crest recedes from the deck. This upward and downward vertical force can exceed the horizontal force. However, for non-plated (grated, open) decks, this vertical force is much lower (i.e. comparable with the horizontal forces), due to the reduced contact area.

5.4.2. Vertical forces

Any member that is immersed or exposed by the passage of a wave train will experience a vertical hydrostatic force of appropriate sign. One should also consider possible dynamic uplift loads arising from waves with crest heights in excess of the soffit or underside level of the platform or suspended pier structure. Results from studies indicate that the pressures can be significantly greater than the corresponding hydrostatic values for the immersed depths, depending on the wave conditions, the seabed and structure geometries.

There are essentially three types of water wave induced uplift pressures on horizontal decks/platforms in both deep water (offshore oil production platforms) and shallow water (jetties, piers etc). At the instant of contact between the wave crest and the soffit of the deck, an impact pressure is exerted which is extremely large in magnitude and very short in duration. This is followed by a slowly varying positive

pressure and then by a slowly varying negative pressure. These are described in more detail as follows.

- **Impact pressure:** Severe local damage, fatigue failure and local yielding are caused by a dynamic impact pressure acting on a very small area for an extremely short duration. Available experimental evidence shows that impact pressures exhibit large variations in both magnitude and duration differing significantly under identical conditions. Laboratory studies have shown that the reason for this is air entrainment.

- **Slowly varying positive pressure:** These forces are mainly governed by wave height and deck clearance above the still water level. As the wave front propagates beneath the platform, outshooting jets are evident at the wave front as impact occurs continuously along this front. This impact is followed by a slowly varying pressure, when more of the wave crest comes into contact with the underside of the deck as the free surface of the water alongside the platform starts to rise up above the soffit level. A difference in elevations between the fluid underneath the platform and that alongside the platform starts to develop which gives rise to the generation of the slowly varying positive pressure.

- **Slowly varying negative pressure:** Eventually, the free surface of the undisturbed wave starts to fall below the soffit level; the free surface underneath the platform begins to move inwards in the lateral direction, which causes the contact area between the platform and the wave to diminish. During this stage, a slowly varying negative pressure is generated caused by the water pressure acting downwards on the inundated deck. This is mainly governed by the width of the platform and the wave height.

Kaplan's model

Kaplan (1992) and Kaplan *et al* (1995) developed a model, essentially built up from methods described by Morison (see BS 6349 Part 1, 2000) and Bea *et al* (1999), to determine the vertical force on horizontal flat plate deck elements. The occurrence of wave impact forces on flat horizontal decks, associated with inundation due to large waves, was illustrated by events in the Ekofisk field in Norway (Kaplan, 1992, Kaplan *et al*, 1995). The Ekofisk platform deck was composed of flat plating, which may experience large loads. Other platforms have their decks composed of a finite number of beams on which grating is placed, so that a reduced 'hard structure' region is present. For such cases horizontal deck loads are then usually the dominant loads on the deck structure. The nature of the loads on flat plate decks differs from that on horizontal cylinders.

Kaplan's model can be expressed by:

$$F_z = (\rho \frac{\pi}{8} l^2 \ddot{\eta} + \rho \frac{\pi}{4} \dot{\eta} l \frac{\partial c}{\partial t} + \frac{\rho}{2} \dot{\eta} |\dot{\eta}| l C_d) b \tag{5.4}$$

where ρ is the water density, l is the wetted length, C_d is the drag coefficient, $\partial l/\partial t$ is the variation of wetted length with time, and η is the surface elevation, where $\ddot{\eta}, \dot{\eta}$ denote acceleration and rate of change with time.

The wetted length l and $\partial l/\partial t$ are determined from the relative degree of wetting of the flat deck underside, which occurs as the incident wave travels along the deck from its initial contact location.

This model was later modified to more accurately represent the effects of the different aspect ratios of deck platforms as Equation (5.4) represented a model that was effectively two-dimensional (for small wetted length-span ratios).

The modified equation to give a 3-dimensional model is given by (Kaplan *et al*, 1995):

$$F_z = \left(\rho \frac{\pi}{4} \dot{\eta} l \frac{\partial l}{\partial t} \frac{1 + \frac{1}{2}(l/b)^2}{\left[1 + (l/b)^2 \right]^{\frac{3}{2}}} + \rho \frac{\pi}{8} \frac{l^2 \ddot{\eta}}{\left[1 + (l/b)^2 \right]^{\frac{3}{2}}} + \frac{\rho}{2} \dot{\eta} |\dot{\eta}| l C_d \right) b. \tag{5.5}$$

This was later simplified by Bolt (1999) to give a general mathematical expression for wave forces, which can be described as:

$$\begin{aligned} F_i &= \frac{d}{dt}[M_i V_i] + M_i \frac{dV_i}{dt} + \text{drag} + \text{buoyancy} \\ &= \frac{dM_i}{dt} V_i + M_i \frac{dV_i}{dt} + \rho S_i \frac{dV_i}{dt} + \text{drag} + \text{buoyancy}. \end{aligned} \tag{5.6}$$

M_i is the added mass. The first term on the right hand side is the impact force term; the second term represents the inertia term, and the third term is due to pressure gradient effects in an unsteady flow. The pressure gradient acts on a 'closed' body such as an accelerated flow with spatial dependence (as in a wave field). Initial development of the model considered open decks and the pressure gradient was excluded. For closed structures, the term is retained and a vertical buoyancy term is appropriate for structures with a hollow deck.

These equations represent a continually varying force as a function of time during wave passage. This is illustrated in Figure 5.9 where time series for the total force acting on a deck and the wave crest elevation are shown, together with time series for each of the force components.
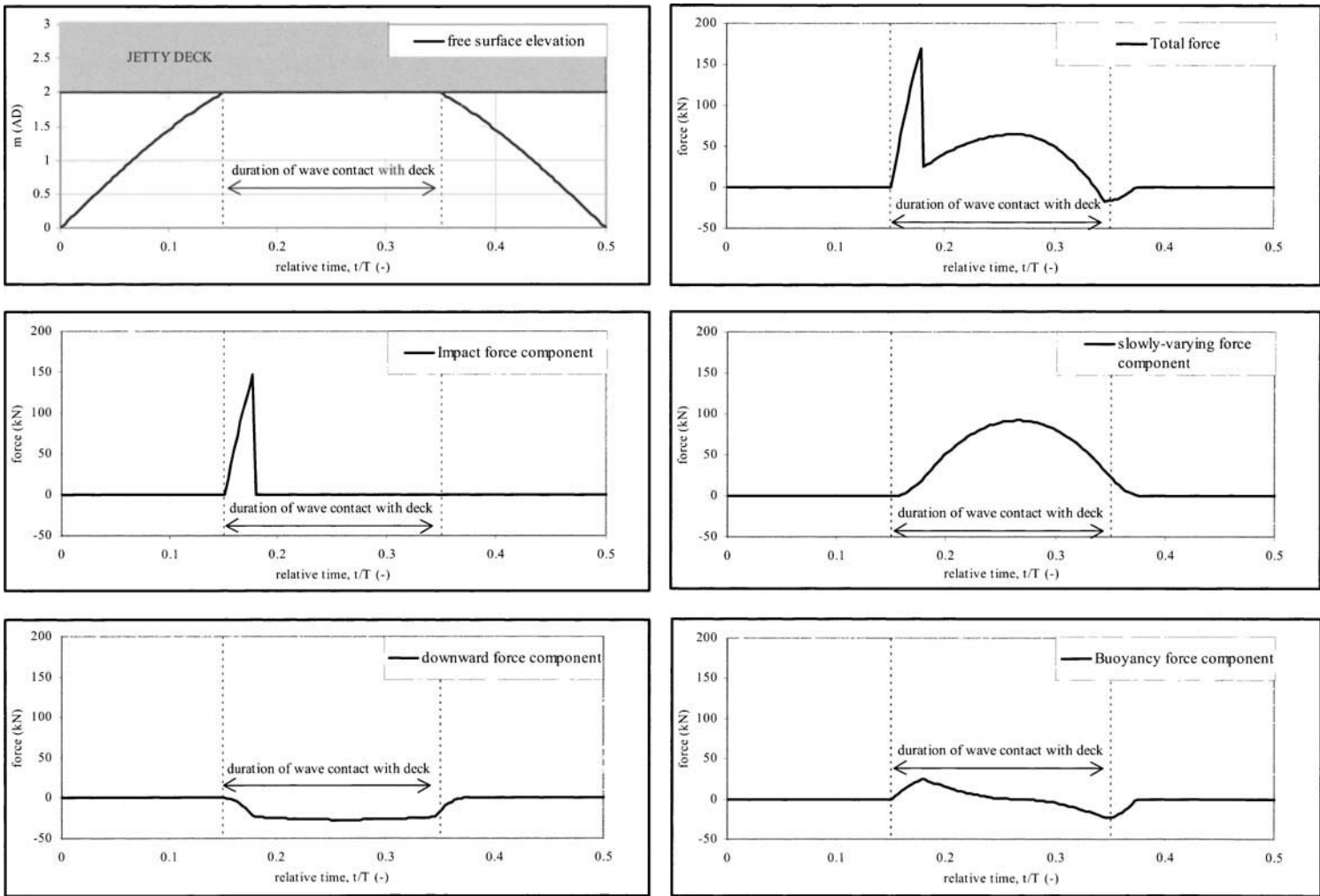
Figure 5.9. Typical time series of forces predicted using Kaplan's model

Since large waves are also generally long compared with the dimensions of a platform deck, the spatial variability of the wave properties along the deck is not considered in evaluating the above expression, i.e. the wave function variability is only considered as a function of time. The major contribution to vertical forces on the deck is due to the solid horizontal deck plating which interacts with the wave region near the upper crest portion when the waves are sufficiently high to result in such water contact (see top left graph in Figure 5.8).

Until 1995, the theoretical vertical force on flat plate decks had not been verified directly by laboratory studies. It did, despite this, provide a basis for the use of the theoretical method for estimating such loads as a consequence of successful prediction of loads on moving vessels. However, Kaplan in 1995 managed to compare theory with experiment and found good agreement. For a configuration with a grating of 40% solidity, the theoretical values of vertical forces were in the range of 20–25% of those with a solid deck. This general range was the same as that reported in the test data. No differences were found in the horizontal forces in the theoretical model, for the same wave conditions, whether grating or solid plating is present as the deck horizontal-plating surface. The measured horizontal forces showed only small differences in magnitude for the same wave conditions, whether the deck plating was solid or porous. Thus the present theoretical modelling provides a useful guide to calculating the force levels associated with the use of a porous type of deck plating thereby enabling a useful prediction of different wave impact loads acting on the offshore platforms. This is supported by correlation between theory and experiment. The variation in results is associated with the variability in the incident wave characteristics as well as the force measurements themselves, with maximum forces within about 10–15% of the measured values.

Other wave loading models

Other models are also available and have been previously reviewed, such as the Shell model, Statoil model, Amoco model and so on (Bolt, 1999). Conclusions from the review were that the appropriate choice of wave-in-deck load calculation method would ultimately depend on the purpose for which the analysis was being performed. On that basis, it was seen that the Shell model would enable the significance of wave-in-deck loads on individual platform reliability to be established. However, for instances where detailed study of the effects of inundation is required or where there is potential for water to enter the deck, giving rise to substantial vertical loads, a variant of the Kaplan model may be preferred.

5.4.3. Horizontal forces

Slamming force

It is important to recognise that slender members can be subject to high loads due to wave breaking or, in the case of members in the free surface zone, waves slamming on the members as they first become submerged. These load mechanisms can cause high local stresses or additional fatigue in member or joint welds. The force is defined as:

$$F_s = 0.5 C_s \rho A u^2 \quad \text{(Bea et al, 1999)} \quad (5.7)$$

where A is the area of the vertical face of the horizontal deck subjected to the wave crest, u is the horizontal fluid velocity in the wave crest, and C_s is the slamming coefficient ($2 < Cs < 20$, see Tickell (1994)).

BS 6349 Pt 1 (2000) recommends a similar equation for the vertical slam force for a cylindrical member:

$$F_s = 0.5C_s \rho v_\eta l W_s \qquad (5.8)$$

where l is the length of the cylinder, W_s is the diameter of the cylinder, and v_η is the vertical velocity of the water surface given by the rate of change of surface elevation η with time.

For horizontal members close to the mean water level, BS 6349 Pt 1 recommends that account should be taken of the wave slamming loads caused by the sudden immersion of the member. It is possible to calculate the horizontal slam force using the above equations and replacing the vertical velocity component with a horizontal velocity component. This may then be added to the pile drag force, to get the total horizontal force component.

The force is considered to be the imposed horizontal slamming force. However, the induced ('effective') slamming force is given as:

$$F_s' = F_e F_s \qquad (5.9)$$

where F_e is the dynamic loading factor that reflects the loading characteristics (such as duration, time history and periodicity of the imposed loading) and platform deck response characteristics (response periods [reflecting mass and stiffness], degree of overloading [inducing non-linearities] and damping).

For a very short duration impact force (e.g. $t_d = 0.01$–0.1 s) relative to the natural period (T_n) of the platform deck, the elastic dynamic response of the deck can be formulated as an impulse-momentum problem. The dynamic amplification factor (C_{dyn} = maximum dynamic force/maximum static force) can be shown as:

$$C_{dyn} = 2\pi\alpha(t_d/T_n) = F_e \text{ (for elastic, non damped response)} \qquad (5.10)$$

where t_d is the duration of the impact loading, T_n is the natural period of the deck, and α reflects the time-magnitude characteristics of the impact loading.

Inundation force

Equations for the horizontal drag force, the vertical lift force and the horizontal inertia force can be defined (Bea *et al* 1999).

The horizontal drag force can be formulated as:

$$F_d = 0.5\rho C_d A_u^2 \qquad (5.11)$$

The vertical lift force can be formulated as:

$$F_l = 0.5\rho C_l A u^2 \qquad (5.12)$$

The horizontal inertia force can be formulated as:

$$F_i = \rho C_m V a \qquad (5.13)$$

where C_d is the drag coefficient, A is the area subjected to wave action, C_l is the lift coefficient, C_m is the inertia coefficient, V is the volume of the deck inundated, u is the water particle velocity, and a is the water particle acceleration.

The horizontal lift forces are expected to be relatively small compared with the horizontal drag forces. The maximum horizontal force developed on the platform deck by the wave crest will be formulated based on the horizontal drag force or effective slamming force. The primary issues associated with this formulation are evaluating the elevation of the wave crest (which determines the amount of the deck inundated) and the water velocity in the wave crest. Methods for deriving these parameters are discussed in Sections 5.3 and 3.5.3.

5.5.   RECENT TEST DATA AND DESIGN GUIDANCE

5.5.1. Introduction

Recent physical model studies at HR Wallingford measured wave forces on jetty deck and beam elements (see Allsop and Cuomo (2004), Tirindelli *et al* (2002)) (Figure 5.10).
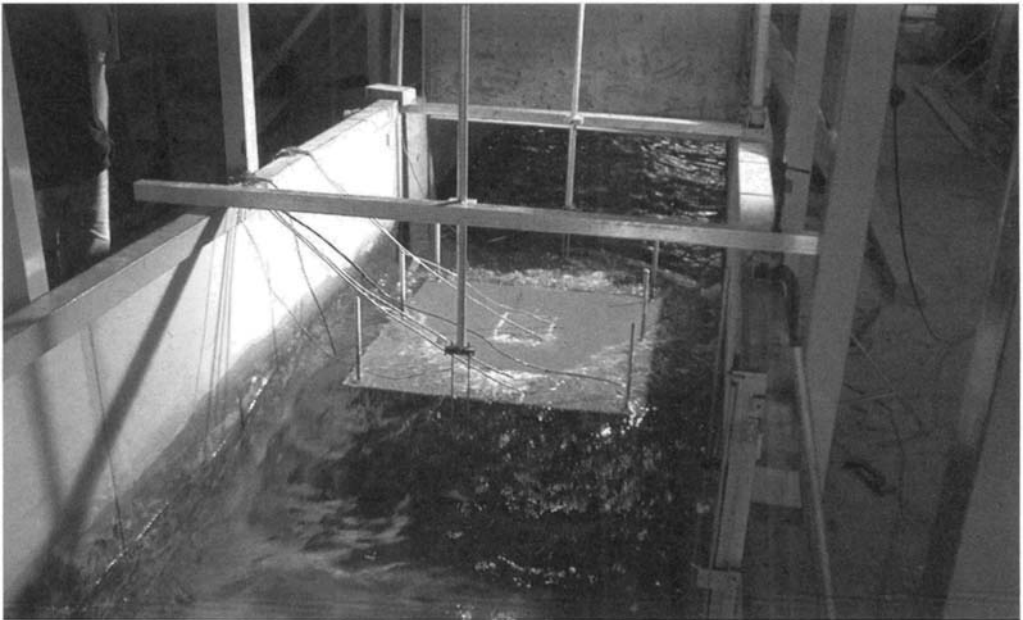
Figure 5.10.   Physical model of jetty deck, configuration 1 (courtesy HR Wallingford)

The model was designed based on consultation with an industrial steering group to ensure that the configuration and dimensions of the elements were typical of real structures, such as the jetty head shown in Figure 5.11. The model was constructed at a scale equivalent to 1:25 based on dimensions of a 'typical' jetty. The model structure and wave conditions were also approximately equivalent to some offshore installations at 1:50. As most of the results are presented in dimensionless form, any particular scale ratio is irrelevant.

A comprehensive test programme considered the following configurations:

- Configuration 1 – deck with downstand beams
- Configuration 2 – flat deck
- Configuration 3 – deck with downstand beams (as for configuration 1) with side panels to limit three-dimensional flow effects.

The model set up was such that three-dimensional flow effects could occur with configurations 1 and 2, due to inundation of the deck from the sides (Figure 5.12). A further test series (configuration 3) therefore included side panels to exclude sideways flow, thus allowing some quantification of the importance of these effects.

Figure 5.11. Dabhol jetty head under construction (courtesy Besix–Kier)
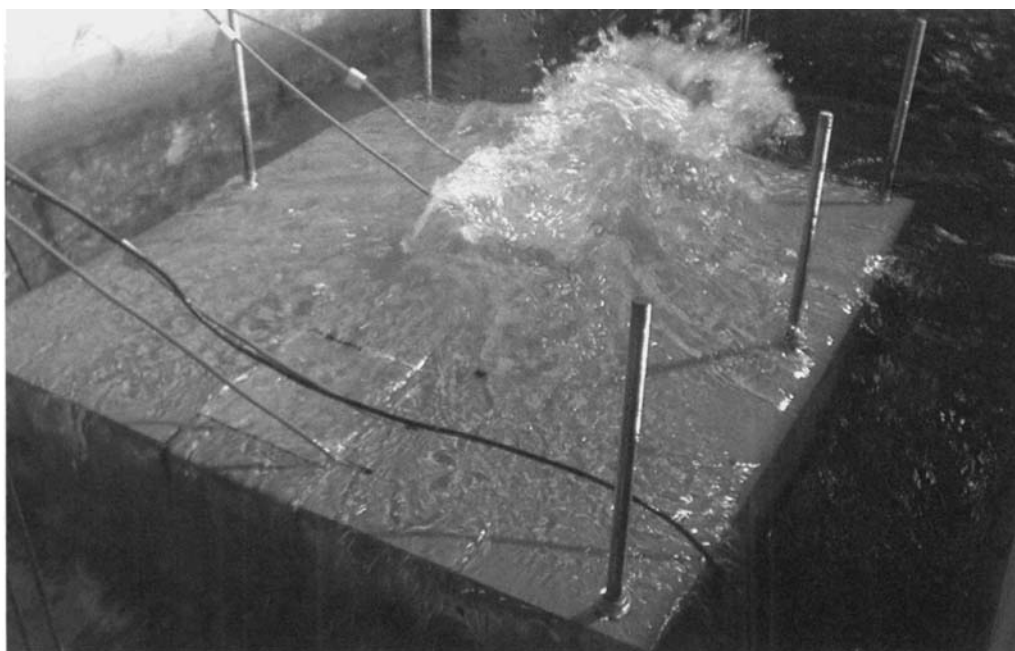
Figure 5.12.   Model set-up showing three-dimensional flow effects (courtesy HR Wallingford)

Forces were measured on internal and seaward deck and beam elements. The jetty deck configuration and measurement elements are illustrated in Figure 5.13, with dimensions of the structure elements given in model and prototype units. The range of test conditions considered in the tests is given in Table 5.3.

Table 5.3.   Test conditions

Parameter	Model	Prototype (at 1:25)
H_s (m)	0.1–0.22	2.5–5.5
T_m (s)	1–3	5–15
Water depth, h (m)	0.75, 0.6***	18.75, 15***
Clearance, c_l (m)	0.06 – 0.16* 0.01 – 0.11**	1.5–4* 0.25–2.75**
Wave height to clearance ratio, H_s/c_l	1.1–18	1.1–18
Wave height to water depth ratio, H_s/h	0.13–0.33	0.13–0.33
Relative water depth, h/L_m	0.1	0.48
Sampling frequency (Hz)	200	40

*   Configurations 1 and 3   **   Configuration 2   *** Configuration 3 only
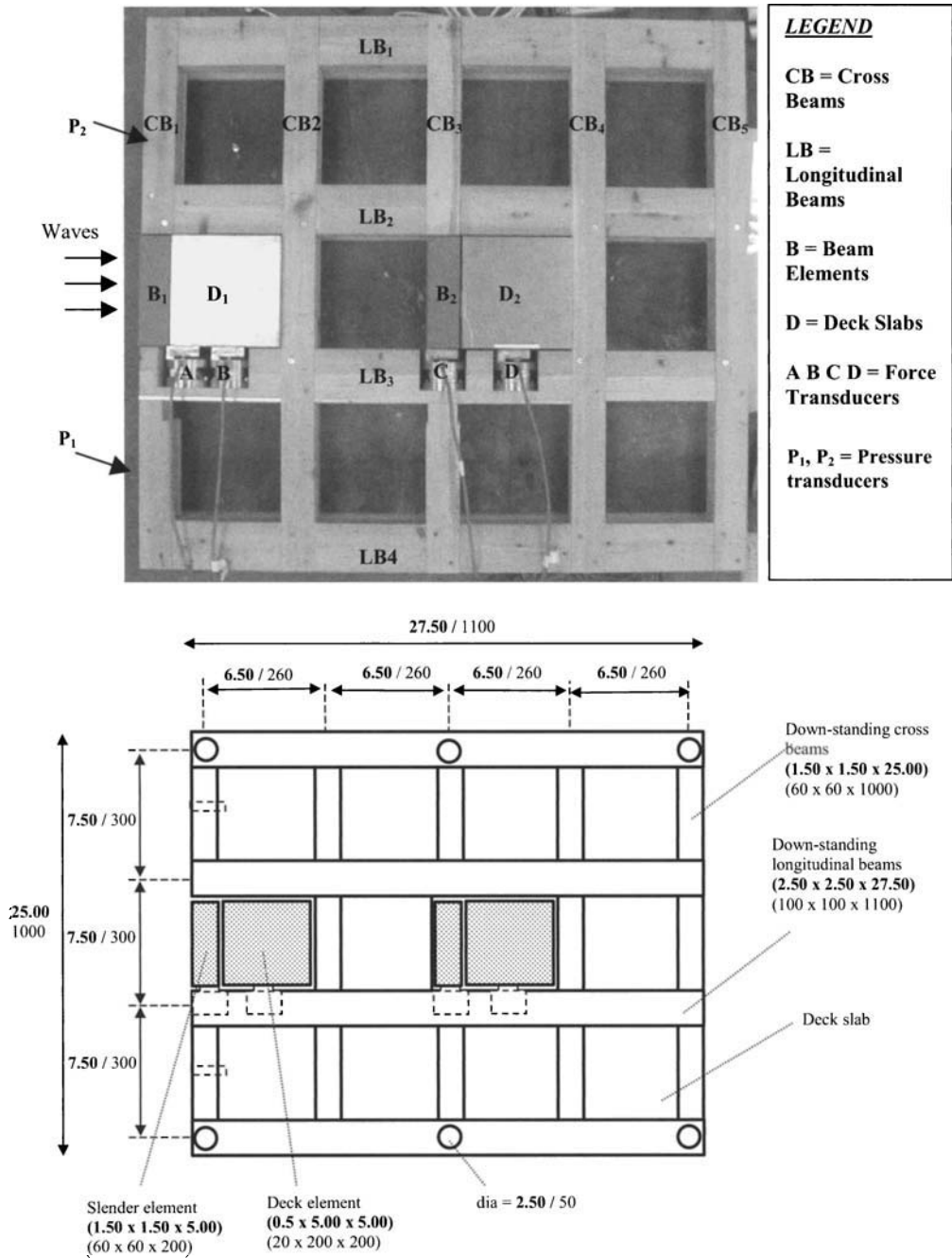
Figure 5.13. Model test device: downstanding frame of cross and longitudinal beams – plan views
Note: dimensions are given as **prototype** (model)

The following force parameters were extracted from the measured test data for each of the test elements (as defined in Figure 5.14):

F_{max} Impact force (short duration, high magnitude)

$F_{qs+, v\,or\,h}$ Maximum positive (upward or landward) quasi-static (pulsating) force

$F_{qs-, v\,or\,h}$ Maximum negative (downward or seaward) quasi-static (pulsating) force
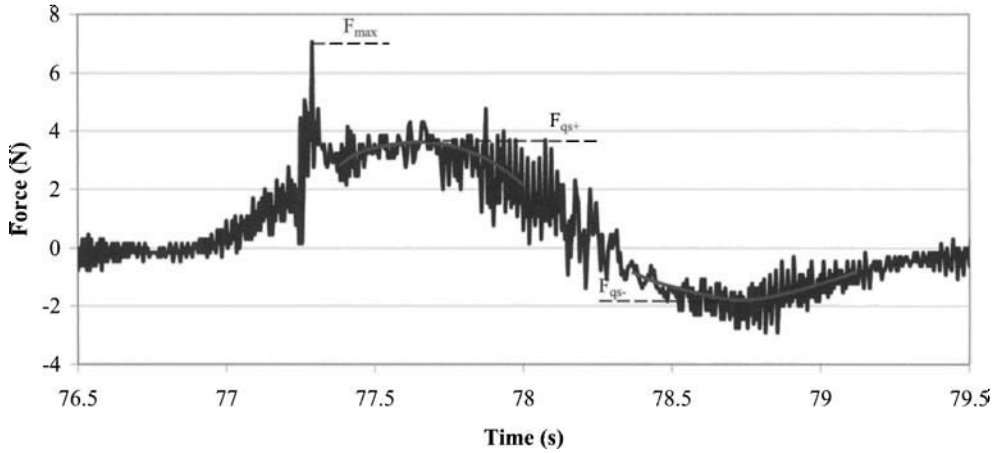
Figure 5.14.   Definition of force parameters (from Allsop and Cuomo, 2004)

Comparisons of these measured force components were made with predictions using the Kaplan model, which was found to underestimate the measured forces.

The measured forces are presented in non-dimensionalised format that can be used to provide design guidance for different wave conditions and element sizes. Forces described at $1/250^*$ statistical level ($F_{1/250}$ is the average of the four highest values recorded during each test of 1000 waves) are non-dimensionalised by a notional wave force that can be readily calculated with information at hand to the designer. This 'basic wave force' F_v^* is calculated for a wave reaching the predicted maximum crest elevation, η_{max}, whilst assuming no (water) pressure on the reverse side of the element. F_v^* is defined by a simplified pressure distribution using hydrostatic pressures, p_1 and p_2, at the top and bottom of the particular element being considered (see Figure 5.15):

$$p_1 = [\eta_{max} - (b_h + c_l)] \cdot \rho g \qquad (5.14)$$

$$p_2 = (\eta_{max} - c_l) \cdot \rho g \qquad (5.15)$$

---

* It should be noted that all loads described by Allsop and Cuomo (2004) are at 1/250 level, that is the average of the highest four loads in 1000 waves. For most test conditions, many waves will have generated loads, so $F_{1/250}$ is relatively well supported. For a few tests, however, there may be relatively fewer loads contributing to $F_{1/250}$ defined in this way, and the measure may be less stable.

where p_1, p_2 are the pressures at top and bottom of the element, b_w, b_h are the element width and height, b_l is the element length, c_l is the clearance, and η_{max} is the maximum wave crest elevation, derived using Equation (5.2) or other higher order wave theory as appropriate.

Integrating over the underside of the deck gives the basic vertical wave force, F^*_v as:

$$F^*_v = \int_{b_w} \int_{b_l} p_2 \cdot dA \cong b_w \cdot b_l \cdot p_2. \tag{5.16}$$

The basic horizontal wave force, F^*_h, is defined as follows:

$$F^*_h = \int_{b_w} \int_{c_l}^{\eta_{max}} p_{hyd} \cdot dA = b_w \cdot (\eta_{max} - c_l) \cdot \frac{p_2}{2} \qquad \text{for} \quad \eta_{max} \leq c_l + b_h \tag{5.17}$$

and

$$F^*_h = \int_{b_w} \int_{c_l}^{c_l + b_h} p_{hyd} \cdot dA = b_w \cdot b_h \cdot \frac{(p_1 + p_2)}{2} \qquad \text{for} \quad \eta_{max} > c_l + b_h. \tag{5.18}$$
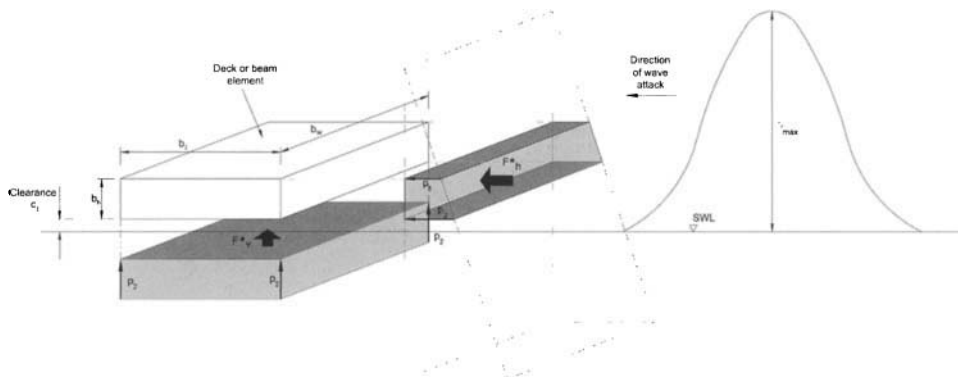
Figure 5.15.   Definition of 'basic wave forces' F^*_v and F^*_h

Dimensionless forces are presented against the dimensionless group $(\eta_{max} - c_l)/H_s$. When written as $(\eta_{max}/H_s) - (c_l/H_s)$ this parameter firstly assesses the relative elevation of the wave crest (η_{max}/H_s), often between 1.0 and 1.3, then the relative excess of the wave over the clearance (c_l/H_s). Over the test range, relatively little effect of either wave steepness or relative depth was detected in these data, although that conclusion may be specific to the relative size of the test elements considered.

Slowly-varying vertical and horizontal (quasi-static) forces, F_{qs+} and F_{qs-}, are discussed in Sections 5.5.2 and 5.5.3. Discussion of shorter duration, higher magnitude impact forces is given in Section 5.5.4.

6. Berthing and mooring loads

6.1. BERTHING LOADS

The previous chapters have described the hydraulic loads that may be applied to exposed jetties. However, it is important to note that these loads may still be small in comparison with mooring and berthing loads and the structural design must accommodate the wide range of loads that may be applied to the structure.

The British Standard Maritime Code BS 6349 Part 4 (1994) provides guidance on the assessment of berthing loads including facilities situated in exposed locations. In the absence of any further advances in berthing design guidance it is recommended that the designer should follow the recommendations given in BS 6349 Part 4. It is important to note that, as stated in the British Standard, the berthing velocity for exposed locations will be larger than for sheltered locations.

6.2. MOORING LOADS

6.2.1. Introduction

Design of an appropriate mooring system requires assessment of the full range of loads acting on the moored vessel. These may include:

- wind
- currents
- wave loads
  - o   ocean or long period swell waves
  - o   vessel-generated waves
- tidal rise and fall (not addressed in these guidelines)
- change in draught or trim due to cargo operations (not addressed in these guidelines)
- ice (not addressed in these guidelines).

Wind and current loads

Guidance in the British Standards suggests that principal horizontal forces are normally due to wind and current loading on vessels, for berths in sheltered locations. The reader is directed to OCIMF (1994) and OCIMF (1997) for guidance on wind- and current-induced loads.

Wave loads

In the case of berths at jetties in exposed locations, wave loads may be significant. The dynamic and complex nature of the wave loads, ship, fender, and mooring lines response makes it difficult to make a simple initial assessment of the line and fender loads and vessel movements.

This section provides initial guidance on wave-induced mooring line loads, fender forces and movements for vessels berthed at exposed jetties for use at the concept and feasibility design stage. A series of lookup graphs has been developed to help designers establish indicative values for the early stages of design. It is important that the designer ensures that at the detailed design stage a rigorous assessment of mooring loads for the specific vessels in question is undertaken using appropriate numerical or physical modelling techniques.

The loads have been determined based on arrangements for mooring lines given in BS 6349 Pt 4 (1994) and OCIMF (1978). The arrangement used comprises 12 lines (2 forward, 2 aft, 2 forward breast, 2 aft breast, 2 forward springs, and 2 aft springs) and ten fenders, as shown in Figure 6.2.

It should be noted that the determined loads may not apply to layouts different from that shown. For instance, it is quite common that fewer than ten fenders are used in such layouts, in which case the results from the lookup graphs should be treated with caution (although if the fore and aft fenders are similarly located the results may be similar). The mooring line layout used in determining the loads is relatively generic and the lookup graphs for mooring line forces and vessel response may be applicable in other cases.

When designing for mooring line loads, it is normal to design such that, in the event of overloading, the mooring equipment fixings will fail before the jetty structure is damaged.

6.2.2. Derivation of lookup graphs for wave loads

Computer models of wave forces and moored ship motions were used in combination to determine the responses of a typical vessel for preliminary design only. Results are collated in dimensionless form to enable designers to identify their particular design case for initial concept or feasibility design purposes.

Figure 6.1.   Jetty head and mooring dolphins under construction, Dabhol (courtesy Besix–Kier)

⊙ line number

▣ fender number
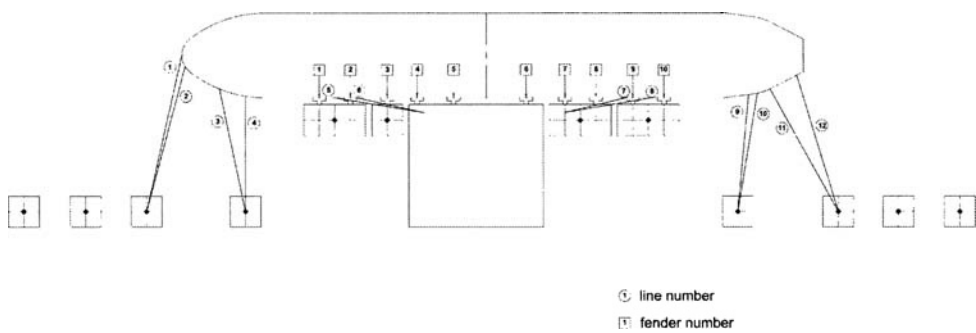
Figure 6.2.   Mooring configuration adopted for derivation of wave force lookup graphs

Mooring lines were modelled as elastic springs. All lines were modelled as having the same spring rate (stiffness), which is expressed in terms of a dimensionless mooring stiffness parameter, μ:

$$\mu = \frac{\lambda . L_{bp}}{\Delta} \tag{6.1}$$

where λ is the stiffness (spring rate) of the mooring lines (tonnes per metre extension), L_{bp} is the length of the vessel between perpendiculars (m), and Δ is the displacement mass of the vessel (tonnes).

Results are presented for mooring line stiffness parameters, $\mu = 0.0125$, 0.05 and 0.1. The range of values is intended to be realistically representative of the range of relative mooring line stiffnesses that might be used in practice to moor ships of different sizes. Typical line stiffnesses are noted in Table 6.1. The spring rate of each of the fenders was 40 times that of the mooring lines in all cases.

Table 6.1. Typical line stiffnesses

Vessel DWT (tonnes)	Vessel displacement (tonnes)	Fibre ropes Stiffness (t/m)	Wire ropes Stiffness (t/m)
15–20 000	20–25 000	10	30
20–40 000	25–50 000	11.5	35
40–70 000	50–85 000	13.5	40
70–120 000	85–144 000	20	60

Notes: Rope types and stiffnesses are taken from BS 6349 Pt 4 (1994)
Stiffnesses calculated assuming approximate typical length of 30 m for fibre ropes, or compliant tail of 10 m attached to wires
DWT or dead weight tonnage is the total weight of cargo etc. that a ship can carry when immersed to the appropriate load line

The graphs have been derived for the ballast scenario as this can often induce greater movements and resulting loads, compared with the laden scenario. An under-keel clearance of 53% of vessel draft was assumed (which is equivalent to 10% under-keel clearance when the vessel is laden). The vessel type considered was an oil tanker.

Wave heights and periods were varied, but all tests represented long-crested sea conditions. Waves were random, and a JONSWAP wave spectrum was used. The wave directions used are shown in Figure 6.3.

The range of parameters used to derive the lookup graphs is summarised in Table 6.2.
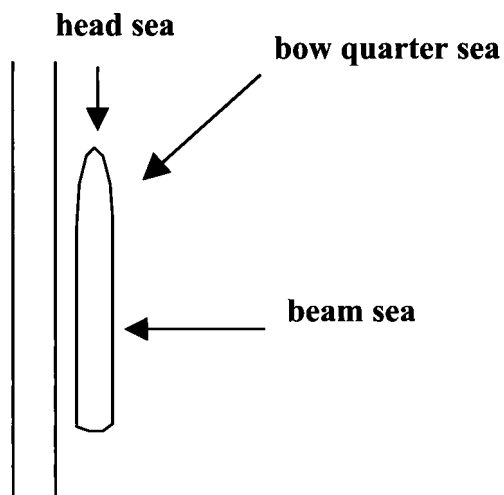
Figure 6.3. *Definition of wave directions*

Table 6.2. *Parameters used in derivation of graphs*

Mooring configuration	BS 6349 recommended for lines: 12 lines (2 forward, 2 aft, 2 forward breast, 2 aft breast, 2 forward springs, and 2 aft springs) and ten fenders (see Figure 5.1)
Vessel	Oil tanker
Vessel loading scenario	Unladen (ballast condition)
Wave directions	3 no. (see Figure 5.1)
Water depth	under-keel clearance 53% of vessel draft (equivalent to under-keel clearance of 10% when laden)
Line stiffness	3 ($\lambda = 0.0125$, 0.05, 0.1)
Fender stiffness	40 times line stiffness
Wave height, period	variable
Vessel size	variable

The key vessel responses presented in the graphs are:

- **mooring line loads**
  The graphs present the maximum individual load of the 12 lines, $F_{max,line}$, non-dimensionalised by the displacement mass of the vessel, Δ

- **fender loads**
  The graphs present the maximum individual load of the 10 fenders $F_{max,fender}$, non-dimensionalised by the displacement mass of the vessel, Δ

- **motion – sway and surge**
  The graphs present the maximum motion response non-dimensionalised by vessel length, L_{bp}.

All the graphs (Figures 6.5–6.16) present results against wave steepness (H_s/L_p) for a range of relative vessel lengths (the ratio of vessel length to peak wavelength: L_{bp}/L_p). L_p is calculated for the depth of water at the berth. Separate graphs are also presented for each of the different line stiffnesses. Note the calculated dimensionless line stiffness, μ, as defined in Equation (6.1) is used as a reference for all of the graphs.

A worked example using the lookup graphs is given in Box 6.1.

It should be noted that the methodology can be used only for conceptual design with the design vessel being an oil tanker. Under no circumstances should the results from the exercise be used directly in detailed design.

Figure 6.4.   Small timber jetty where berthing has damaged a support pile (courtesy Doug Ramsay)
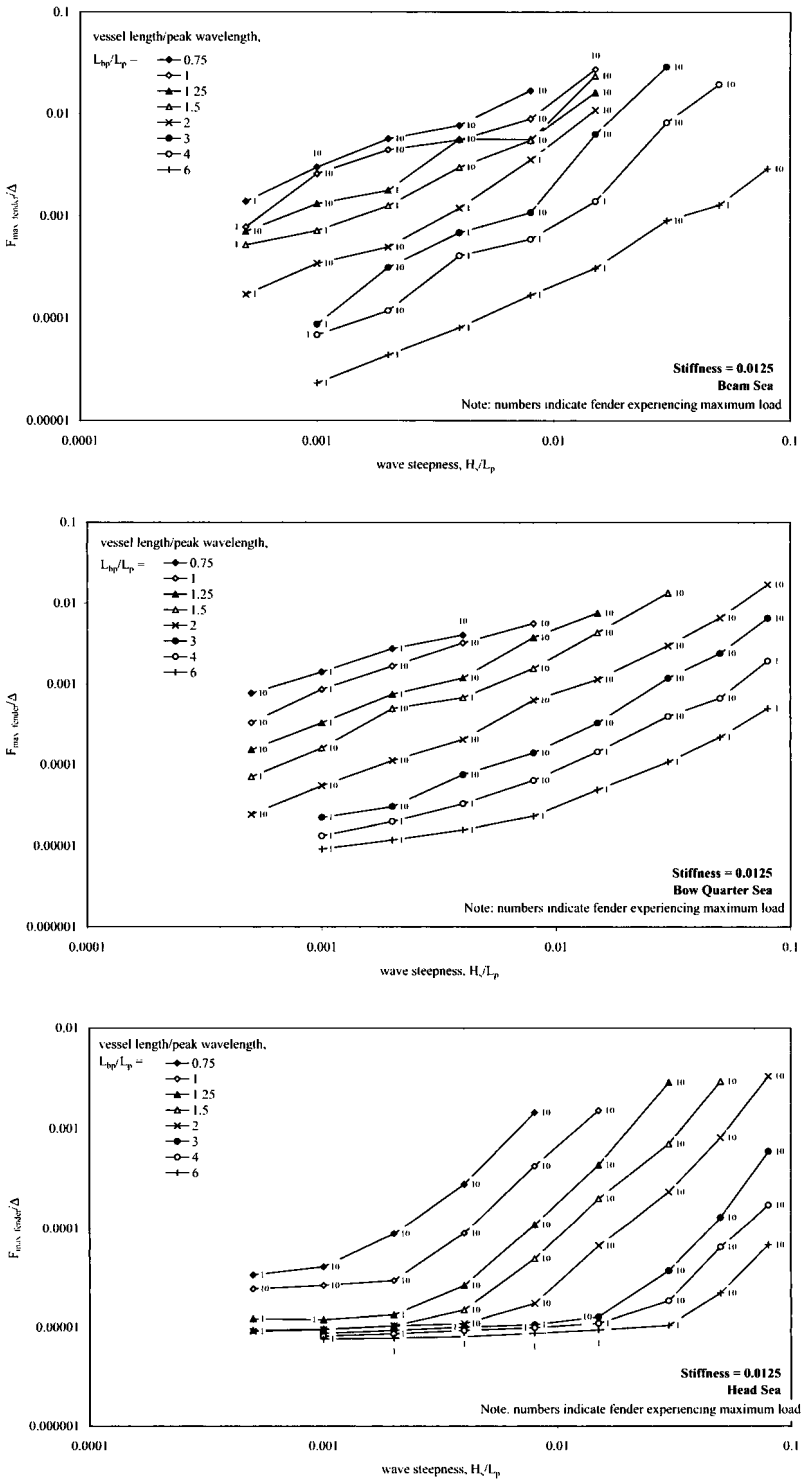
Figure 6.5.   *Fender loads – stiffness = 0.0125*

Note: Graphs are provided for use in concept/feasibility design purposes only
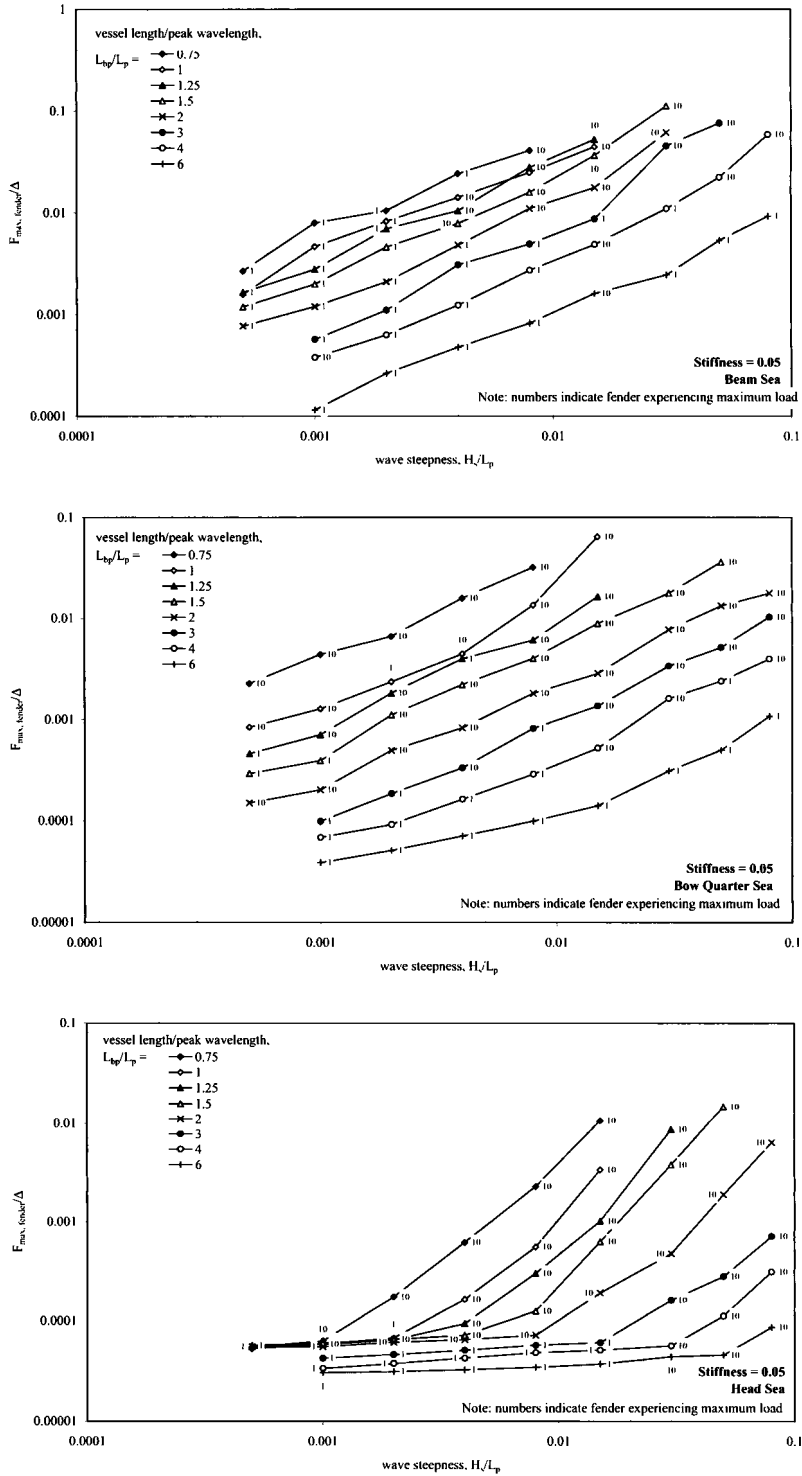
Figure 6.6.   Fender loads – stiffness = 0.05

Note: Graphs are provided for use in concept/feasibility design purposes only
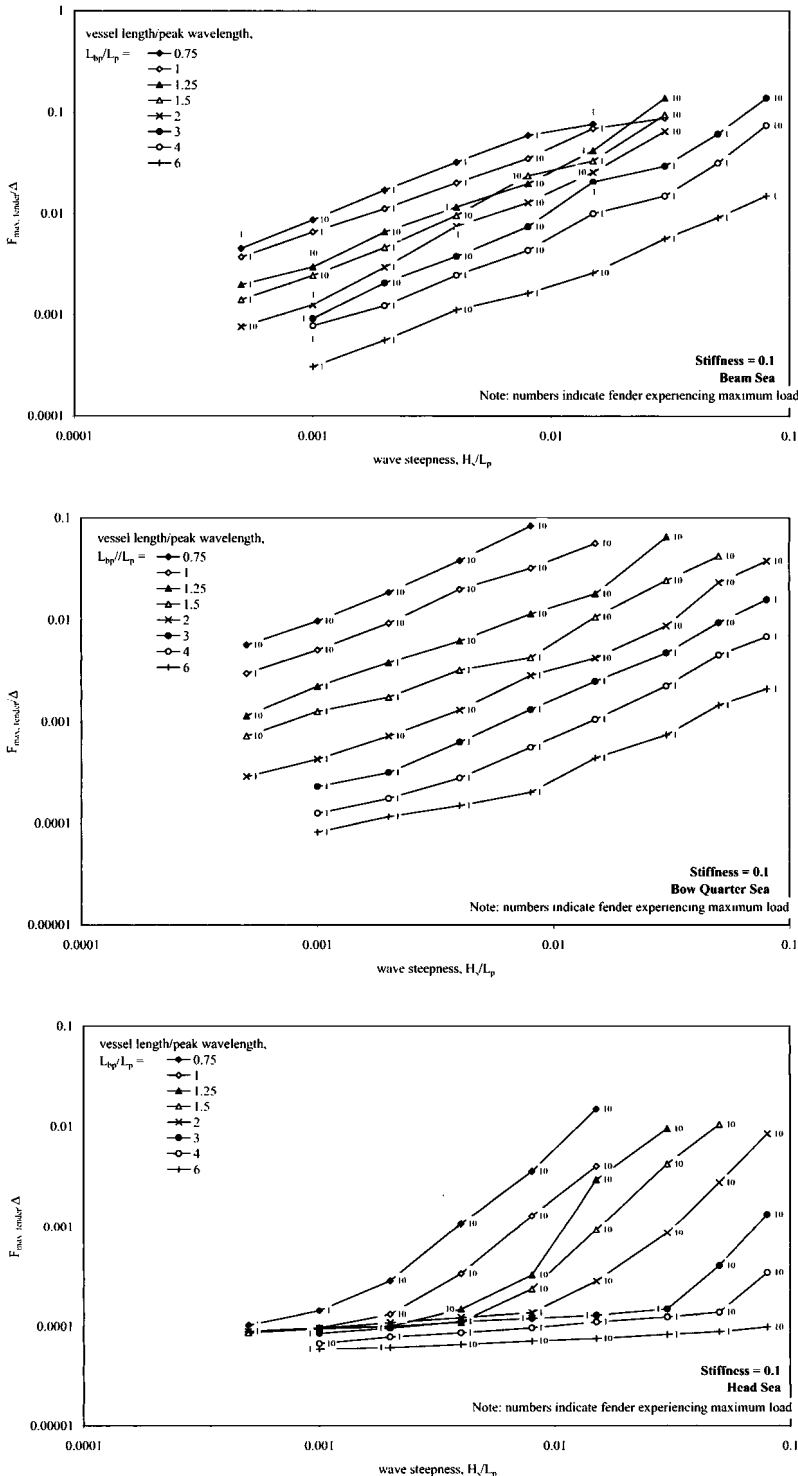
Figure 6.7.   *Fender loads – stiffness = 0.1*

Note: Graphs are provided for use in concept/feasibility design purposes only
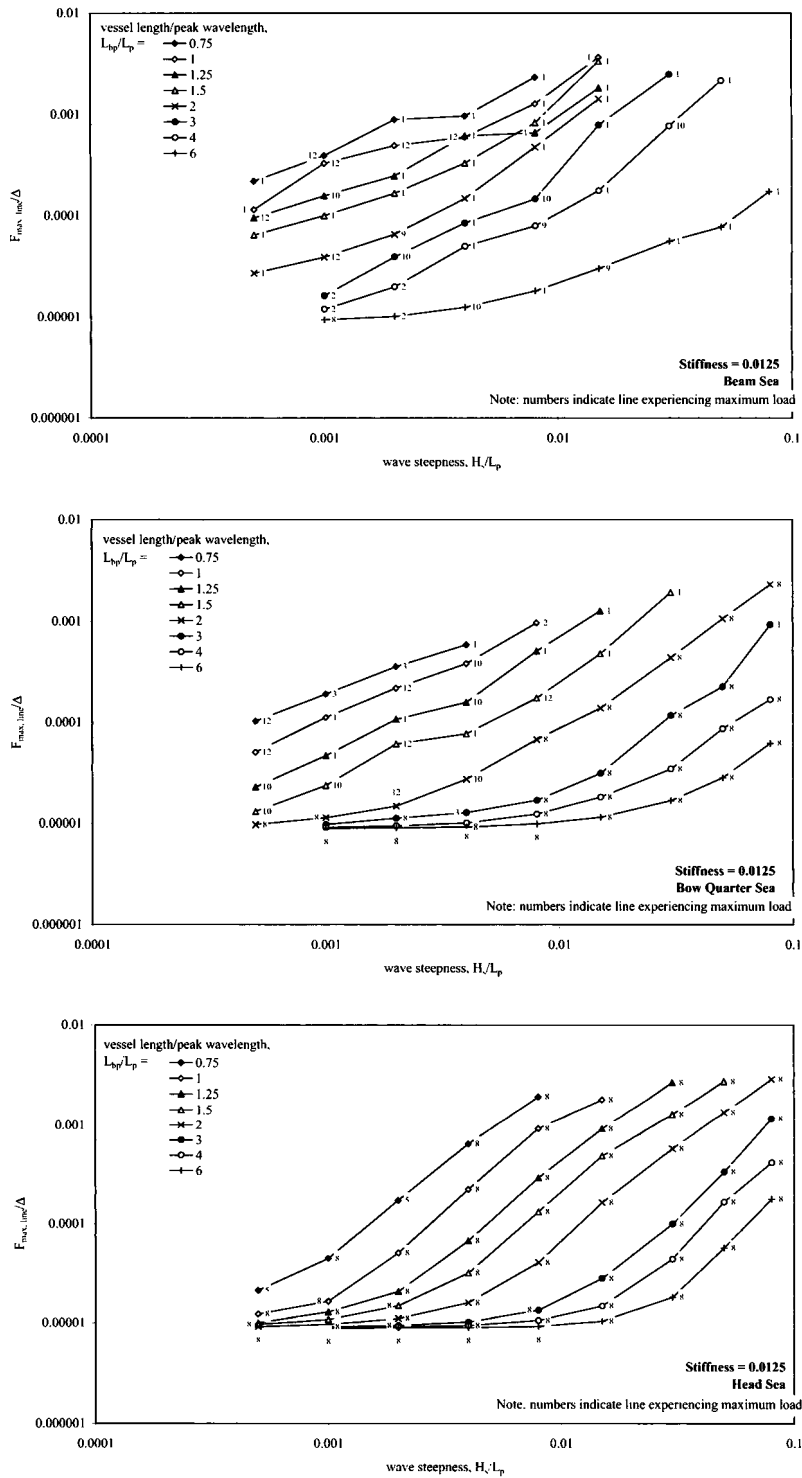
Figure 6.8.   *Mooring line loads – stiffness = 0.0125*

Note: Graphs are provided for use in concept/feasibility design purposes only
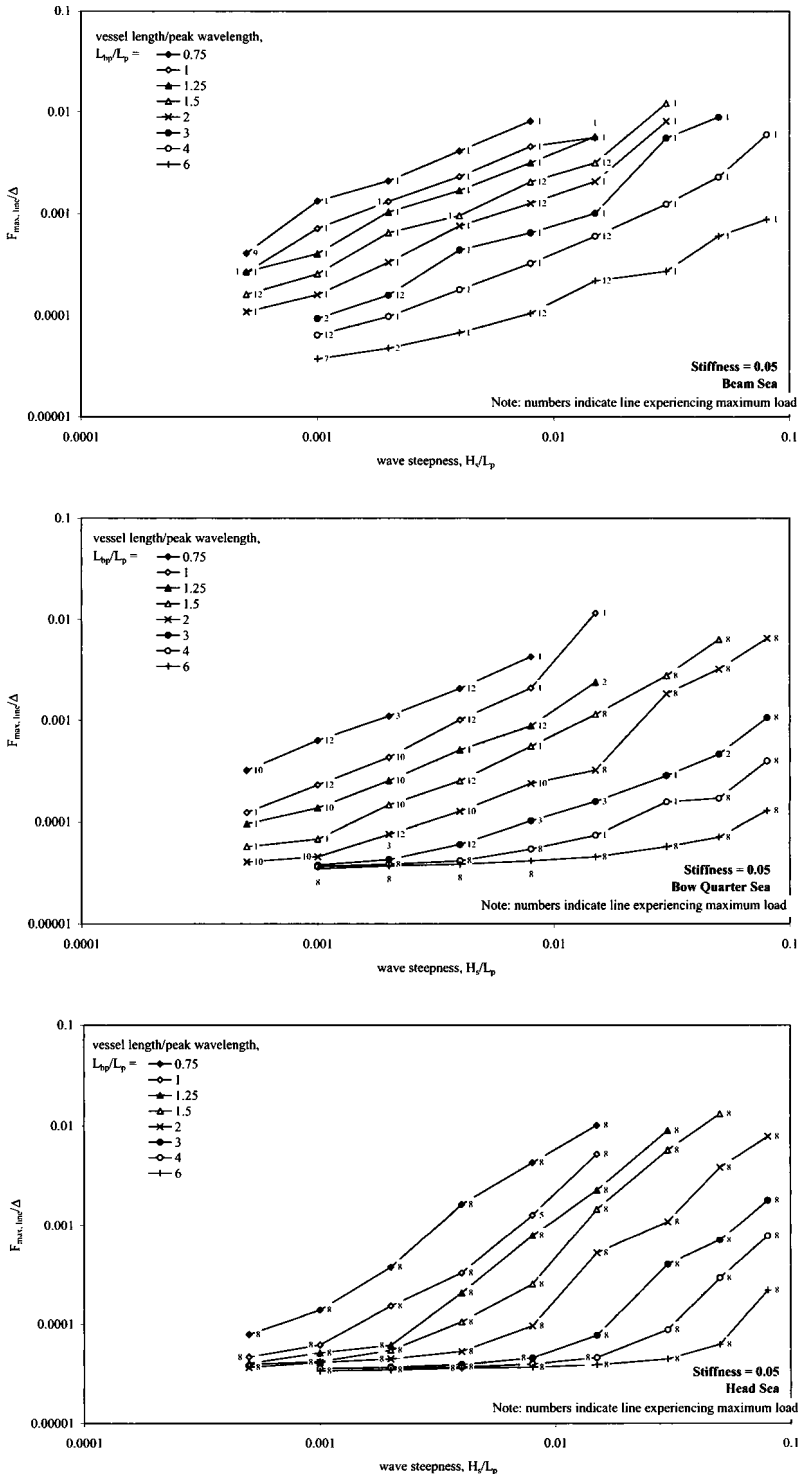
Figure 6.9.   *Mooring line loads – stiffness = 0.05*

Note: Graphs are provided for use in concept/feasibility design purposes only
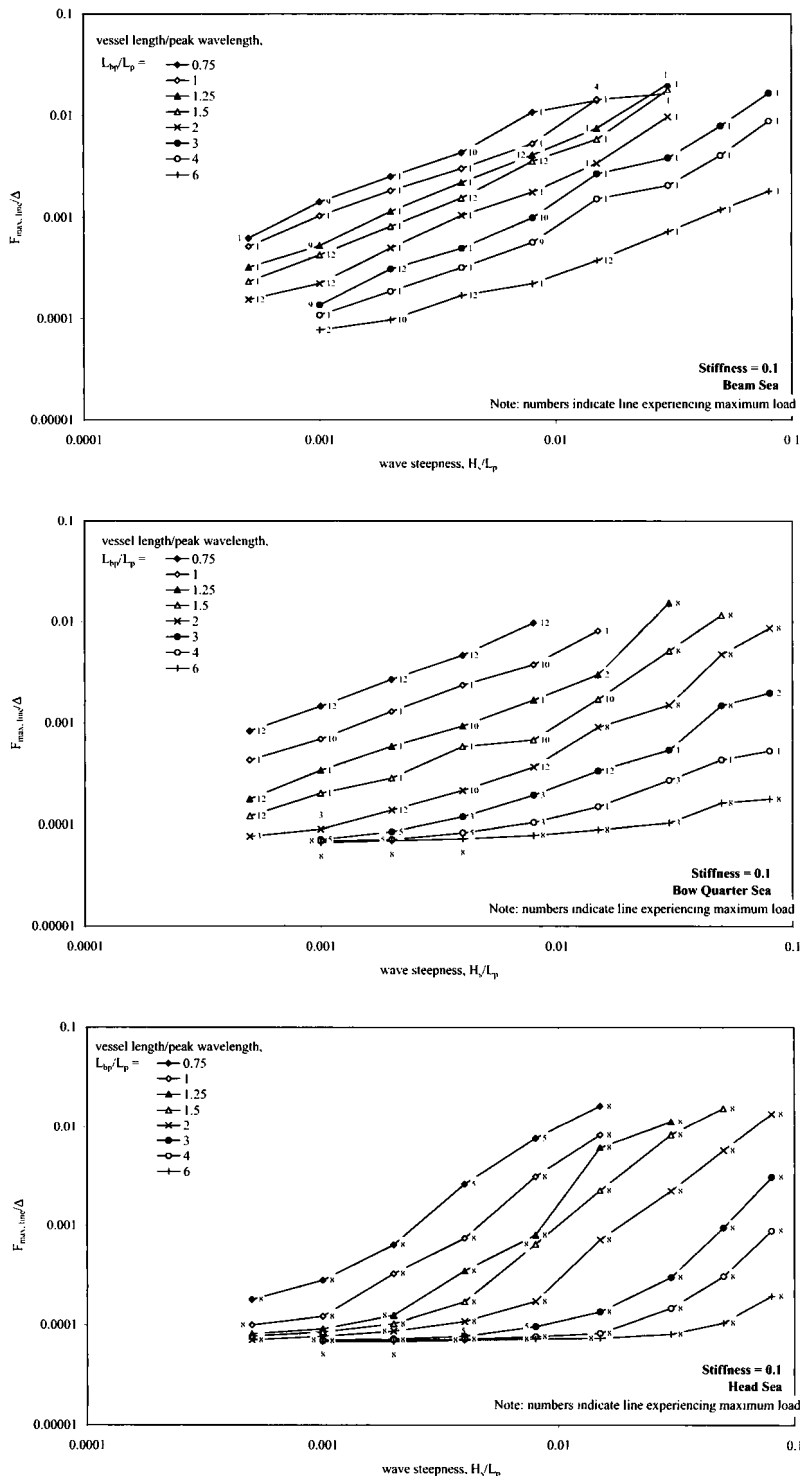
Figure 6.10.   Mooring line loads – stiffness = 0.1

Note: Graphs are provided for use in concept/feasibility design purposes only
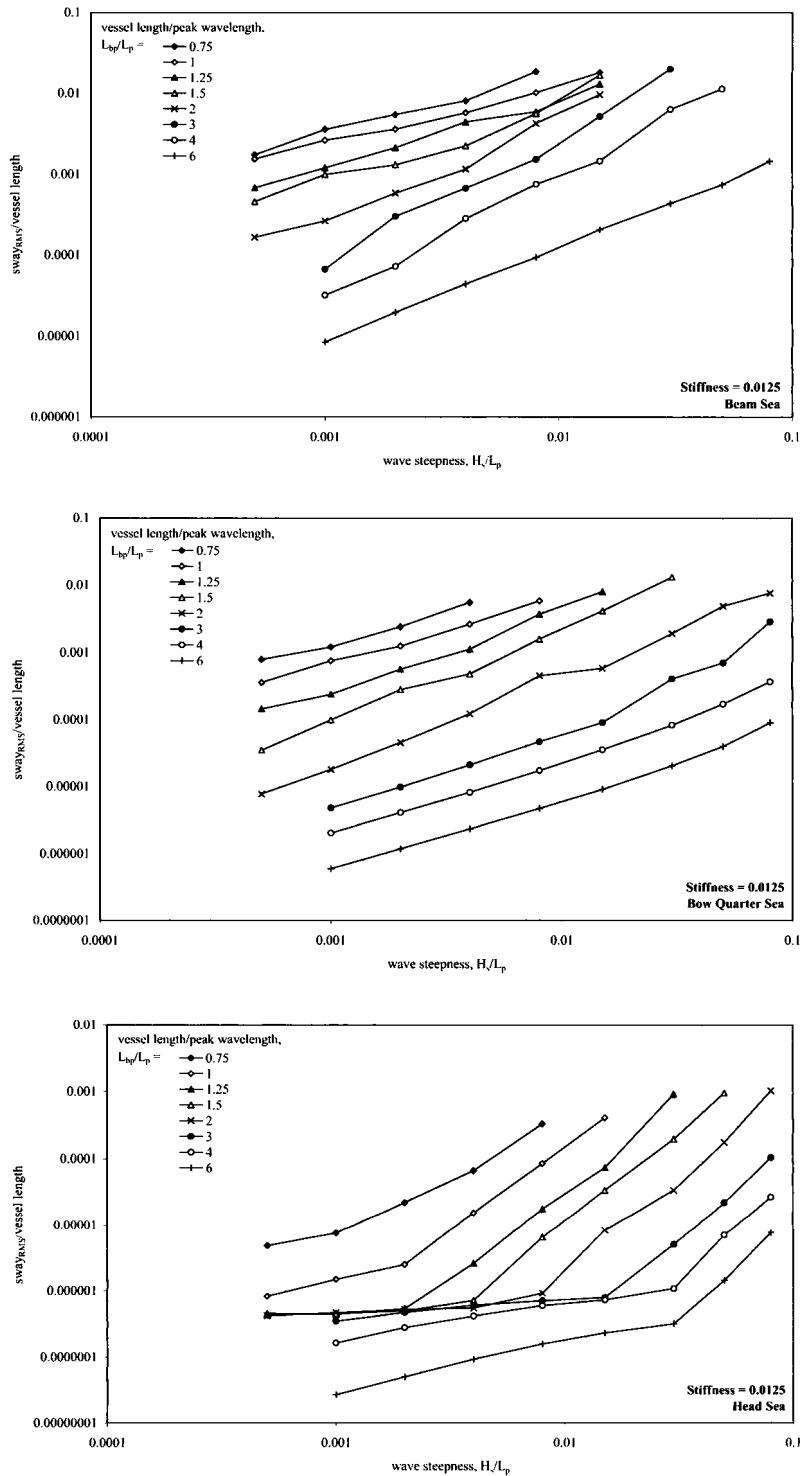
Figure 6.11. *Sway – stiffness = 0.0125*

Note: Graphs are provided for use in concept/feasibility design purposes only
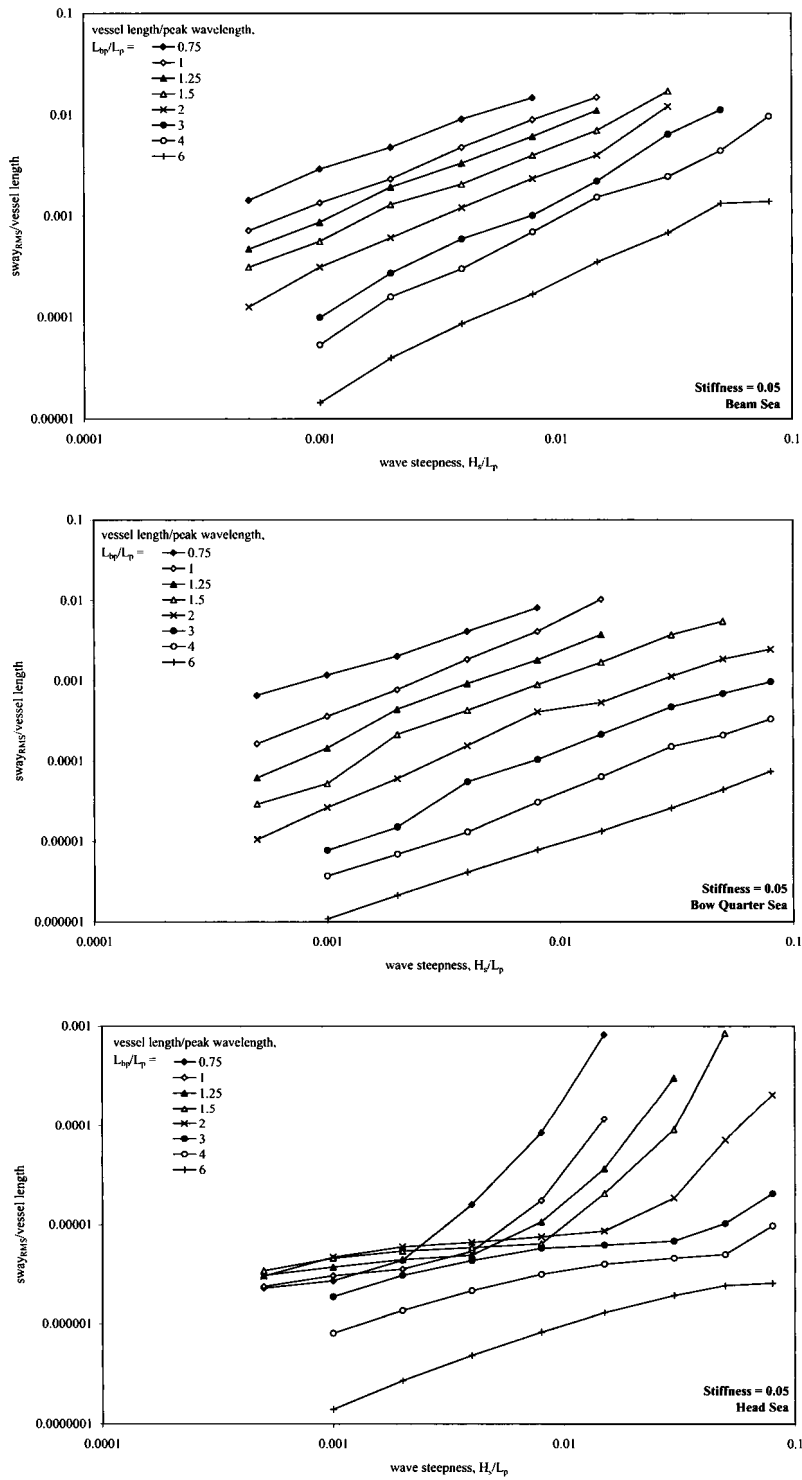
Figure 6.12.   *Sway – stiffness = 0.05*

Note: Graphs are provided for use in concept/feasibility design purposes only
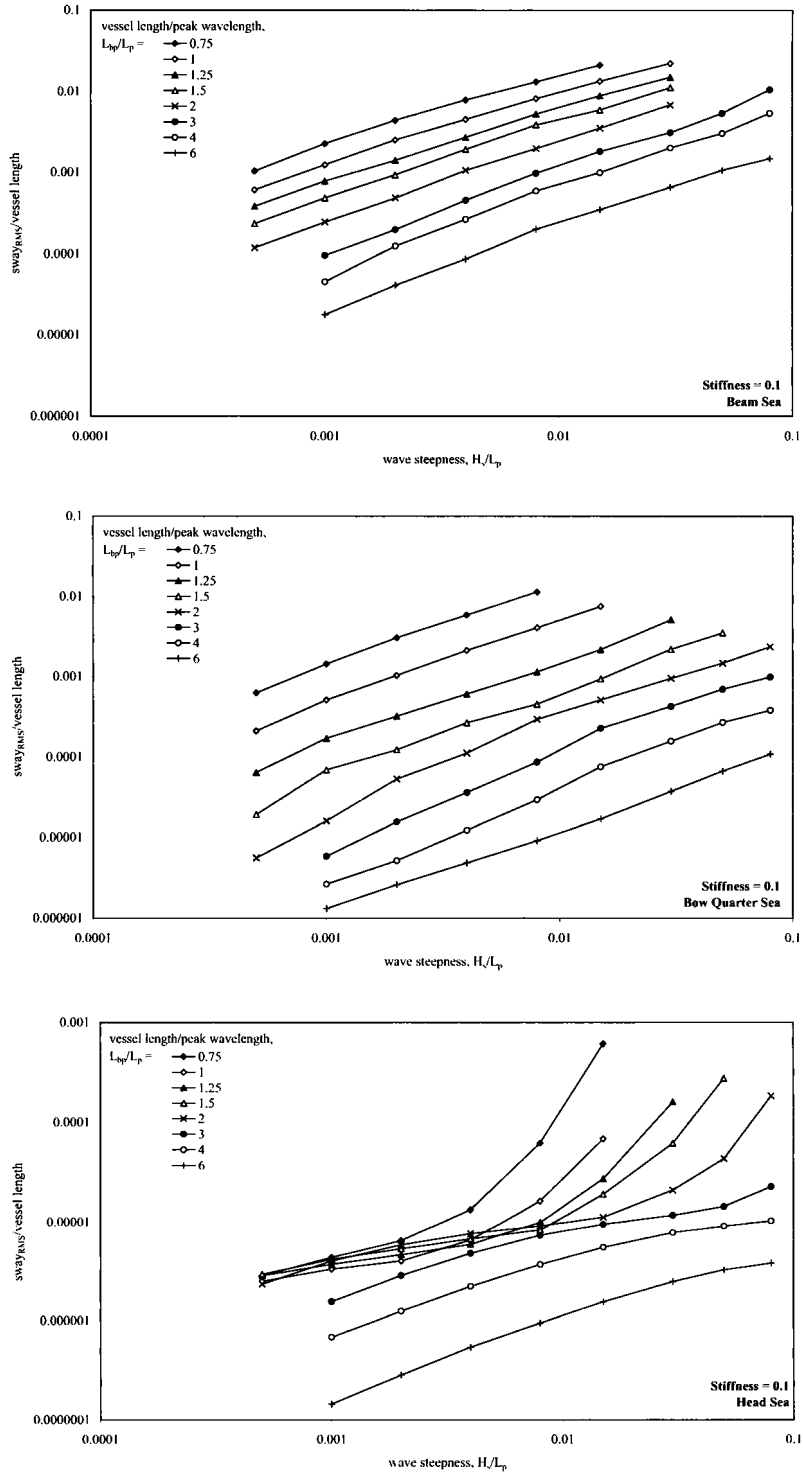
Figure 6.13.   Sway – stiffness = 0.1

Note: Graphs are provided for use in concept/feasibility design purposes only
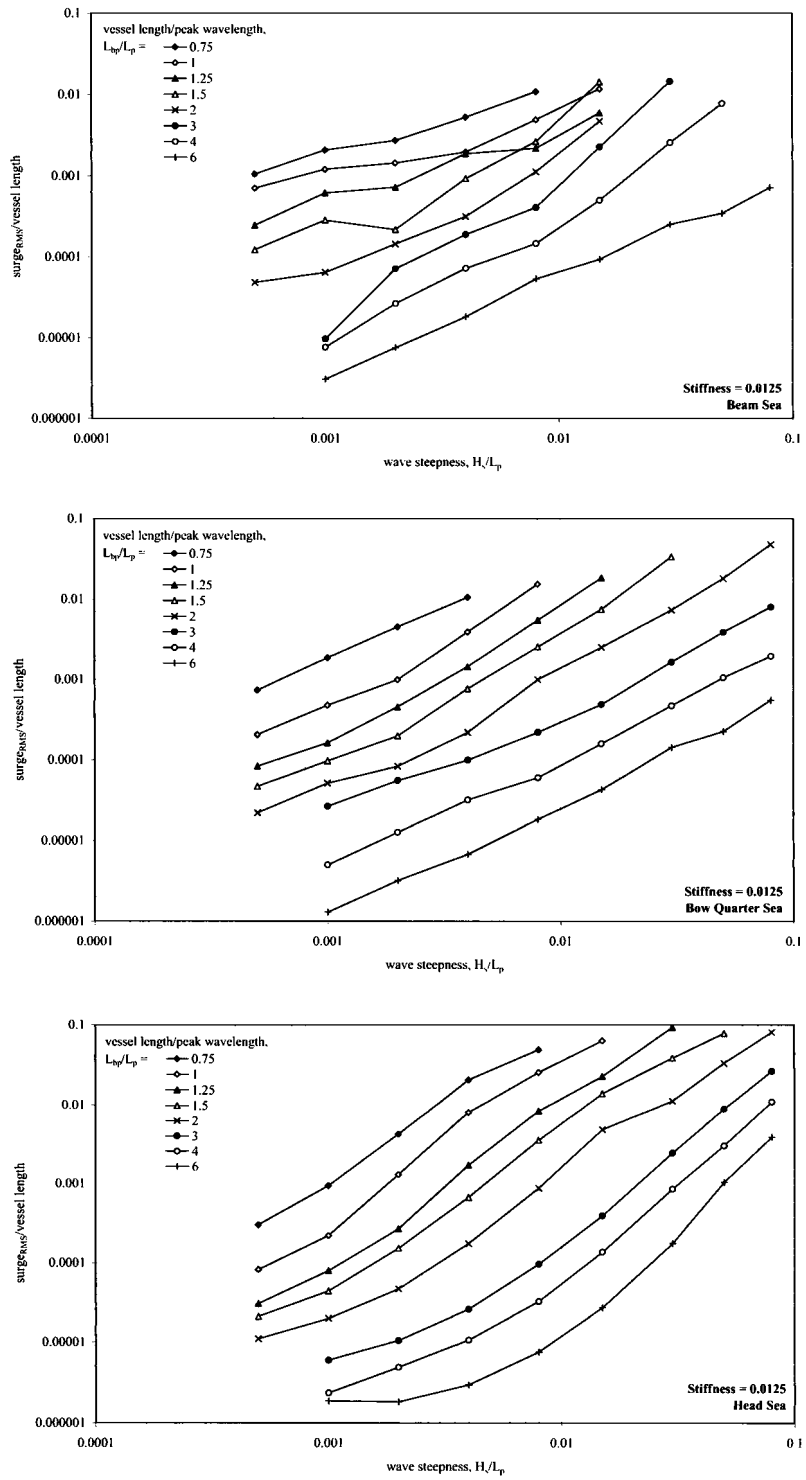
Figure 6.14.   Surge – stiffness = 0.0125

Note: Graphs are provided for use in concept/feasibility design purposes only
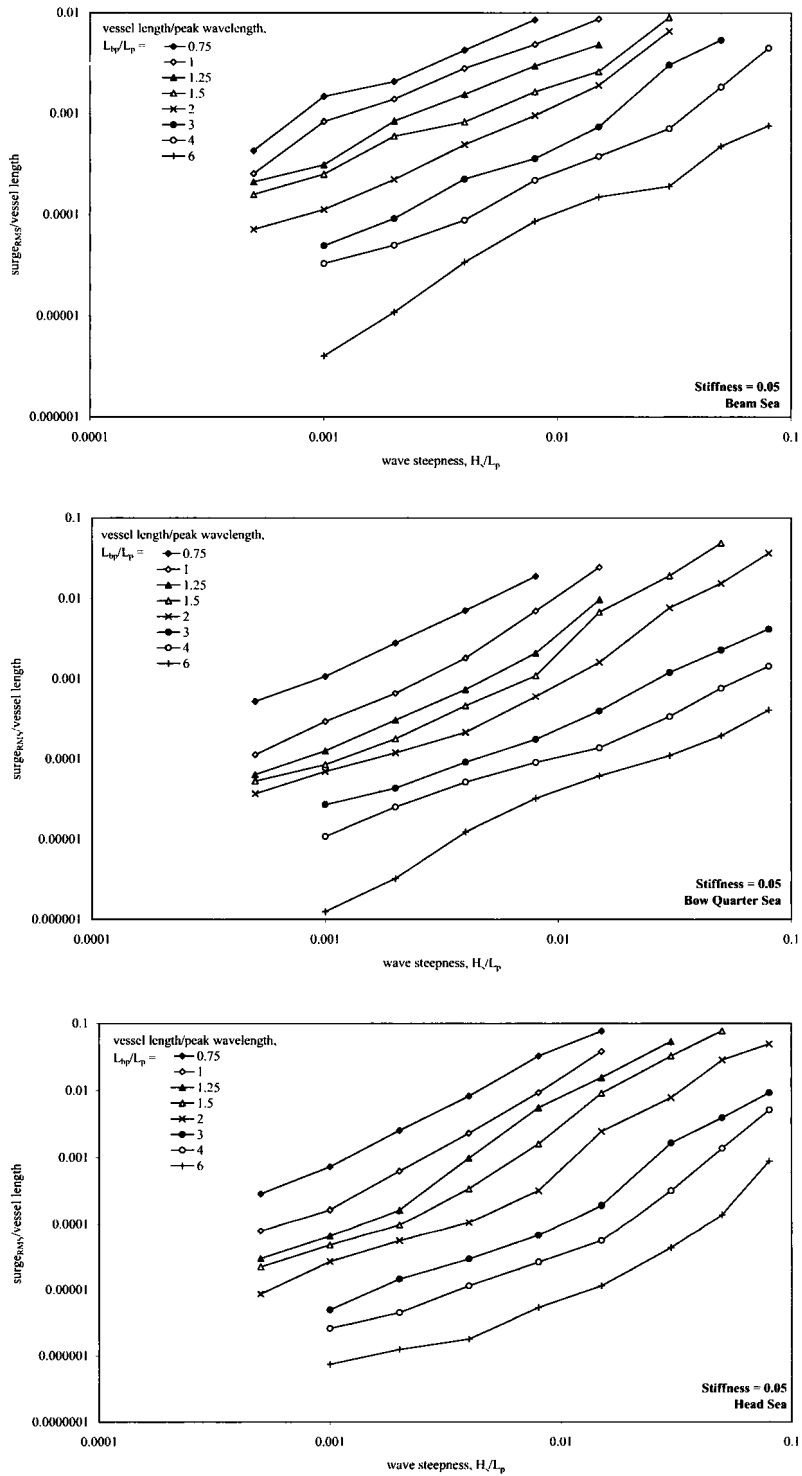
Figure 6.15.   *Surge – stiffness = 0.05*

Note: Graphs are provided for use in concept/feasibility design purposes only
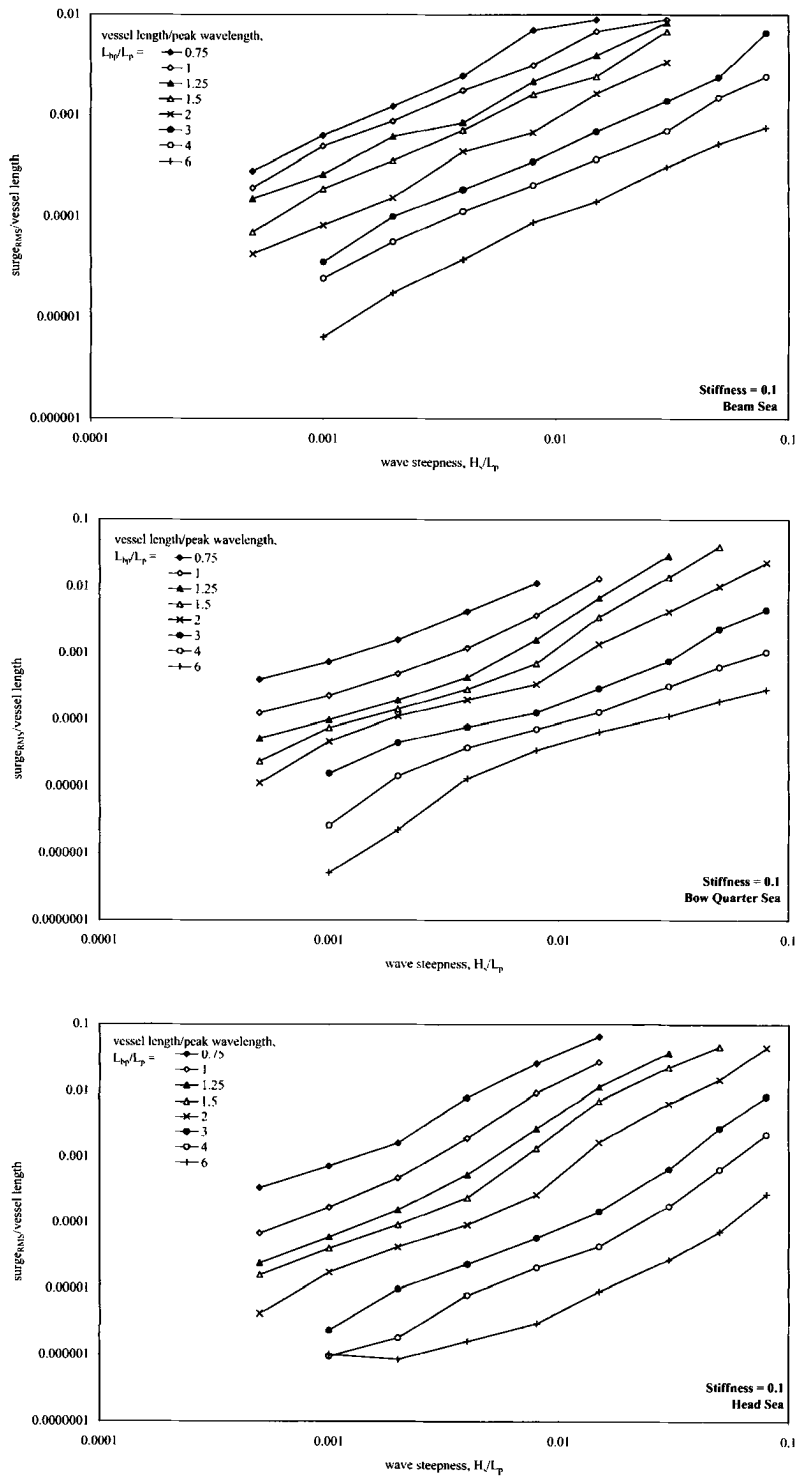
Figure 6.16.   Surge – stiffness = 0.1

Note: Graphs are provided for use in concept/feasibility design purposes only

---

Box 6.1. Worked example – calculation of mooring loads

A berth must accommodate a chemical tanker with the following characteristics:

> Deadweight tonnage, DWT = 20 000 t
> Displacement (DT) = 25 000 t
> L_{bp} = 165 m

The following frequent conditions are known to exist at the location of the berth that is sheltered by a breakwater:

> H_s = 0.32 m
> L_p = 223 m

Mooring lines have yet to be specified, so taking a representative stiffness from Table 6.1:

> Fibre rope stiffness = 11.5 t/m

Calculate the dimensionless stiffness, μ, from Equation (6.1):

$$\mu = \frac{\lambda \cdot l_{bp}}{DT} = \frac{11.5 \times 165}{25000} = \mathbf{0.076}$$

Calculate the value of vessel length(L_{bp})/peak wavelength(L_p):

$$\frac{165}{223} = \mathbf{0.74}$$

Calculate the wave steepness H_s/L_p:

$$\frac{0.32}{223} = \mathbf{0.0014}$$

Determine the most appropriate wave direction from Figure 6.3 as being '**bow quarter sea**'.

Determining forces and movements: as a dimensionless stiffness of 0.076 has been calculated the graphs corresponding to dimensionless stiffnesses of 0.05 and 0.1 are used for the lower and upper limits respectively.

Box continues

Box 6.1 Worked example – calculation of mooring loads (continued)

The following dimensionless values are obtained from the graphs.

	Softer limits	Stiffer limits
$F_{max.fender}/\Delta$	0.007	0.02
$F_{max.line}/\Delta$	0.0011	0.003
$Sway_{rms}$/vessel length (L_{bp})	0.0015	0.0025
$Surge_{rms}$/vessel length (L_{bp})	0.002	0.002

Multiplying the dimensionless forces by the displacement (DT) and multiplying the movements by the vessel length (L_{bp}) the results can be summarised below.

	Lower	Upper
$F_{max.fender}$	175 t	500 t
$F_{max.line}$	27.5 t	75 t
$Sway_{rms}$	0.25 m	0.41 m
$Surge_{rms}$	0.33 m	0.5 m

7. Scour

7.1. INTRODUCTION

The aim of this chapter is to provide the user with guidance for the prediction of scour effects around jetty piles in exposed locations. The guidance is not expected to be exhaustive but should be sufficient to identify if there is a problem and, if so, the scale of the problem. It may be that more detailed model studies will be required to investigate the problem in more detail. The reader is referred to Whitehouse (1998) for a more detailed discussion of scour issues.

A useful flowchart detailing the steps for undertaking scour calculations is given by Whitehouse (1998) and is reproduced in Figure 7.1.
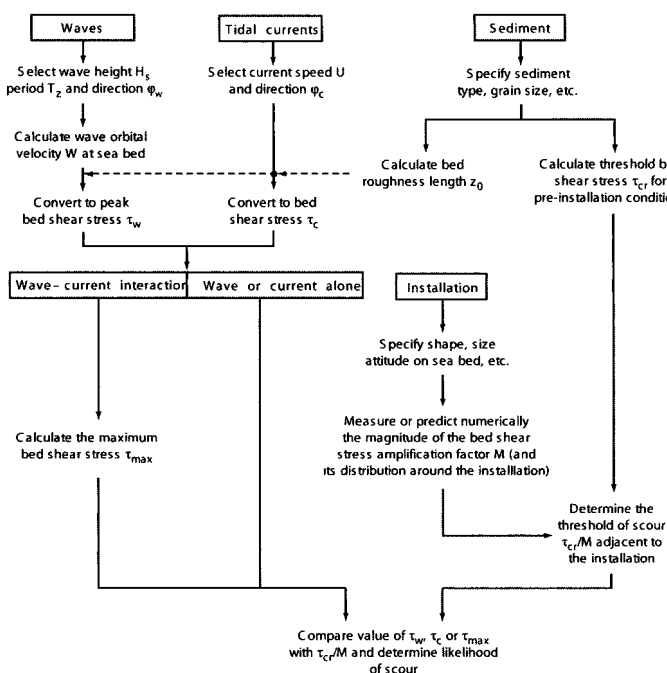
Figure 7.1.   Flowchart for scour calculations (after Whitehouse, 1998)

Much of this chapter considers the case of a single pile. Effects due to multiple pile groups are discussed in Section 7.4. Design guidance addresses waves, currents and the combination of waves and currents.

Key parameters referred to in this chapter are:

- *bed shear stress, τ_0*

- *Shield's parameter, θ,* or dimensionless shear stress, which is used to identify the onset of movement of sediment:

$$\theta = \frac{\tau_0}{g(\rho_s - \rho)d} \tag{7.1}$$

where ρ_s is the density of sediment grains, ρ is the density of water and d is the grain size.

- *Keulegan–Carpenter number, KC, which relates the magnitude of the wave orbital motion with the dimensions of the structure being considered:*

$$KC = \frac{U_w T_w}{D} \tag{7.2}$$

where U_w is the wave orbital velocity amplitude at the seabed (m/s), T_w is the wave period (s), and D is the pile diameter (m).

Reference is made to *clear water scour* and *live bed scour*. Clear water scour only occurs in the vicinity of the pile. Live bed scour occurs where the ambient shear stress, τ_0, exceeds the critical shear stress, τ_{cr}, everywhere on the bed. Clear water scour occurs when the shear stress, τ_0, is less than the critical value for sediment motion, τ_{cr}, but $M\tau_0$ exceeds τ_{cr}, where M is the shear stress amplification factor due to the pile ($M = 4$ for a single pile).

7.2. SCOUR UNDER STEADY FLOW

The scour around a slender cylindrical pile diameter, D, on a sand bed in a steady unidirectional flow with velocity, U, and flow depth, h, has been examined by many authors in relation to river engineering, as summarised by Whitehouse (1998). The scour development around this simplest of structures provides a benchmark that can be adopted and extended to more complex cases with different shapes, time-varying flow, etc. The pile is considered to be slender when the pile diameter to water depth ratio $D/h < 0.5$. In practice, this is the case for many exposed jetties constructed in the coastal region.

7.2.1. Scour pattern

Laboratory observations indicate that scouring of sediment at single piles initially takes place in two shallow depressions situated at 45° either side of the centreline of the cylinder. These observations correlate closely to patterns of shear stress amplification measured by Hjorth (1975) (see Whitehouse (1998)).

The scoured areas coalesce with time, forming a conical shaped hole around the entire cylinder of nearly constant depth and with side slopes at near the angle of repose for the sediment bed material (generally 25° to 35° for sand) (see Figure 7.2). Scour depressions reducing in depth in the streamwise direction are formed either side of the cylinder. The sediment removed from around the pile is deposited between these two depressions in the 'shadow' of the pile and at the downstream extent of the wake vortex system (Figure 7.3).
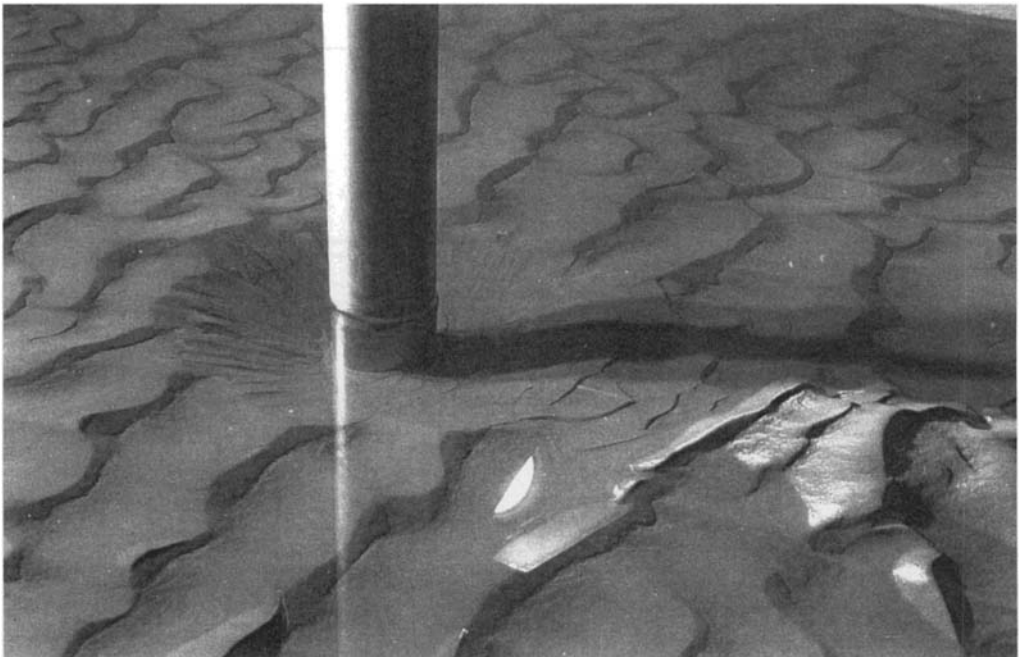
Figure 7.2.   Scour around a pile due to steady flow from left to right: clear-water scour $U/U_{cr} \approx 0.9$ (reproduced by permission of BP International Ltd.)

The magnitude and extent of the flow field that controls the depth of scouring S is in the region ±60° from the flow axis around the periphery of the cylinder. The final extent, $x_{s,}$ of the scour pit from the cylinder wall is controlled by the angle of repose of the sand ϕ, i.e. $x_s = S_e/\tan \phi$. Typically $S_e = 1.3D$ (as shown in Figure 7.4) and $\phi = 30°$ giving

$$x_s = \frac{1.3D}{\tan 30°} \rightarrow 2.25D \cdot \tag{7.3}$$

Thus the overall diameter of the scour pit will be around $6D$, including the pile.
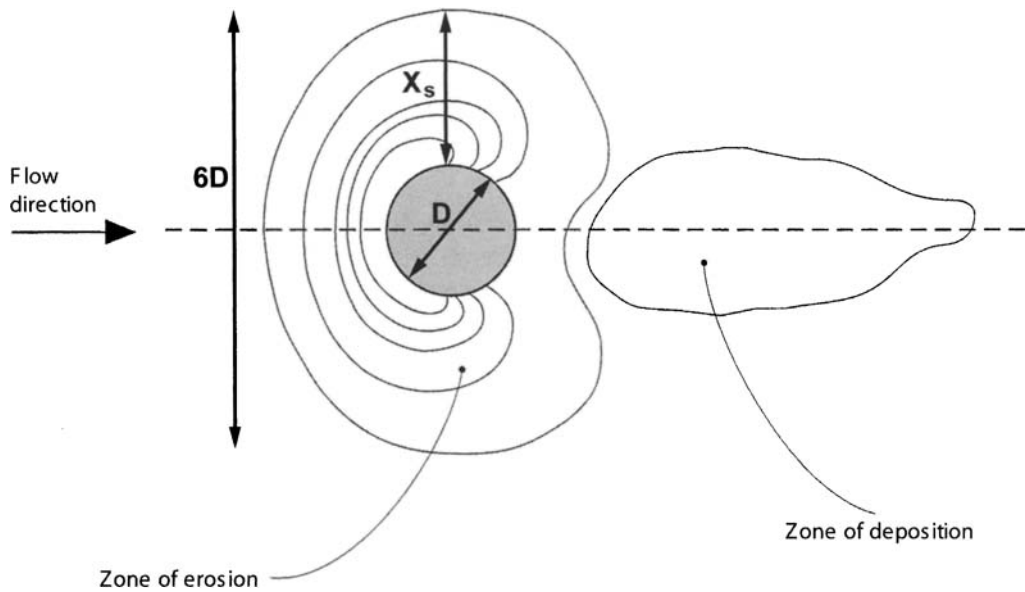
Figure 7.3.   Characteristic equilibrium scour hole pattern for a vertical cylinder in steady flow
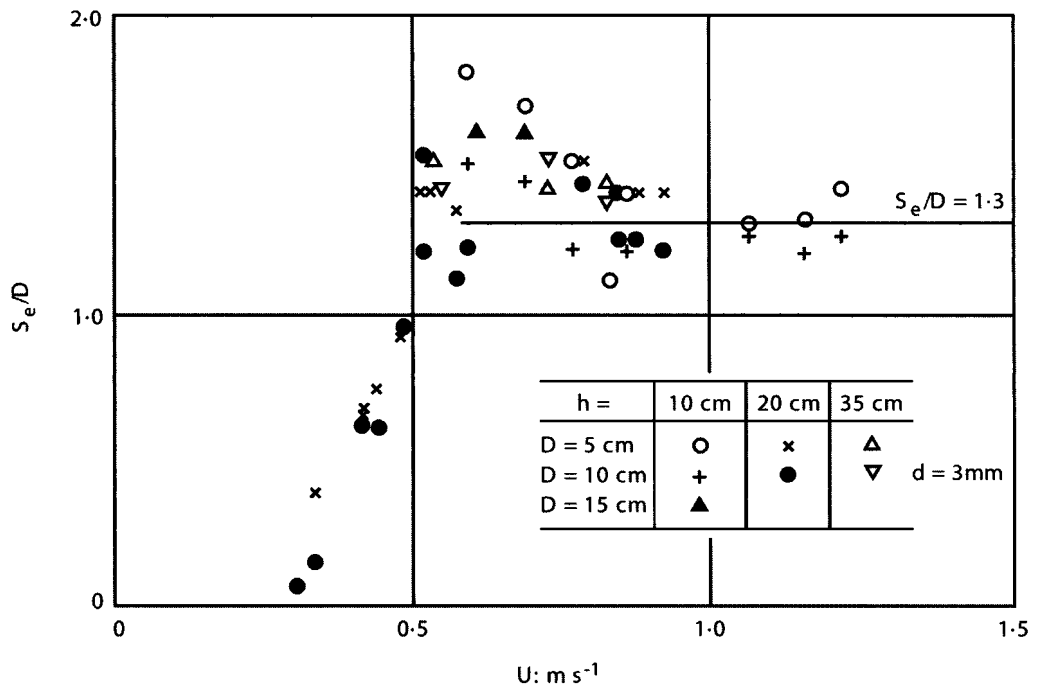
Figure 7.4.   Variation of scour depth with flow speed (reproduced from Breusers, 1972, by permission of Delft Hydraulics)

Figure 7.5.   Shellhaven Refinery. Relatively sheltered environment where peak currents are typical 1–1.5 m/s (courtesy Costain)

7.2.2. Scour depth

The depth of scour at a pile is generally assumed to scale with the diameter of the pile D (Carstens, 1966; Breusers, 1972). The equilibrium value of the scour depth, S_e, increases linearly with increasing flow velocity, U, (Figure 7.4) and therefore increasing shear stress, τ (Figure 7.6). The equilibrium scour depth increases from zero at $\tau_0 = \tau_{cr}/M$ to $\tau_0 = \tau_{cr}$, where the amplification factor $M = 4$ for a single pile.
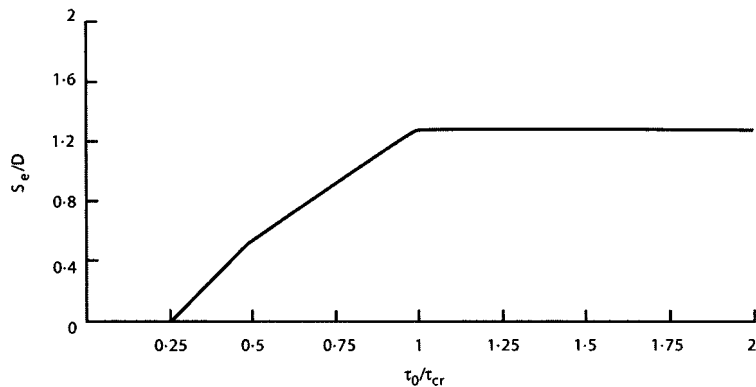
Figure 7.6.   *Scour development at a single pile in steady flow: variation of equilibrium scour depth with shear stress*

For larger values of τ_0 the variation in the equilibrium scour depth with increasing τ_0 is relatively constant, possibly with a 10% reduction (Breusers and Raudkivi, 1991) or a periodic fluctuation related to the passage of ripples through the scour hole. The fluctuation in the scour depth due to the passage of large bedforms should be taken into account as the scour depth could fluctuate by ±50% of the bedform height. The bedform height can be calculated using the methods given in Soulsby (1997).

Published results, as discussed by Whitehouse (1998), indicate some variation in maximum equilibrium scour depth, from less than $S_e = 1.0D$ up to $S_e = 2.4D$, which is considered to be conservative.

Individual sets of measurements have tended to produce quite reasonable trends for the variation of S_e/D with increasing velocity (10% error) but when a compilation of data is examined the scatter is much larger. Imberger *et al* (1982) collected data from laboratory tests for two different sediment and pile diameter combinations and combined their results with the data from five previous studies. The comparison suggested a scatter of 50% from a best fit line to the scour depth data as a function of the ratio u_*/u_{*cr}, where the shear velocity u_* is defined as $(\tau_0/\rho)^{0.5}$. This scatter is most likely due to the uncertainty in the values of u_* and u_{*cr}. A graph showing this comparison of results is presented by Whitehouse (1998). A step-by-step methodology for calculation of the depth of scour due to a steady current is given in Box 7.1.

Box 7.1. Calculation of scour depth due to steady current for single pile
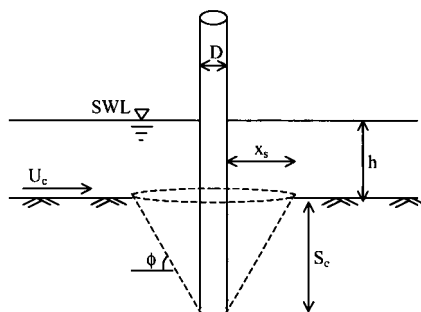
1. Identify input parameters:

   - current velocity (depth-averaged), U_c (m/s)
   - pile diameter, D (m)
   - grain size, d_{50} (m) and density of sediment grains, ρ_s (kg/m^3)

2. Calculate drag coefficient, C_d, for hydraulically rough flow:

   $$C_d = [0.4/\{ln(h/z_0)-1\}]^2 \tag{i}$$

   where $z_0 = 2.5d_{50}/30$ \hfill (ii)

3. Calculate bed shear stress, τ_0:

   $$\tau_0 = 0.5\rho C_d U_c^2 \tag{iii}$$

4. Calculate Shield's parameter θ:

   $$\theta = \tau_0/g(\rho_s-\rho)d_{50} \tag{iv}$$

5. Calculate critical Shield's parameter θ_{cr}, using method of Soulsby (1997) for $D^* < 10$ (fine sand):

   $$\theta_{cr} = [0.30/(1 + 1.2D^*)] + 0.55[1-\exp(-0.02D^*)] \tag{v}$$

   or for $D^* > 10$ use:

   $$\theta_{cr} = 0.24/D^* + 0.55[1-\exp(-0.02D^*)] \tag{vi}$$

   where $D^* = d_{50}((\rho_s/\rho - 1)g/v^2)^{1/3}$ \hfill (vii)

   v = kinematic viscosity of water = 1.17×10^{-6} m^2/s for seawater at 16°C

Box continues

Box 7.1. Calculation of scour depth due to steady current for single pile (continued)

6. Check parameter range and calculate equilibrium scour depth, S_e:

$S_e = 1.3D$ for $\theta/\theta_{cr} > 1$ (viii)

$S_e = 1.3 [2(\theta/\theta_{cr})^{1/2}-1.0] D$ for $0.25 < \theta/\theta_{cr} < 1$ (ix)

It should be noted that there is a high degree of uncertainty in scour depth as illustrated by Figure 7.4 and S_e/D may reach values of up to 1.9.

7.3. SCOUR DUE TO WAVES

7.3.1. Scour pattern

Where the cylinder diameter is less than 20% of the local maximum wavelength of the sea surface waves (or bottom orbital velocity amplitude) the effects of wave diffraction are minimal. The scour pattern proceeds first with the development of scour depressions either side of the pile, at 90° to the centreline of the cylinder (Sumer *et al*, 1992; Abou-Seida, 1963).

Ultimately the scour pattern is not too dissimilar to the current only case, but without the pair of shallow streamwise depressions extending downstream. The wave-induced scour pattern for a square pile is similar to the circular pile case (Sumer *et al*, 1993).

7.3.2. Scour depth

The scour depth in oscillatory wave flow has been examined in several papers but the most comprehensive study was by Sumer *et al* (1992). Most authors agree that the local scour around a pile due to waves is smaller than the steady current value. Based upon extensive laboratory data, Sumer *et al* correlated the equilibrium scour depth with the Shield's parameter and the Keulegan–Carpenter (KC) number. Live-bed scour data ($\tau_w > \tau_{cr}$) demonstrated first that the equilibrium scour depth due to waves is considerably smaller than due to a steady current, i.e. $S_e/D < 1$ for KC < 55, and second that there is a good correlation between the scour depth and the KC number (Figure 7.7). The relationship is approximated by:

$$\frac{S_e}{D} = 1.3\{1 - \exp[-0.03(KC - 6)]\}, \quad \text{for KC} \geq 6. \tag{7.4}$$

The scour depth is negligible for KC <6. The scour depth for large KC numbers, greater than 100, is similar to the steady flow value of 1.3D. This limiting value of KC below which the influence of the reversing flow becomes significant was also quoted by Breusers and Raudkivi (1991). A step-by-step methodology for calculating scour depth due to waves is given in Box 7.2.
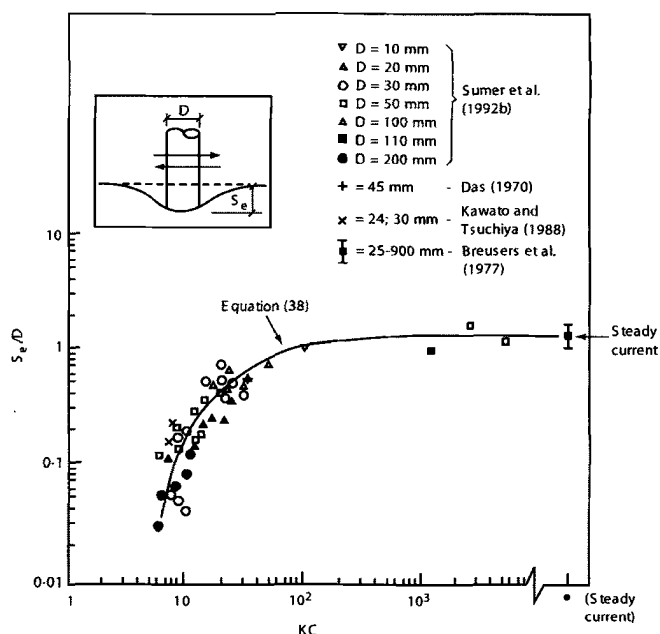
Figure 7.7.   Correlation between equilibrium scour depth at circular pile and Keulegan–Carpenter number: live-bed conditions (reproduced from Sumer et al, 1992, by permission of the ASCE)

Box 7.2. Calculation of scour depth due to waves for single pile
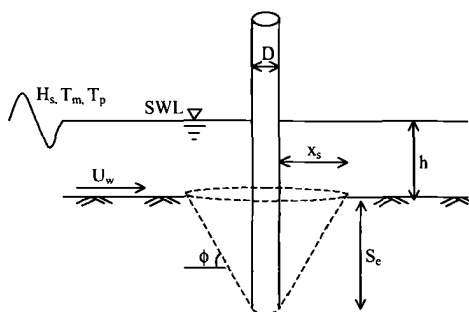
1.   Identify input parameters:
    wave height, H_s (m), wave period, T_m or T_p (s), water depth, h (m)
    pile diameter, D (m)
    grain size, d_{50} (m) and density of sediment grains, ρ_s (kg/m^3)

Box continues

Box 7.2. Calculation of scour depth due to waves for single pile (continued)

2. Calculate wave orbital velocity at seabed, U_w:

$$U_w = \pi H_s / [T_p \sinh(2\pi h / L_p)] \qquad\qquad (i)$$

3. Calculate bed shear stress, τ_0:

$$\tau_0 = 0.5 \rho f_w U_w^2 \qquad\qquad (ii)$$

where $f_w = 1.39 (A/z_0)^{-0.52}$ (iii)

$\qquad\quad A = U_w T_p / 2\pi$ (iv)

$\qquad\quad z_0 = 2.5 d_{50} / 30$ (v)

4. Calculate Shield's parameter θ:

$$\theta = \tau_0 / g(\rho_s - \rho) d_{50} \qquad\qquad (vi)$$

Calculate critical Shield's parameter θ_{cr}, using method of Soulsby (1997) for $D^* < 10$ (fine sand):

$$\theta_{cr} = [0.30/(1 + 1.2 D^*)] + 0.55[1 - \exp(-0.02 D^*)] \qquad\qquad (vii)$$

or for $D^* > 10$ use:

$$\theta_{cr} = 0.24/D^* + 0.55[1 - \exp(-0.02 D^*)] \qquad\qquad (viii)$$

where $D^* = d_{50}((\rho_s/\rho - 1)g/v^2)^{1/3}$ (ix)

v = kinematic viscosity of water = 1.17×10^{-6} m^2/s for seawater at 16°C

5. Calculate Keulegan–Carpenter number, KC:

$$KC = U_w T_w / D \qquad\qquad (x)$$

6. Calculate equilibrium scour depth, S_e:

$$S_e = 1.3\{1 - \exp[-0.03(KC - 6)]\}D \text{ for } KC > 6 \qquad\qquad (xi)$$

$$S_e = 1.3D \text{ for } KC > 100 \qquad\qquad (xii)$$

7. Consider storm effects – scour depth at peak of storm may be significantly greater, see Section 6.3.4, which suggests maximum scour depth during storm is 4 to 7 times greater than that at end of storm.

Tests performed by Sumer *et al* with KC > 1000 indicate that the maximum scour depth in a tidally reversing flow is also similar to the steady flow value

(Equation (7.4)), although the role of backfilling of scour holes on alternate tides is not explicitly addressed.

The effect of pile cross-sectional shape has been studied by Sumer *et al* (1993) in tests on circular piles and square piles at orientations of 90° and 45° (corner into flow). The data indicate that the equilibrium scour depth for KC > 100 approaches a constant value of $S_e/D = 1.3$ for circular piles and $S_e/D = 2$ for square piles. This is a 50% increase in the wave-induced scour depth at a square pile as opposed to 30% for the steady flow case (Section 7.2.5). The variation in scour depth with KC number for the different pile shapes/orientations was more complicated for KC < 100.

Discussion of the temporal development of scour due to waves is given by Whitehouse (1998).

7.3.3. Breaking waves

The main effect of breaking waves in the sea is to provide an additional source of turbulence in the water column. If the water depth is shallow enough to cause wave breaking (Southgate, 1995), the extra turbulence will enhance the suspended sediment-carrying capacity of the flow. Bijker and de Bruyn (1988) measured greater scour depths (up to $S_e/D = 1.9$) when breaking waves were superimposed on a current, i.e. 46% larger than the current-only situation. The available data on this topic are sparse.

7.3.4. Storm effects

In general there is a lack of published investigations on the effect of storms on scour at piles. Interesting experimental results have been reported by Di Natale (1991) who measured the time variation in the scour depth at a pile during the passage of a storm. The results from the experiments showed that the peak of the scour development was out of phase with the peak of the storm and that the maximum scour depth recorded during the storm was considerably different (4 to 7 times greater) than that observed at the end of the storm, i.e. backfilling had taken place after the storm had passed.

7.4. EFFECT OF COMBINED WAVES AND CURRENTS

7.4.1. Scour depth

The effect of the combination of waves and a steady current on local scour depth is still unclear. It is generally agreed that the rate of scour in wave-current flow is enhanced. Kroezen *et al* (1982) state that the influence of waves on the scouring rate is of great importance when the steady current alone is too weak to cause scour. Further discussion on studies of the combined effects of currents and waves on scour depth is given in Box 7.3.

> **Box 7.3. Effect of combined waves and currents on scour depth**
>
> Bijker and de Bruyn (1988) found that there was a greater increase in the wave plus current shear stress in the area upstream of the pile than in the vicinity of the pile. They noted that the enhanced transport of sediment towards the pile actually led to a reduction in the scour depth. For the live-bed case they found a maximum scour depth to pile diameter ratio S_e/D of 1.3 for a current alone and 1 to 1.1 for a current and non-breaking waves. Chow and Herbich (1978) found the scour depth in co-linear wave-current flow was 10% deeper than the current-only case. Clark and Novak (1984) determined the maximum equilibrium scour depth (live-bed scour) in laboratory flume experiments with co-linear waves and currents as $1.7D$. Armbrust (1982) found that for large current speeds, relative to the wave orbital velocities, wave action appears to increase the scour depth substantially. Thus it appears that the ratio of wave to current speed as well as their magnitudes influence the scour development in wave-current flow.

7.4.2. Scour pattern

The local scour pattern formed by a co-linear wave-current flow is probably similar to the current-alone case, although the overall scour pattern produced by wave-current flows crossing at other angles will be more complex. This is because the net transport of sediment entrained from the bed by the wave motion will be more or less in the direction of the tidal current.

Bijker and de Bruyn (1988) found the scour hole extent x_s was $3D$ upstream and $5D$ downstream for the current-alone case and this was increased by wave-current flow to $4D$ and $6D$ respectively.

7.5. OTHER INFLUENCES

7.5.1. Time variation of scour

For a given set of environmental conditions the scouring of the sandy sediment at structures initially occurs rapidly but then approaches its ultimate (equilibrium) value asymptotically (Figure 7.8). Whitehouse (1998) discusses methods for assessing the temporal development of scour. As the (maximum) equilibrium scour depth will normally be used in design, the variation of scour depth with time is not considered further here, although the discussion on storm effects in Section 7.3.4 should be considered.
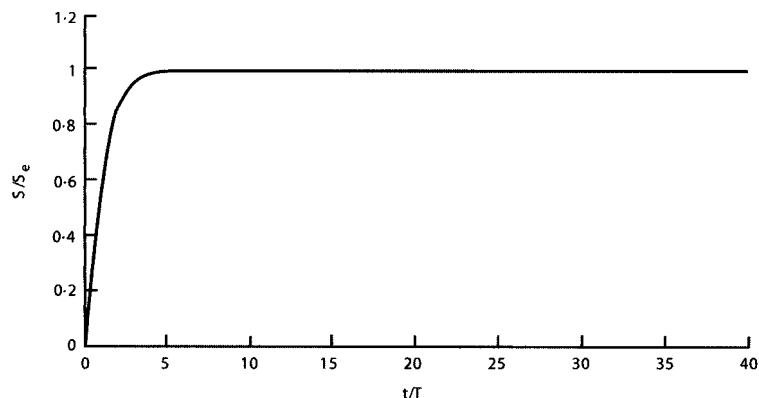
Figure 7.8.   Time variation of scour

7.5.2. Influence of water depth

It is almost certain that some of the scatter in published scour depth data, such as shown Figure 7.4, will be attributable to the effect of shallow water. The effect of water depth on the scour depth at cylindrical piles is generally agreed to be negligible for values of the ratio $h/D > 3$ (see Breusers, 1972; May and Willoughby, 1990; Yanmaz and Altinbilek, 1991). Deep water corresponds to $h/D \geq 5$. Although the measured scour depth is reduced for values of $h/D < 3$, this reduction factor is not of practical significance for most piled structures in the marine environment as typically $h \gg D$.

7.5.3. Pile shape

The effect of pile cross-sectional shape on the equilibrium scour depth has been studied in steady flow experiments (Breusers and Raudkivi, 1991; May and Willoughby, 1990). Taking the scour depth at a circular pile as reference the equilibrium scour depth multiplier for square piles has been determined as 1.3, e.g. $S_{e(square)} = 1.3 S_{e(circular)}$. Attempts at streamlining, for example as for bridge piers in rivers, can achieve a reduction in the scour depth (multiplier = 0.75) but this reduction cannot generally be taken advantage of in the offshore environment due to the effect of the reversing tidal current. The effect of cross-section shape on wave-induced scour is discussed in Section 7.3.2.

7.5.4. Sediment gradation

Studies by Breusers and Raudkivi (1991) to determine the effect of sediment size and gradation on the scour depth have indicated that scour depth will not be limited by the grain size provided that $D > 50d_{50}$. Where the grain size of the natural bed material is very much smaller than the typical diameter of the pile and the bed material tends to

be well sorted, the limiting influence of grain size and grading on scour is probably negligible.

7.5.5. Cohesive sediment

The individual sand particles will be subjected to cohesive forces when the sediment contains more than 10% by weight of cohesive silt sized material. The effects of the cohesion are to increase the resistance of the bed to scour (Mitchener *et al*, 1996) and to produce a more complex shaped scour hole with sideslopes that are steeper than the angle of repose for the constituent sand. The mode of sediment transport for layered mud:sand beds will alternate between suspended and bedload transport as different layers are eroded.

7.5.6. Effect of resistant bed layer

Where a pile of diameter D has been driven in an area with a veneer of erodible sand that is less than $1.0D$ to $2.4D$ thick overlying a resistant layer, e.g. stiff clay, the depth of scouring can be limited. If the resistant layer outcrops upstream of the installation, the sediment load in the flow as it approaches the pile might be lower than the equilibrium carrying capacity of the flow. The significance of this situation is that the flow will have a larger scouring potential than if it was already carrying sediment.

7.5.7. Influence on pile fixity

Studies have shown that the reduction in pile fixity due to the scour around single piles is not as significant as for pile groups (Diamantidis and Arnesen, 1986).

7.6. MULTIPLE PILE GROUPS

In the case of pile clusters, group effects become important, as does the angle of orientation of the pile cluster to the prevailing direction of waves and currents. The main factors to consider are flow interference leading to enhanced flow speeds or turbulence at adjacent piles in some cases and sheltering of piles in others.

7.6.1. Linear arrays of piles

The effect of pile spacing on the scour depth in a steady current has been investigated by various authors in the literature. A summary of these results is given in Table 7.1 for different pile spacings and orientations. For a line of piles, perpendicular to the flow, relative scour depth increases as pile spacing decreases until it exceeds two times the value for the single pile (i.e. proportional to the projected area of the pair of piles).

Table 7.1.   Linear array of piles perpendicular to flow: effect on scour depth in a steady current

Pile spacing	Scour depth at each pile	Reference
single pile	S_e	(see Box 6.1 for derivation of S_e)
>6D (for square piles >5D)	S_e	Breusers (1972); Hirai and Kurata (1982); Basak et al (1975)
2D	$1.4S_e$	Hirai and Kurata (1982)
<2D	$2S_e$	

Interaction effects have also been observed for piles aligned parallel to the flow. Experiments have shown that for pile spacings in the range $1.5D$ to $4D$ the scour depth around the upstream pile was increased by 10% to 20% (Hirai and Kurata, 1982). When the spacing was increased to $6D$ the scour depth at the aft cylinder was reduced to 60% of the single cylinder value as a result of the deposition of scoured sediment taking place in this region.

7.6.2. Pile clusters

The scour interaction of groups of piles can be estimated in many cases from the published literature. Experiments on the scouring pattern obtained both within and downstream from 3×3, 5×3 and 7×3 groups of square, octagonal and hexagonal cross-section piles have been reported by Mann (1991). These experiments used a thin layer of sand on the bed of a flume as a tracer material to indicate the area of the bed that was scoured from around the pile groups and the results were presented in terms of a scour ratio (SR = ratio of scoured area of bed to group area of pile array). The observed value of SR for the 3×3 pile group in head-on flow varied with the pile spacing (centre to centre) is given in Table 7.2.

Table 7.2.   Effect of linear arrays of piles on scour depth (3 ×3 array) after Mann (1991)

Spacing	SR = ratio of scoured area of bed to group area of pile array
3D	1.8
6D	0.9
9D	0.3

The variability in the scour pattern under different angles of attack was also investigated. The value of SR tended to be larger for the case where the array was rotated 45° to the approach flow.

The clear-water scour depth at a group of three cylindrical piles angularly spaced at 120° was studied by Vittal *et al* (1994) with the gap set so that any one of them

could just pass through the gap between the other two (i.e. gap = 2*D*). The scour depth at the pile group due to a steady current was about 40% smaller than the scour depth at a single pile with diameter equal to a circle circumscribing the pile group. The scour depth varied by only 6% with variations in the angle of attack of the flow.

Scour at groups of 3, 4 and 6 piles was investigated in a wave flume by Chow and Herbich (1978). Results obtained indicated an increase in scour depth as pile spacing reduced from 8*D* to 4*D*.

7.6.3. Field observations

The potential for large overall scour depths around piled jetties has been illustrated well by bathymetric data measurements for the research pier at Duck, North Carolina (see Whitehouse, 1998). Field observations of scour at piled structures in the coastal zone can be made at low tide although the influence of shallow water effects in modifying the scour holes local to the pile could be significant as the tide recedes prior to observation. The presence of latticework and cross-bracing can lead to an increase in the levels of flow turbulence around the platform which may contribute to scour.

Figure 7.9.   Jetty under construction. Pile installation can also cause immediate scour or weaken the soil properties around the pile, resulting in longer term scour (courtesy Doug Ramsay)

Figure 7.10. Sedimentation can also affect the usability of the jetty! (courtesy Doug Ramsay)

8. Other design and construction issues

This guidance document focuses on the hydraulic loading exerted upon exposed jetties in the marine environment, as opposed to other design loads which must be considered, and the related design and construction issues. However, many of these issues are heavily interrelated and it would be inappropriate to consider hydraulic loading in complete isolation during the design and construction process. This chapter is therefore intended as an *aide-mémoire* of the key design and construction issues to be considered by the designer.

8.1. KEY CONSTRUCTION ISSUES

8.1.1. Seek contractors' views

Marine construction costs will be heavily dependent on plant costs and their associated downtime rather than direct material costs. Therefore, any optimisation of the structure should be driven by the contractors' plant availability and working methods. For example, it would be inappropriate to include large heavy piles or precast elements in the design if it is beyond the lifting limitations of locally available plant. It is recommended that designers seek advice on construction issues and working methods from prospective contractors. Early involvement of the contractor will help to manage risks during the project development.

8.1.2. Temporary instability

Exposed jetties are usually constructed from floating marine plant, jack-up platforms or using hand-over-hand construction from the landward side (see Figure 8.2). The completed permanent works provide the necessary bracing. In these exposed locations there is often little potential for the contractor to provide temporary bracing to the structure. The temporary stability and environmental loadings applied to the individual structural members during construction can be a greater problem for the

designer than that of the design loading for the permanent works. Caution should therefore be exercised when optimising the design of the structure to accommodate the maximum permanent works loading without giving due consideration to its impact on the temporary construction phase design case.

Figure 8.1. *Aqaba jetty under construction (courtesy Mott MacDonald and C J Associates)*

Figure 8.2. *A 2.4 km jetty and travelling gantry being constructed at Abbot Point Port Development, Queensland, Australia, to handle 8 million tonnes of coal for export to Japan (courtesy Costain)*

8.1.3. Formwork and temporary bracing

The designer should recognise that hydraulic loads may be applied to the formwork and temporary bracing during construction as well as the permanent works. Whilst the selected return period may be smaller for the temporary works, these elements, unless well designed, are very vulnerable to wave action. Alternatives such as permanent formwork may be considered.

Figure 8.3.   Sri Racha Jetty, Thailand, under construction. Use of precast pilecaps allowed infill concrete to be poured without the need for complicated shutters (courtesy Kier)

8.1.4. Modular construction

Exposed jetties by their nature tend to be long structures with repetitive construction details. It is therefore essential that modular construction be maximised to reduce time and associated costs of working in and over water. A jetty being constructed in a modular fashion is shown in Figures 8.3 and 8.4. This issue will reduce the potential to excessively refine the structural elements (such as beams, deck slabs and reinforcement) over the length of the structure to accommodate different exposure levels. However, some optimisation can be accommodated through alterations in the percentage of reinforcement in concrete elements or alterations in the steel section weights as in the case of steel beams rather than adjusting the section sizes themselves. The ability to install quickly using prefabricated elements may result in cost savings, even if the initial material costs are higher than for alternative construction approaches.

Figure 8.4.   Construction of jetty at Banjul, Gambia. The design made use of precast elements to allow modular construction (courtesy Kier)

8.1.5. Constructability

It is critical that achievable tolerances are built into the design, bearing in mind the construction location. This will help avoid unnecessary time delays and resulting cost increases as a result of impractical degrees of accuracy being set. Working closely with the contractor, as discussed in Section 8.1.1 will help to achieve this.

8.1.6. Dangers of relying on airgap

Often designers try to avoid the wave slam problem by raising all the horizontal and other bracing elements above the level of the maximum wave excursion and providing an air gap as a margin of safety (see Section 4.5.2). However, there is often still a requirement for low level tug and small boat berths as well as maintenance access points along the structure that cannot be raised above the level of maximum

wave excursion. Therefore, there may still be a necessity to design for these large wave slam loads at certain locations even if the majority of the structure can be raised up and a safe airgap provided.

8.1.7. Elements designed to fail

Where excessive loading is calculated it may be appropriate for the designer to design the non-critical element to fail when overloaded rather than trying to design the structure to withstand all extreme design events. For instance, low level tug berth fender panels could be designed with a weak element which is designed to fail under the 1:100 year event wave slam. This prevents the surrounding structure from being excessively loaded. However, extreme caution is necessary when applying this technique to ensure that safety of personnel is not compromised. The potential effects on the rest of the structure should also be considered for the scenario where the weak element does not fail (especially as it is very difficult to accurately predict when and how any weak element will fail). Consideration should also be given to the environmental impact of adopting this approach.

8.1.8. Operational limits of marine plant

The inherent exposure of these structures means that the construction plant can be susceptible to significant downtime during construction. Most floating marine plant will have difficulties in operating effectively in significant wave heights of greater than 1 m and find it very difficult to operate at all at significant wave heights greater than 2 m. Small floating plant may find difficulty in operating in much lower wave heights where long period swell conditions exist. Jack-up platforms can operate at greater wave heights but are still vulnerable when being moved between location and during jacking up out of the water or lowering back down into the water. A walking jack-up platform exposed to wave action is shown in Figure 5.1.

8.1.9. Construction schedule

It is unlikely that refinements to the design that only reduce material quantities will have a significant impact on the total capital construction costs. Optimising the construction period will produce much greater cost savings both in terms of plant costs and benefits to the client of opening the facility ahead of schedule. The construction programme should be regularly reviewed as part of the risk management approach.

8.1.10. Capital versus maintenance costs

Facility owners will generally seek to reduce the total costs of the facility. However, in practice there is often a focus on reducing capital construction cost, with a resulting increase in maintenance costs which will occur once the facility is in operation and

can be offset against the revenue at that stage. It should be noted that there may be a requirement for downtime at the berth due to maintenance, which will potentially have an impact on berth operations.
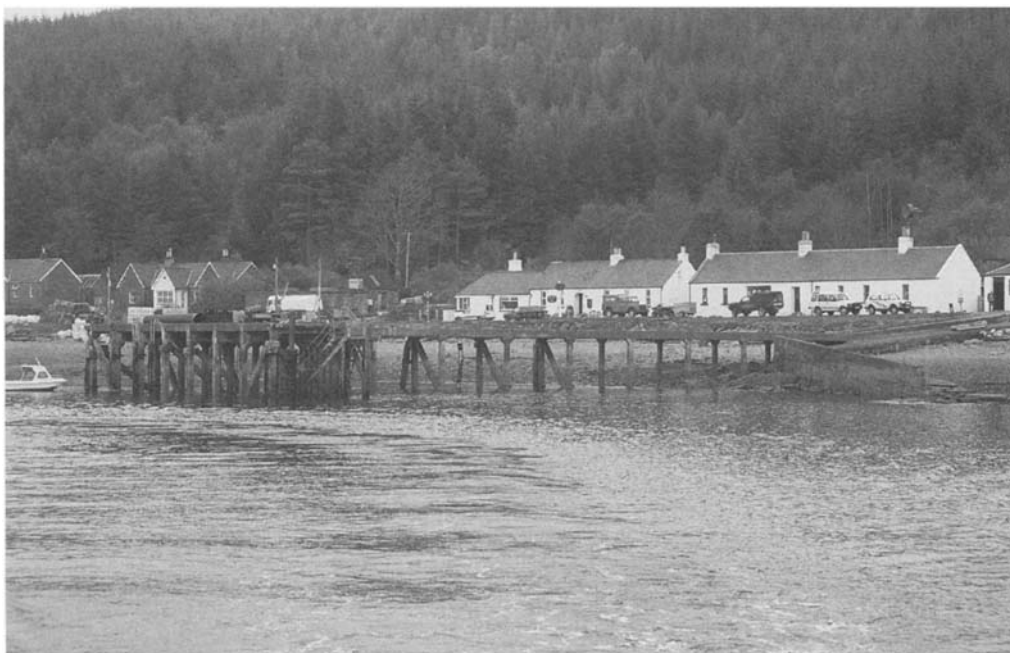
Figure 8.5.   Inverie jetty, UK (courtesy Doug Ramsay)

8.2.   KEY MAINTENANCE ISSUES

8.2.1. Location of plant, conveyors and pipelines

Whilst it may be possible to design the main deck structure to be positioned at a relatively low level, it should be noted that equipment such as plant, conveyors and pipelines will be more susceptible to damage from even relatively benign wave action at such levels. This is particularly important where hazardous material such as oil or gas is being transported along the jetty, or where bulk materials may be subject to degradation through water spray. The problem can be mitigated to some extent by raising the level of the plant, conveyors or pipelines above the deck level.

8.2.2. Access for inspection and maintenance

The remoteness of much of the structure means that access for regular inspection and maintenance of the structure should be carefully considered in the design, in accordance with the requirements of CDM Regulations or other locally applied

guidance or legislation. It may be difficult to provide safe access from support vessels or by retrofitting hanging walkways. These elements should be designed giving consideration to the issues described in Sections 8.1.5 and 8.1.6 above.

Illustrations

Notation

Symbol	Description	Units
a	wave amplitude	m
a_x, a_y	horizontal, vertical water particle acceleration	m/s^2
A	vertical deck area subjected to wave action	m^2
A	projected area of cylinder in Morison's equation	m^2
A	orbital amplitude of wave motion at the bed	m
b	width of deck	m
b_w, b_h, b_l	element width, height and length	m
B	spacing between wave front orthogonals	m
c	wave celerity	m/s
C_l	clearance	m
c_0	deep water wave celerity	m/s
C_b	wave breaker velocity at structure = $(gd)^{0.5}$	m/s
C_{dyn}	maximum dynamic force/maximum static force	-
C_d	drag coefficient	-
C_l	lift coefficient	-
C_m	inertia coefficient	-
C_s	slamming coefficient	-
d	sieve diameter of grains	m
d_{50}	median grain diameter	m
D	pile diameter	m
$D*$	dimensionless grain size = $d_{50}[g(\rho_s/\rho -1)/v^2]^{1/3}$	-
E_{50}	extreme 50 year water surface elevation	m
f_w	wave friction factor	-
F	force	N
F_b	vertical buoyancy force	N
F_d	drag force	N
F_e	dynamic loading factor	N
$F_{h,broken}$	force due to broken waves	N
$F_{h,min}$	minimum or negative force	N
F_h^*, F_v^*	horizontal, vertical 'basic wave force'	N
F_{hqs+}	maximum positive (shoreward) quasi-static (pulsating) horizontal force	N
F_{hqs-}	maximum negative (seaward) quasi-static (pulsating) horizontal force	N
F_i	inertia force	N
F_l	lift force	N
F_{max}	Maximum force, impact force	N
$F_{max.fender}$	maximum force expected on any one fender	t
$F_{max.line}$	maximum force expected on any one mooring line	t
F_s	slam force	N
$F_{s'}$	effective slam force	N
F_{tw}	total wave-induced force	N

Symbol	Description	Units
F_v	force to be determined (e.g. F_{vqs+}, F_{vqs-})	N
F_{vqs+}	maximum positive (upward) quasi-static (pulsating) vertical force	N
F_{vqs-}	maximum negative (downward) quasi-static (pulsating) vertical force	N
F_z	vertical wave force on horizontal deck	N
$F_{1/250}$	average force of four highest recorded test values of 1000 waves	N
g	acceleration due to gravity	m/s^2
h	water depth	m
h_f	exposed height of wall over which wave pressures act	m
H	wave height	m
H_B	breaking wave height	m
H_{max}	highest wave	m
H_s	significant wave height	m
H_0	deep water wave height	m
$H_{1/3}$	average height of highest 1/3 of waves	m
k	wave number = $2\pi/L$	m^{-1}
KC	Keulegan–Carpenter number = $U_w T_w/D$	-
KD	drag coefficient	-
K_i	inertia coefficient	-
K_s	shoaling coefficient	-
K_r	refraction coefficient	-
l	length of cylinder	m
l	wetted length	m
L	wavelength	m
L_p	wavelength, calculated using peak wave period	m
L_{bp}	length between perpendiculars of vessel	m
M	shear stress amplification factor due to presence of structure	-
M_i	added mass	kg
n	ratio of group celerity to phase celerity	-
N	design life	yrs
N_z	number of waves for each test, or during the storm/tide peak	-
p	encounter probability – annual exceedance probability of design event	-
P_{imax}	average wave pressure due to broken waves	N/m^2
p_1, p_2	pressures at top and bottom of element	N/m^2
S_e	equilibrium scour depth	m
S_R	ratio of scour area to group area of pile array	-
$Sway_{rms}$	root mean square sway response expected from the vessel	m
$Surge_{rms}$	root mean square surge response expected from the vessel	m
t	time	s
t_d	duration of the impact loading	s
T	wave period	s
T_m	mean wave period	s
T_n	natural period	s
T_p	peak wave period	s
T_R	return period	yrs
T_w	period associated with amplitude w of wave bottom orbital velocity	s
T_z	zero crossing period	s

Symbol	Description	Units
x_s	lateral extent of scour pit from cylinder wall	m
u	horizontal water particle velocity in the wave crest	m/s
u	incident current velocity	m/s
u^*	friction velocity $= (\tau_0/\rho)^{1/2}$	m/s
u^*_{cr}	critical friction velocity	m/s
U	horizontal component of water velocity	m/s
U_c	depth-averaged current velocity	m/s
U_{cr}	threshold current speed for motion of sediment	m/s
U_w	wave orbital velocity amplitude at seabed	m/s
v	vertical component of velocity	m/s
v_η	vertical velocity of water surface given by rate of change of surface elevation η with time	m/s
V	volume of the deck inundated	m^3
V	displaced volume per unit length in Morison's equation	m^3/m
W	wave orbital velocity at sea bed	m/s
W_s	diameter of the cylinder	m
x_s	final extent of scour pit	m
z_0	bed roughness length	m
α	angle between wave crest and sea bed contour	degrees
α	coefficient for time-magnitude characteristics of impact loading	-
Δ	displacement mass of the vessel	t
ϕ	angle of repose of sediment	degrees
γ	spring rate of the mooring lines	t/m
λ	an aeration constant	-
λ	stiffness of mooring lines	t/m
μ	dimensionless mooring stiffness parameter	-
η	water surface elevation	m
η_{max}	expected maximum crest elevation	m
$\dot{\eta}$	rate of change of water surface elevation	m/s
$\ddot{\eta}$	acceleration of water surface elevation	m/s^2
ν	kinematic viscosity of water	m^2/s
θ	Shield's parameter $= \tau_0/\{g(\rho_s-\rho)d$	-
θ_{cr}	threshold Shield's parameter	-
ρ_s	density of sediment grains	kg/m^3
ρ	density of water	kg/m^3
τ_c	current only shear stress	N/m^2
τ_{cr}	threshold bed shear stress for motion of sediment	N/m^2
τ_0	bed shear stress	N/m^2
τ_w	amplitude of oscillatory bed shear stress due to waves	N/m^2
τ_{max}	maximum bed shear stress	N/m^2
ω	wave angular frequency $= ck$	rad/s

9. References

Abbott, M. B. and Price, W. A. (1994). *Coastal, estuarial and harbour engineers reference book*, E and FN Spon, London.

Abou-Seida, M. M. (1963). *Sediment scour at structures*, Technical Report HEL-4-2, University of California, Berkeley, California.

Allsop, N. W. H. and Calabrese, M. (1998). Impact loadings on vertical walls in directional seas. *Proc. 26th ICCE, June 1998, Copenhagen.* ASCE, New York.

Allsop, N. W. H. and Calabrese, M. (1999). *Forces on vertical breakwaters: effects of oblique or short-crested waves.* Research Report SR465, HR Wallingford, Wallingford.

Allsop, N. W. H. and Cuomo, G. (2004). *Wave loads on exposed jetties.* Report SR583, HR Wallingford, UK.

Allsop, N. W. H. and Hettiarachchi, S. S. L. (1989). *Wave reflections in harbours: design, construction and performance of wave absorbing structures.* Report OD 89, HR Wallingford, February 1989.

Allsop, N. W. H. and Hettiarachichi, S. S. L. (1988). Reflections from coastal structures. *Proc. 21st ICCE, Malaga, June 1988*, pp. 782-794. ASCE, New York.

Allsop, N. W. H. (1995). Vertical walls and breakwaters: optimisation to improve vessel safety and wave disturbance by reducing wave reflections. Chapter 10 in *Wave forces on inclined and vertical wall structures*, pp. 232-258, ed. N. Kobayashi, and Z. Demirbilek. ASCE, New York.

Allsop, N. W. H. (2000). Wave forces on vertical and composite walls. Chapter 4 in *Handbook of Coastal Engineering*, pp. 4.1-4.47, ed. J. Herbich. McGraw-Hill, New York.

Allsop, N. W. H., Durand, N. and Hurdle, D. P. (1998). Influence of steep seabed slopes on breaking waves for structure design. *Proc. 26th ICCE, Copenhagen,* pp. 906 – 919. ASCE, New York.

Allsop, N. W. H., Kortenhaus, A., McConnell, K. J. and Oumeraci, H. (1999). New design methods for wave loadings on vertical breakwaters under pulsating and impact conditions. *Proc. Coastal Structures '99, Santander.* Balkema, Rotterdam.

Allsop, N. W. H., McKenna, J. E., Vicinanza, D. and Whittaker, T. J. T. (1996). New design formulae for wave loadings on vertical breakwaters and seawalls. *25th International Conference on Coastal Engineering, September 1996, Orlando.* ASCE, New York.

Allsop, N. W. H., Vicinanza, D. and McKenna, J. E. (1996). *Wave forces on vertical and composite breakwaters.* Strategic Research Report SR 443, pp. 1-94, HR Wallingford, March 1996, Wallingford.

American Petroleum Institute (1993). *Planning, designing and constructing fixed offshore platforms – load and resistance factor design,* 1st Edition (including supplement 1, Feb 1997).

American Petroleum Institute (2000). *Planning, designing and constructing fixed offshore platforms – working stress design,* 20th edition.

Armbrust, S. F. (1982). *Scour about a cylindrical pile due to steady and oscillatory motion.* MSc Thesis, Texas A and M University, May 1982.

Basak, V., Basamisli, Y. and Ergun, O. (1975). *Maximum equilibrium scour depth around linear-axis square cross-section pier groups.* Devlet su isteri genel mudurlugi, Report No 583, Ankara (in Turkish).

Battjes, J. A. (1982). Effects of short-crestedness on wave loads on long structures. *Applied Ocean Research,* Vol. 4, No. 3, pp.165-172.

Battjes, J. A. and Groenendijk, H. W. (2000). Wave height distributions on shallow foreshores. *Coastal Engineering,* Vol. 40, pp.161-182, Elsevier Science.

Bea, R.G., Xu, T., Stear, J. and Ramos, R. (1999). Wave forces on decks of offshore platforms. *J. Waterway, Port, Coastal and Ocean Eng.,* Vol. 125, No. 3. Proc. ASCE, New York.

Besley, P. (1999). *Overtopping of seawalls – design and assessment manual* R and D Technical Report W 178. Environment Agency, Bristol.

Besley, P. and Allsop, N. W. H. (2000). Wave overtopping of seawalls, breakwaters and related structures. Chapter 6 in *Handbook of Coastal Engineering,* pp. 6.1-6.21, ed. J. Herbich. McGraw-Hill, New York.

Bijker, E. W. and de Bruyn, C. A. (1988). Erosion around a pile due to current and breaking waves. *Proc. 21st Int. Conf. Coastal Eng., Malaga,* Vol. 2.

Blackmore, P. A. and Hewson, P. (1984). Experiments on full scale impact pressures. *Coastal Engineering,* Vol. 8, pp. 331-346. Elsevier, Amsterdam.

Bolt, H. M. and Marley, M. (1999). *Regional sensitivity and uncertainties in airgap calculations.* Paper 5.1, Airgap Workshop, Imperial College, June 1999, HSE/E and P Forum, BOMEL, Maidenhead.

Bolt, H. M. (1999). *Wave-in-deck load calculation methods.* Paper 4.3, Airgap Workshop, Imperial College, June 1999. HSE/E and P Forum, BOMEL, Maidenhead.

Bradbury, A. P. and Allsop, N. W. H. (1988). Hydraulic effects of breakwater crown walls. *Proc. Conference on Design of Breakwaters,* pp. 385-396, Institution of Civil Engineers. Thomas Telford, London.

Bradbury, A. P., Allsop, N. W. H. and Stephens, R. V. (1988). *Hydraulic performance of breakwater crown walls.* HR Report SR 146, Hydraulics Research, Wallingford.

Breusers, H. N. C. and Raudkivi, A. J. (1991). *Scouring, IAHR-AIRH Hydraulic Structures Design Manual,* Vol. 2, Balkema, Rotterdam.

Breusers, H. N. C. (1972). *Local scour near offshore structures,* Delft Hydraulics Laboratory, Publication No 105.

British Standards Institution (1988). *British Standard Code of Practice for Maritime Structures. Part 2: Code of Practice for design of quay walls, jetties and dolphins.* BS 6349: Part 2: 1988. British Standards Institution, London.

British Standards Institution (1994). *British Standard Code of Practice for Maritime Structures. Part 4: Code of Practice for design of fendering and mooring systems.* BS 6349: Part 4: 1994. British Standards Institution, London.

British Standards Institution (1991). *British Standard Code of Practice for Maritime Structures. Part 7: Guide to the design and construction of breakwaters.* BS 6349: Part 7: 1991. British Standards Institution, London.

British Standards Institution (2000). *British Standard Code of Practice for Maritime Structures, Part 1: General Criteria.* BS 6349: Part 1: 2000 (and Amendments 5488 and 5942). British Standards Institution, London.

Burcharth, H. F. (1991). Introduction of partial coefficients in the design of rubble mound breakwaters. *Proc. Conf. Coastal Structures and Breakwaters,* Institution of Civil Engineers, 6-8 November 1991. Thomas Telford, London.

Burcharth, H. F. (1994). The design of breakwaters Chapter 29 in *Coastal, estuarial and harbour engineers reference book*, pp. 381-424, eds. M. B. Abbott and W. A. Price. E and FN Spon, London.

Burcharth, H. F. and Hughes, S. (2001). Fundamentals of design Chapter VI-5 in: *Coastal engineering manual, Part VI: Design of Coastal Project Elements*, ed. S. Hughes. Engineer Manual 1110-2-1100, U.S. Army Corps of Engineers, Washington, DC.

CERC (1984). *Shore protection manual.* US Army Corps of Engineers.

CIRIA (1996). *Beach management manual.* CIRIA Report 153.

CIRIA/CUR (1991). *Manual on the use of rock in coastal and shoreline engineering*, ed. J.D. Simm. Special Publication 83, CIRIA, London.

Carpenter, K. E. and Powell, K. A. (1998). *Toe scour at vertical walls: mechanisms and protection methods.* Strategic Research Report SR 506, HR Wallingford, Wallingford.

Carstens, M. R. (1966). Similarity laws for localised scour. *Proc. ASCE, J. Hydraulics Div.*, Vol. 92, No. 3, pp. 13-36.

Chan, E. S. and Melville, W. K. (1988). *Deep water plunging wave pressures on a vertical plane wall.* Proc. Royal Soc., London.

Chan, E. S. and Melville, W. K. (1989). Plunging wave forces on surface-piercing structures. *J. Offshore Mechanics and Arctic Engineering*, Vol. 111, May 1989.

Chan, E. S., Cheong, H. F. and Gin, K. Y. H. (1995). Breaking wave loads on vertical walls suspended above mean sea level. *J. Waterway, Port, Coastal, and Ocean Div.*, ASCE, July/August, 1995.

Chan, E.S., Cheong, H. F. and Tan, B. C. (1995). Laboratory study of plunging wave impacts vertical cylinders. *Coastal Engineering,* Vol. 25, pp. 87-107, Elsevier Science BV, Amsterdam.

Chien, C. H., Chiou, Y. D. and Lai, G. H. (1995). Irregular impulsive wave forces on solid wall breakwater. *Proc. Conf. HYDRA 2000*, Vol. 3, pp. 269-280, Thomas Telford, London.

Childs, K. M. (1896). Perforated wave barriers in small boat piers. *Proc. Ports '86.* ASCE, New York.

Chow, W. Y. and Herbich, J. B. (1978). *Scour around a group of piles.* Paper OTC 3308, Offshore Technology Conference, Houston, May 1978.

Christakis, N., Waller, M. N. H., Beale, R. G. and Dennis, J. M. (1998). Analysis of the impact of waves on the underside of decks using the Volume of Fluid (VOF) method. *Computational Mechanics in UK, 6th Annual Conference of Association for Computational Mechanics in Engineering (ACME), Exeter*, pp.133-137.

Clark, A. and Novak, P. (1984). Local erosion at vertical piles by waves and currents, in: *Sea Bed Mechanics, Proc. IUTAM-IUGG Symp*, ed. B. Denness. Graham and Trotman, London, September 1984, pp. 243-249.

Cuomo, G., Allsop, N. W. H. and McConnell, K. J. (2003). Dynamic wave loads on coastal structures: analysis of impulsive and pulsating wave loads. *Proc. Conf. Coastal Structures 2003*. ASCE/CPRI, Portland.

Daemrich, K. F. and Mathais, H. J. (1999). Overtopping at vertical walls with oblique wave approach. *Proc. Conf. COPEDEC V, Cape Town*, pp. 1294-1301. COPEDEC, Sri Lanka.

Demirbilek, Z. and Vincent, L. (2002). *Water Wave Mechanics* Chapter II-1 in: *Coastal Engineering Manual, Part II*: Coastal Hydrodynamics, ed. L. Vincent. Engineer Manual 1110-2-1100, U.S. Army Corps of Engineers, Washington, DC.

Det Norske Veritas (1991). *Environmental conditions and environmental loads*. Classifications Notes No. 30.5.

Di Natale, M. (1991). *Scour around cylindrical piles due to wave motion in the surf-zone*. Coastal Zone '91, Long Beach, California, USA, July 1991.

Diamantidis, D. and Arnesen, K. (1986). Scour effects in piled structures – a sensitivity analysis. *Ocean Engineering*, Vol. 13, No. 5, pp. 497-502.

EAU (1996). *Recommendations of the Committee for the Waterfront Structures, Harbours and Waterways*.

Fowler, R. E and Allsop, N. W. H. (1999). Codes, standards and practice for coastal engineering in the UK. *Proc. Coastal Structures '99, Santander, Spain*. Balkema, Rotterdam.

Franco, C. and Franco, L. (1999). Overtopping formulae for caisson breakwaters with non-breaking 3-D waves. *J. Waterway, Port, Coastal and Ocean Engineering*, Vol. 125, No. 2, March/April 1999, pp. 98-107 ASCE, New York.

Franco, C., van der Meer, J. W., and Franco, L. (1996). Multi-directional wave loads on vertical breakwaters. *Proc. 25th International Conference on Coastal Engineering, Orlando*. ASCE, New York.

Goda, Y. (1971). Expected rate of irregular wave overtopping of seawalls. *Coastal Engineering in Japan*, Vol. 14, pp. 45-51. JSCE, Tokyo.

Goda, Y. (1974) New wave pressure formula for composite breakwaters. *Proc. 4th International Conference on Coastal Engineering*.

Goda, Y. (1985). *Random seas and maritime structures*. University of Tokyo Press, Tokyo. (out of print).

Goda, Y. (2000). *Random seas and design of maritime structures*. Advanced Series on Ocean Engineering – Volume 15. World Scientific, Singapore.

Hallam, M. G., Heaf, N. J. and Wootton, L. R. (1978). *Dynamics of Marine Structures*. CIRIA Publications, Underwater Engineering Group, London.

Hattori, M. (1994). Wave impact pressures on vertical walls and the resulting wall deflections. *Proceedings of Workshop on Wave Barriers in Deep Waters*, pp. 332-346. Port and Harbour Research Institute, Yokosuka.

Hattori, M., Arami, A. and Yui, T. (1994). Wave impact pressures on vertical walls under breaking waves of various types. *Coastal Engineering*, Special Issue on Vertical Breakwaters, Vol. 22, pp. 79-115. Elsevier Science BV, Amsterdam.

Hirai, S. and Kurata, K. (1982). Scour around multiple and submerged circular cylinders. *Memoirs Faculty of Engineering*, Osaka City Univ., Vol. 23, pp. 183-190.

Hiroi, I. (1919). On a method of estimating the force in waves. *Bulletin of Engineering Department*, Tokyo Imperial University, Vol. 10, No. 1, pp. 19.

Hjorth, P. (1975). *Studies on the nature of local scour*. Bulletin,. Series. A, No. 46, Dept. of Water Resources Engineering., Lund Institute Technology, Lund, Sweden.

HMSO (1974). *The Offshore Installation (Construction and Survey) Regulations*. Statutory Instrument 289.

HMSO (1996). *The Offshore Installations and Wells (Design and Construction etc) Regulations*. Statutory Instrument 1996/913.

International Organisation for Standardization (ISO), 1999. *Fixed steel structures standards* (draft).

IPCC (2001). *Technical summary: Climate change 2001: Impacts, adaptation and vulnerability*. http://www.ipcc.ch/pub/wg2TARtechsum.pdf

Imberger, J., Alach, D. and Schepis, J. (1982). Scour around circular cylinder in deep water. *Proc. 18th Int. Conf. Coastal Eng.*, Vol. 2, pp. 1522-1554. ASCE.

Isaacson, M. and Prasad, S. (1993). Wave slamming on a horizontal cylinder. *Proceedings of the Third International Offshore and Polar Engineering Conference, Singapore*, Vol. 3, 274-281.

Ito, Y. (1971). Stability of mixed type breakwaters – A method of probable sliding distance. *Coastal Engineering in Japan*, Vol. 14, pp. 53-61, JSCE, Tokyo.

Jensen, O. J. (1983). Breakwater superstructures. *Proc. Conf. Coastal Structures '83, Arlington*, pp. 272-285. ASCE, New York.

Kaplan, P. (1992). *Wave impact forces on offshore structures: re-examination and new interpretations.* Paper OTC 6814, 24th Offshore Technology Conference, Houston.

Kaplan, P., Murray, J. J. and Yu, W. C. (1995). *Theoretical analysis of wave impact forces on platform deck structures.* Volume 1-A. *Offshore Technology.* OMAE Copenhagen, June 1995, Offshore Mechanics and Arctic Engineering Conference.

Kirkgoz, M. S. (1982). Shock pressure of breaking waves on vertical walls. *Journal of the Waterway Port Coastal and Ocean Division*, Vol. 108, No. 1, pp. 81-95.

Kirkgoz, M. S. (1990). An experimental investigation of a vertical wall response to a breaking wave impact. *Ocean Engineering*, Vol. 17, No. 4, pp. 379-391. Elsevier Science, Oxford.

Kirkgoz, M. S. (1995). Breaking wave impacts on vertical and sloping coastal structures. *Ocean Engineering*, Vol. 22, No. 1, pp. 35-48. Elsevier Science, Oxford.

Kroezen, M., Vellinga, P., Lindenberg, J. and Burger, A. M. (1982). *Geotechnical and hydraulic aspects with regard to seabed and slope stability.* Delft Hydraulics Laboratory, Publication No. 272, June 1982, Delft, Netherlands.

Le Mehauté, B. (1976). *An Introduction to Hydrodynamics and Water Waves.* Springer-Verlag, New York.

Longuet-Higgins, M. S. (1952). On the statistical distribution of the heights of sea waves. *J. Marine Research*, 11, 245-266.

McConnell, K. J., Allsop, N. W. H. and Flohr, H. (1999). Seaward wave loading on vertical coastal structures. *Proc. Coastal Structures '99*, Santander, Spain. Balkema, Rotterdam.

Mann, K. (1991). *Sedimentation at jetties.* HR Wallingford Report SR 285.

May, R. P. and Willoughby, I. R. (1990). *Local scour around large obstructions.* HR Wallingford Report SR 240.

Minikin, R. R. (1950). *Winds, waves and maritime structures: studies in harbour making and in the protection of coasts.* Charles Griffin, London.

Minikin, R. R. (1963). *Wind, waves and maritime structures: studies in harbour making and in the protection of coasts.* 2nd edition. Griffin, London.

Mitchener, H. J., Torfs, H. and Whitehouse, R. J. S. (1996). Erosion of mud/sand mixtures. *Coastal Engineering*, Vol. 29, pp. 1-25.

Muir Wood, A. M. (1969). *Coastal hydraulics.* MacMillan, London

Müller, G. and Walkden, M. (1998). Survivability assessment of shoreline wave power stations. Paper OMAE98-0539, *Proc. 17th Int. Conf. Offshore Mech. and Arctic Engineering, Lisbon.*

Nath J. H. (1984) Marine roughened cylinder wave force coefficients. *Proceedings 19th International Coastal Engineering Conference*, Volume 3, pp. 2710-2725.

Norwegian Petroleum Directorate (1994). *Offshore Regulations.*

Oil Companies International Marine Forum (1994). *Prediction of wind and current loads on VLCCs.* OCIMF, London.

Oil Companies International Marine Forum (1997). *Mooring equipment guidelines.* 2nd edition. OCIMF, London.

Oumeraci, H., Allsop, N. W. H., de Groot, M. B., Crouch, R. S. and Vrijling, J. K. (2000). Probabilistic Design Methods for Vertical Breakwaters (PROVERBS). *Proc. Coastal Structures '99, Santander, Spain.* Balkema, Rotterdam.

Oumeraci, H. (1994). Scour in front of vertical breakwaters – review of problems. *Proceedings of Workshop on Wave Barriers in Deep Waters*, pp. 281-307, Port and Harbour Research Institute, Yokosuka, Japan.

Oumeraci, H., Kortenhaus, A., Allsop, N. W. H., De Groot, M. B., Crouch, R. S., Vrijling, J. K. and Voortman, H. G. (2000). *Probabilistic design tools for vertical breakwaters.* Balkema, Rotterdam.

Pearson, J., Bruce, T. and Allsop, N. W. H. (2000). *Violent overtopping of seawalls.* Poster paper 38, Abstracts for 27th Int. Coast. Eng. Conf. National Committee on Coastal and Ocean Eng, Institution of Engineers. Australia, Barton.

Pedersen, J. and Burcharth, H. F. (1992). Wave forces on crown walls. *Proc. 23rd ICCE, Venice.* ASCE, New York.

Pedersen, J. (1996). *Wave forces and overtopping on crown walls of rubble mound breakwaters – an experimental study.* Series paper 12, Hydraulics and Coastal Eng. Lab., Aalborg University, Denmark.

PIANC (1997). *Guidelines for the design of armoured slopes under open piled quay walls.* Report of Working Group 22 of PTC II, supplement to Bulletin No. 96, PIANC, Brussels.

Pos, J. D. (1991) *Wave and current forces on vertical, inclined and horizontal slender cylindrical members of offshore structures.* CSIR Report EMA-T 9102, South Africa.

Rienecker, M. M. and Fenton, J. D. (1981). A Fourier approximation method for steady water waves. *J. Fluid Mech.*, 104, 119-137.

Römisch, K. and Hering, W. (2002). *Input data of propeller induced velocities for dimensioning of bed protection near quay walls – a comment on existing recommendations.* PIANC Bulletin No. 109, Brussels.

Sainflou, G. (1928). Essai sur les diques maritimes verticales. *Annales des ponts et chaussées*, Vol. 98, No. 1, pp. 5-48.

Sarpkaya, T. and Cakal, I. (1983). A comprehensive sensitivity analysis of the OTS data. *Proceedings of the Offshore Technology Conference*, OTC-4616 1, 317-326.

Sarpkaya, T. (1986). *In-line and transverse forces on smooth and rough cylinders in oscilatory flow at high Reynolds numbers.* Naval Postgraduate School, California, Report NPS69-86-003.

Sarpkaya, T. and Storm, M.A. (1985). In-line force on a cylinder translating in oscillatory flow. *Applied Ocean Research*, Vol. 7, No. 4, 188-196.

Shih, R. W. K. and Anastasiou, K. (1992). A laboratory study of the wave-induced vertical loading on platform decks. *Proc. ICE, Water Maritime and Energy*, Vol. 96, No. 1, pp. 19-33. Thomas Telford, London.

Shih, R. W. K. and Anastasiou, K. (1989). *Wave induced uplift pressures acting on a horizontal platform.* Paper submitted for OMAE 1989.

Smith, D., Birkinshaw, M. and Bolt, H. M. (1999). *Airgap determination – meeting the challenge.* Paper 1.1, Airgap Workshop, Imperial College, June 1999, HSE/E and P Forum. BOMEL, Maidenhead.

Smith, G. M. and van Gent, M. R. A. (1998). Wave impacts on a jetty deck. Summary paper 137 in *Book of Abstracts for 26th Int. Conf. on Coastal Eng.*, pp. 274-275. ICCE 98 c/o Danish Hydraulics Institute, Horsholm, Denmark.

Sorenson, R. M. (1993). *Basic wave mechanics for coastal and ocean engineers.* Wiley, London.

Soulsby, R. L. (1997). *Dynamics of marine sands: a manual for practical applications.* Thomas Telford, London.

Southgate, H. N., (1995). Prediction of wave breaking processes at the coastline. In: Rahman, M. (ed.), *Advances in Fluid Mechanics,* vol. 6. Computational Mechanics Publications, Southampton, UK.

Stansberg, C-T. (1991). *Extreme Wave Asymmetry in Full Scale and Model Scale Experimental Wave Trains.* OMAE 91, Stavanger, 1991.

Sterndorff, M. J. and Groenbech, J. (1999). *A numerical model for prediction of wave loads on offshore platform decks.* Paper 4.2, Airgap Workshop, Imperial College, June 1999, HSE/E and P Forum. BOMEL, Maidenhead.

Sumer, B. M., Fredsøe, J. and Christiansen, N. (1992). Scour around vertical pile in waves. *Proc. Am. Soc. Civ. Engrs, J. Waterway, Port, Coastal and Ocean Engineering.*

Sumer, B. M., Christiansen, N. and Fredsøe, J. (1993). Influence of cross section on wave scour around piles. *Proc. ASCE, J. Waterway, Port, Coastal, and Ocean Engineering,* Vol. 119, No. 5, pp.477-495.

Sumer, B. M. and Fredsøe, J. (1997). Hydrodynamics around cylindrical structures. *Advanced Series on Ocean Engineering,* Vol. 12. World Scientific, Singapore.

Tawn, J. A., Coles, S. G. and Ledford, A. W. (1995). *HSE joint probability study: Phase II report,* Department of Mathematics and Statistics, Lancaster University.

Thoresen, C. (1988). *Port design: guidelines and recommendations.* Tapir Publishers, Trondheim.

Tickell, R. G. (1994). Wave forces on structures, Chapter 28 in *Coastal, estuarial and harbour engineers reference book,* pp. 369-380, eds. M. B. Abbott and W. A. Price. E and FN Spon, London.

Tirindelli, M., Cuomo, G., Allsop, N. W. H. and McConnell, K. J. (2002). Exposed jetties: inconsistencies and gaps in design methods for wave-induced forces. *Coastal Conundrums, 28th International Conference on Coastal Engineering, ICCE 2002, Cardiff UK.* ASCE, New York.

Torrini, L., McConnell, K. J. and Allsop, N. W. H. (1999). Simplified dynamic analysis of wave impact loadings on vertical/composite breakwaters. *Proc. Coastal Structures '99, Santander, Spain.* ASCE, New York.

Toumazis, A. D., Shih, W. K. and Anastasiou, K. (1989). Wave impact loading on horizontal and vertical plates. *Proc. IAHR 89 Conf., Ottawa, Canada*, 21-25 August 1989, pp. c209-c216.

U.S. Army Corps of Engineers (2002). *Coastal engineering manual*. Engineer Manual 1110-2-1100, U.S. Army Corps of Engineers, Washington, D.C. (in 6 volumes). (http://bigfoot.wes.army.mil/cem001.html)

van der Meer, J. W., d'Angremond, K. and Juhl, J. (1994). Probabilistic calculations of wave forces on vertical structures. *Proc. 24th ICCE, Kobe*, pp. 1754-1767. ASCE, New York.

van der Meer, J. W. (1993). *Conceptual design of rubble mound breakwaters*. Publication No. 483. Delft Hydraulics, Delft.

Vincent, L., Bratos, S., Demirbilek, Z. and Weggel, J. R. (2002). Estimation of nearshore waves. Chapter II-3 in *Coastal Engineering Manual, Part II*: Coastal Hydrodynamics, ed. L. Vincent. Engineer Manual 1110-2-1100, U.S. Army Corps of Engineers, Washington, DC.

Vitall, N., Kothyari, U. C. and Haghighat, M. (1994). Clear-water scour around bridge pier group. *Proc. ASCE, J. Hydraulic Engrg.*, Vol. 120, No. 11, pp. 1309-1318.

Weckman, J., Bigham, G. N. and Dixon, R. O. (1983). Reflection characteristics of a wave-absorbing pier. *Proc. Conf. Coastal Structures '83, Arlington, March 1983*, pp. 953-960. ASCE, New York.

Whitehouse, R. J. S. (1998). *Scour at marine structures*. Thomas Telford, London.

Yanmaz, A. M. and Altinbilek, H. D. (1991). Study of time-dependent local scour around bridge piers. *Proc. ASCE, J. Hydraulic Engrg.*, Vol. 117, No. 10, pp. 1247-1268.